The role of the transcription factor SRF in the inhibition of senescence in human and porcine smooth muscle cells

der Fakultät für Biologie
der EBERHARD KARLS UNIVERSITÄT TÜBINGEN

zur Erlangung des Grades eines Doktors
der Naturwissenschaften

von

Nina Konjer
aus Nordhorn
vorgelegte
D i s s e r t a t i o n

2009

Tag der mündlichen Prüfung:	29. Oktober 2009
Dekan:	Prof. Dr. H.A. Mallot
1. Berichterstatter:	Prof. Dr. A. Nordheim
2. Berichterstatter:	Dr. O. Heidenreich

Table of contents

1 Introduction 8

1.1 *Serum Response Factor (SRF)* 9

1.1.1 Structure and characteristics of *SRF* 9
1.1.2 Splice variants of SRF 10
1.1.3 DNA binding 11
1.1.4 Activation of *SRF* 12
1.1.5 Interactions with partner proteins 13
1.1.6 Functions of *SRF* 15
1.1.7 *SRF* target genes 17

1.2 Cell cycle of eukaryotic cells 18

1.2.1 Phases of the cell cycle 18
1.2.2 Regulation of cell cycle 19
1.2.3 Checkpoints 21
1.2.4 Senescence 23

1.3 Smooth muscle cells (SMCs) 26

1.3.1 Origin of smooth muscle cells 26
1.3.2 Structure and functions of smooth muscle cells 27
1.3.3 Arterial and venous SMCs 27
1.3.4 Contraction of smooth muscle cells 28
1.3.5 Phenotypic modulation 30
1.3.6 Malfunctions of SMCs 31

1.4 RNA Interference 33

1.4.1 Design of siRNAs 33
1.4.2 Transfection of siRNAs 34
1.4.3 Mechanism of RNA interference 35
1.4.4 Applications for siRNAs 36

2 Aims of this work 37

3 Materials 38

3.1 Chemicals and reagents 38

3.2 Consumable material 43

3.3 Buffers and stock solutions 44

3.4 Laboratory equipment and technical devices 47

3.5 Oligonucleotides 48

3.5.1 Primers for real-time RT-PCR 48
3.5.2 Primer for RT-PCR and sequencing 50
3.5.3 siRNAs 50

3.6 Cells 51

4 Methods 52

4.1 Cell culture 52

4.1.1 Isolation of primary porcine SMCs 52
4.1.2 Thawing and freezing of cells 52
4.1.3 siRNA hybridization 52
4.1.4 Transfection 53
4.1.5 Harvest of cells 53
4.1.6 Senescence β-galactosidase activity staining 53

4.2 Protein analysis 55

4.2.1 Protein determination 55
4.2.2 SDS-PAGE 55
4.2.3 Blotting and protein detection 55
4.2.4 Antibody crossreactions 56
4.2.5 Stripping 56
4.2.6 Loading control 57
4.2.7 Quantification of Western films 57

4.3 RNA analysis 58

4.3.1 RNA determination 58
4.3.2 cDNA synthesis 58
4.3.3 Real-time RT-PCR 58
4.3.4 RT - PCR 59
4.3.5 Agarose gel separation of PCR products 60
4.3.6 Gel extraction 60
4.3.7 Sequencing of PCR products 60

4.4 Statistical analysis 61

4.4.1 Definition of independent analysis 61
4.4.2 Significance test 61

5 Results 62

5.1 Sequencing of cDNA for Sus scrofa SRF 62

5.2 Testing of siRNAs on human smooth muscle cells 69

5.2.1 Test of different siRNAs against *SRF* and verification of siGL2 as neutral control siRNA using human smooth muscle cells 69
5.2.2 Transfection procedure does not induce an interferon response 70

5.3 Effectiveness of siSRF797-transfection in human and porcine smooth muscle cells 71

5.3.1 *SRF* mRNA and protein are significantly downregulated after transfection with siSRF797 in human and porcine SMCs 71
5.3.2 *SRF* target genes are also affected after siSRF797 treatment 73

5.4 Induction of senescence after downregulation of SRF 74
5.4.1 *SRF* depletion induces senescence in human and porcine SMCs 74
5.4.2 Analysis of cell cycle-specific genes in human SMCs after reduction of SRF with siRNAs 76
5.5 Downregulation of SKP2 as possible inducer of senescence 80
5.5.1 Transfection of siSKP2 in human smooth muscle cells 80
5.5.2 Downregulation of *SKP2* leads to an induction of senescence in human SMCs 81
5.5.3 Analysis of *SRF* and its target gene *TAGLN* after downregulation of *SKP2* 82
5.5.4 Analysis of *CDKN1B* and *TP53* levels after siSKP2-transfection 83
5.6 CDKN1B as main inducer of senescence upon downregulation of SRF 85
5.6.1 Transfection of siCDKN1B and cotransfection of siSRF797 and siCDKN1B in human SMCs 85
5.6.2 Cotransfection of siSRF797 and siCDKN1B leads to a rescue of the senescent phenotype 88
5.6.3 Analysis of *TP53* and *SKP2* levels after cotransfection of siSRF797+siCDKN1B 90
6 Discussion 92
6.1 *Sus scrofa* as model organism for cardiologic studies 92
6.2 siSRF797 is a highly efficient and specific siRNA against *SRF* in different mammalian cells 93
6.3 Downregulation of SRF triggers senescence in human and porcine SMCs 94
6.4 The TP53-CDKN1A axis and its possible role in siSRF797-triggered senescence 95
6.5 Role of SKP2 and CDKN1B in siSRF797-triggered senescence 96
6.6 Conclusions and Outlook 98
7 Summary 100
8 Zusammenfassung 101
9 Abbreviations 102
10 Table of figures 104
11 References 106
12 Acknowledgement 123

1 Introduction

The nomenclature used in this thesis corresponds to the gene nomenclature, which was established by the HUGO Gene Nomenclature Committee (HGNC) (see http://www.genenames.org).

The rules for *Homo sapiens* are also applied for non-human primates, domestic species and for everything that is not a mouse, rat, fish, worm and fly and therefore it is also used for *Sus scrofa*.

- Full gene names are not italicized and greek symbols are never used.
- Gene symbols are italicized and all letter are in upper case.
- Proteins are designated as not italicized, but also all upper case.
- mRNA and cDNA use the gene symbol and formatting conventions, so italicized and all in upper case.

The rules for mouse and rat are the following:

- Gene symbols are italicized, with only the first letter in uppercase and the remaining letters in lowercase
- Proteins are designated as not italicized, the first letter in uppercase and the remaining letters in lowercase
- mRNA is symbolized as the gene symbol.

1.1 *Serum Response Factor (SRF)*

The gene encoding the human transcription factor *serum response factor* (*SRF*) is positioned on chromosome 6 at the location 6p21.1. The complete gene consists of 10325 nucleotides, which are separated in 7 exons, 6 introns, 5' and 3' untranslated regions. The exons are in total 1530 nucleotides and encode for the SRF protein that is composed of 508 amino acids (www.ncbi.nlm.nih.gov).

Figure 1 – The human *SRF* gene
This figure depicts the structure of the human *SRF* gene. The thick light red fields indicate exons, the thin lines represent introns and the dark red fields mark the 5' and 3' untranslated regions.

SRF belongs to the MADS transcription factor family (MCM1, Agamous, Deficiens and SRF) and is an evolutionary highly conserved transcription factor (Treisman, 1987; Norman et al., 1988).

1.1.1 Structure and characteristics of SRF

The SRF protein is comprised of 508 amino acids. The highly conserved MADS box is situated between amino acids 142-198 (Johanson et al., 1993). Its DNA binding domain is located between the amino acids 133-235 and the dimerization domain between amino acids 168-235 (Norman et al., 1988). The nuclear localization sequence can be found between amino acids 95-100. The transactivation domain is situated at the 3' end between the amino acids 339-508 (Johanson et al., 1993).

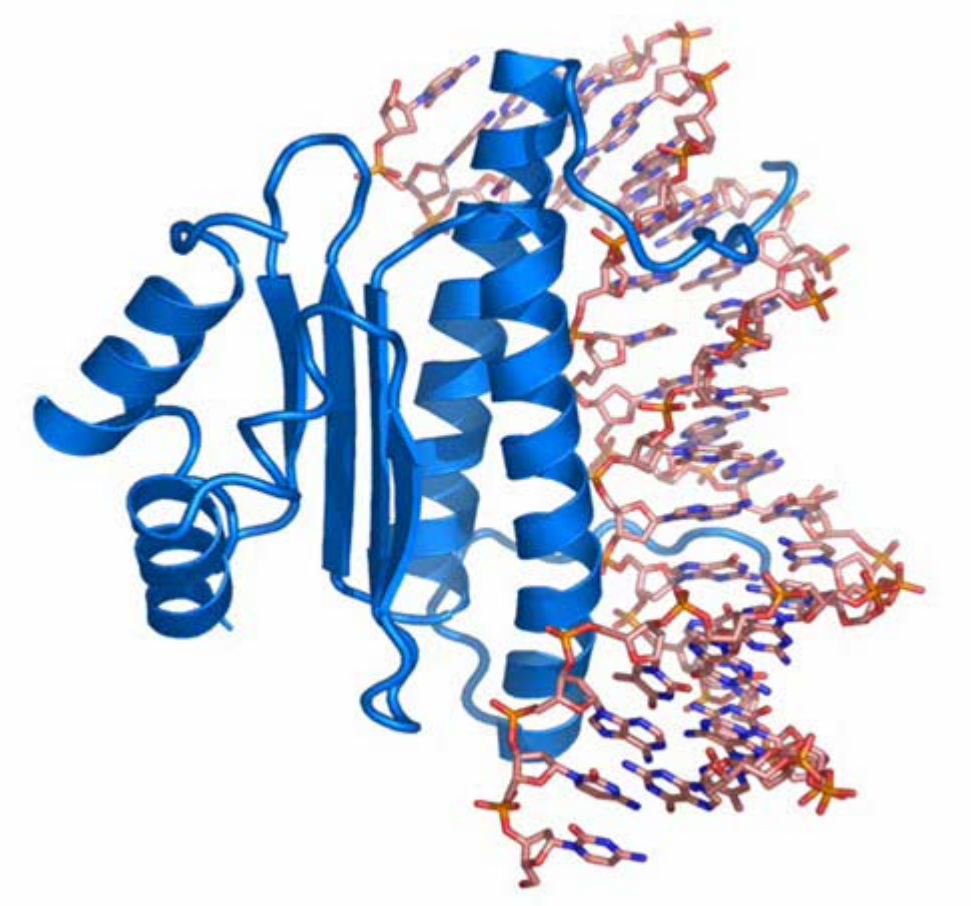

Figure 2 – An SRF-dimer (blue) binds to DNA (Pellegrini et al., 1995)

1.1.2 Splice variants of SRF

Belaguli et al. demonstrated in 1999 that there are five isoforms of Srf. Srf-FL stands for full-length Srf. Its calculated mass is 51.6 kDa but its apparent mass is 67 kDa due to posttranscriptional modifications such as glycosylation (Schröter et al., 1990; Reason et al., 1992), phosphorylation (Heidenreich et al., 1999; Misra et al., 1991) and sumoylation (Matsuzaki et al., 2003). SRF-FL is encoded by all seven exons and is the most prominent isoform in nearly all human tissues (Davis et al., 2002). Three other isoforms, which are generated through alternative splicing, have the ability to bind DNA due to an intact MADS box (Kemp et al., 2000). The fifth isoform that was discovered by Belaguli in 1999 lacks exon 5 and functions as dominant-negative mutant. It represses Srf-dependent transcription.

1.1.3 DNA binding

SRF binds to a specific DNA sequence that is called CArG box. The consensus sequence for CArG boxes is $CC(A/T)_6GG$ (Minty et al., 1986). Insertations or substitutions at positions -3 or 3 (see figure 3) lead to a reduced affinity, whereas a substitution in positions -2 to 2 lead to a very weak or no affinity at all and prevent thereby binding of SRF (Phan-Dinh-Tuy et al., 1988; Leung et al., 1989; Hautmann et al., 1998).

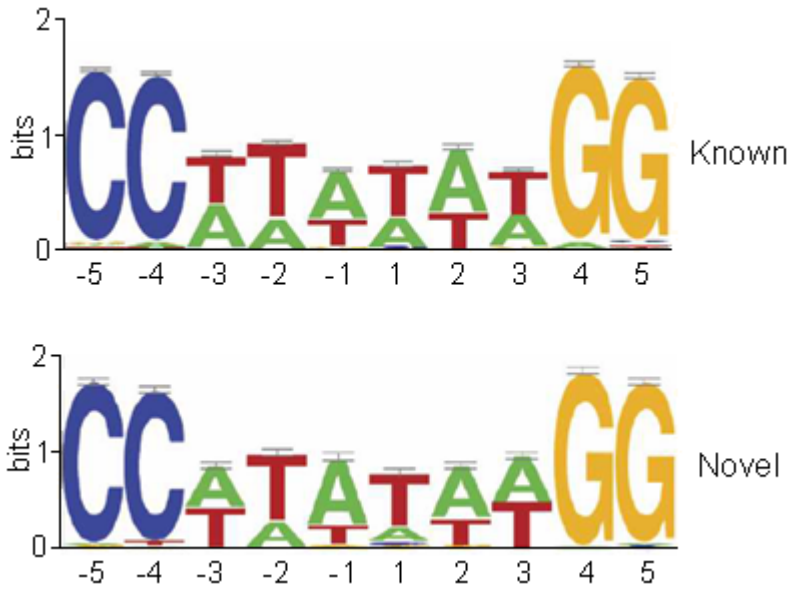

Figure 3 – Sequence logos of known and novel SRF-binding sequences (Sun et al., 2006)

The CArG box can be found in promoters of immediate early genes, for example *FOS* and *EGR1*, and in muscle specific genes like *ACTA1* and *TAGLN* (Sobue et al., 1999). The Serum Response Element (SRE) is 23 bp long and consists of the CArG box and an Ets-motif GGA(A/T). The SRE is present in many genes that are associated with cell cycle regulation and proliferation (Gilman et al., 1986; Treisman, 1986, 1987; Prywes et al., 1987).

1.1.4 Activation of *SRF*

There are two pathways that can lead to a transcriptional activation of *SRF*, the MAP-kinase pathway and the Rho-actin pathway (Gineitis et al., 2001). Spencer et al. showed in 1996 that the *SRF* gene is also regulated by the SRF protein, so there might be a feedback mechanism.

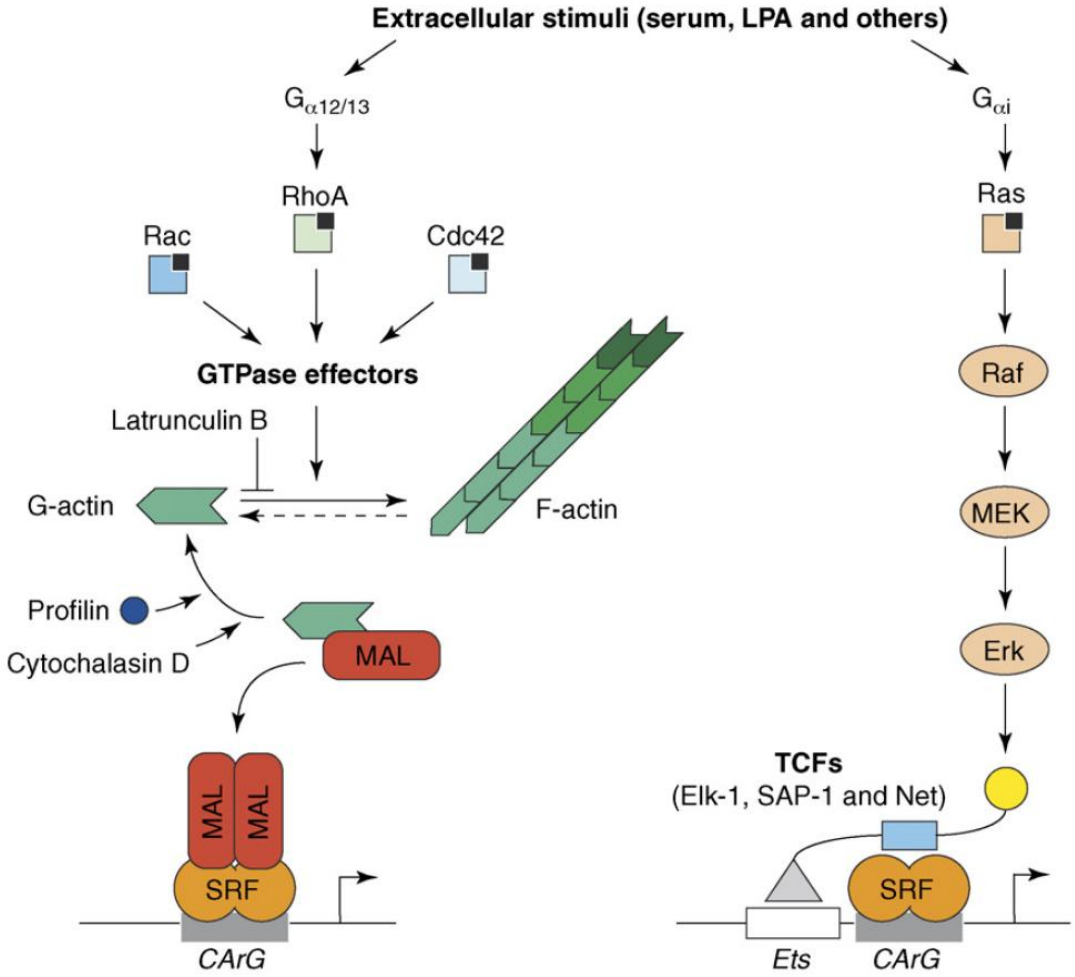

Figure 4 – Schematic overview of the two principal pathways that regulate SRF activity in non-muscle cells (Posern et al., 2006).
Both pathways are activated by G-protein coupled receptors. The Rho-actin pathway (left) is activated by $G_{\alpha 12/13}$ and the actin tread milling cycle, which leads to a activation of SRF by MAL. The MAP kinase pathway (right) is stimulated by activation of $G_{\alpha i}$, which leads to Ras-ERK signalling and starts transcription via TCF-SRF complexes.

Figure 4 shows the two pathways of *SRF* activation. The Rho-actin pathway (left) uses the actin tread milling cycle to increase free MAL, which can then activate SRF. The MAP kinase pathway (right) leads to a phosphorylation of TCFs by ERK. Phosphorylated TCFs bind to the Ets DNA recognition site and SRF in the 'grappling hook' model and start transcription (for review see Posern et al., 2006).

1.1.5 Interactions with partner proteins

SRF-dependent gene transcription is specified by the interaction of SRF with different cofactors. These combinations are very distinct for the role of *SRF* in the different gene programs (for review see Miano, 2006).

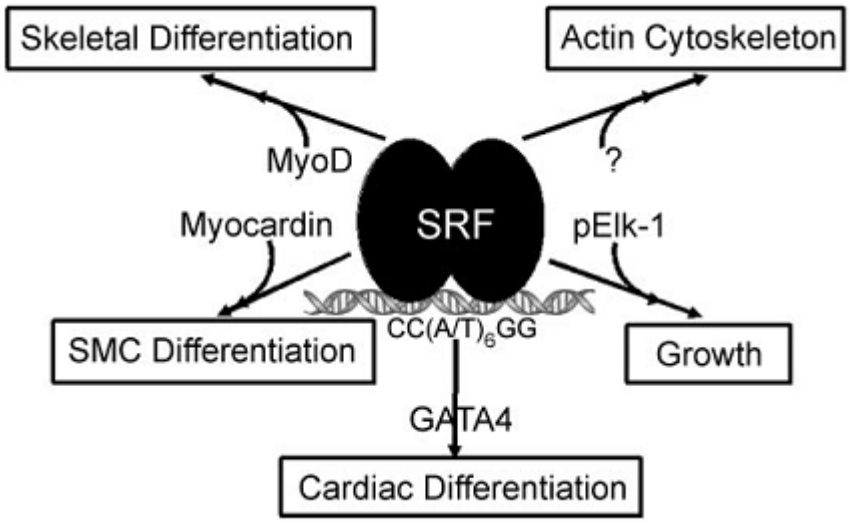

Figure 5 – This schema illustrates some of the SRF-dependent gene programs that are specified by the recruitment of cell-restricted cofactors. (Miano, 2006)

SRF binds to the CArG box as a homodimer and forms with cofactors multi-protein complexes. One of the first discovered cofactors of SRF are the TCFs (ternary complex factors), which belong to the family of Ets-proteins. ELK1, ELK3 and ELK4 build the group of TCF-proteins. Together with one of these proteins, SRF forms the so-called ternary complex and starts translation. (Shaw et al., 1989; Hipskind et al., 1991).

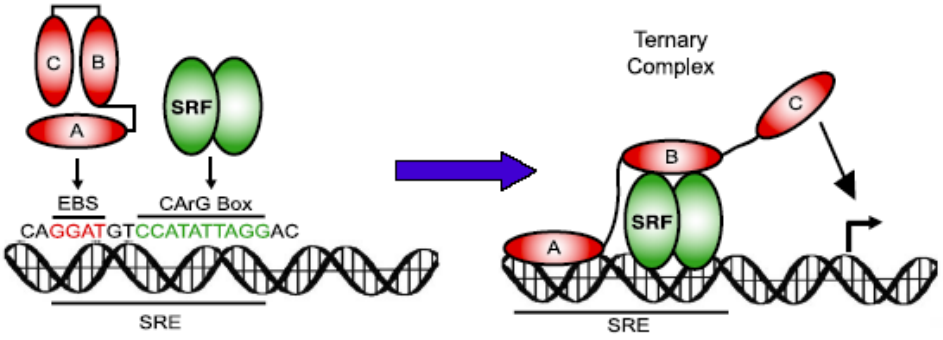

Figure 6 – Formation of a ternary complex at the c-fos promoter
The homodimer of SRF (green) binds to the CArG box, whereas the A-box of the TCF (red) binds to EBS-domain. The protein-protein-interaction takes place over the B-box of the TCF and the MADS-box of SRF (for review see Buchwalter et al., 2004)

Other cofactors of SRF belong to the Myocardin related transcription factor family (MRTF), which is a member of the SAP-domain protein family. There are three members of the MRTF family: MYOCD, MRTF-A/MKL1 and MRTF-B/MKL2 (Wang et al., 2002; Aravind et al., 2000). MYOCD is mainly expression in heart- and smooth-muscle tissues and activates *SRF*-dependent muscle-specific genes (Wang et al, 2001). The other members MRTF-A/MKL1 and MRTF-B/MKL2 are ubiquitously expressed. Therefore, they play probably a more general role than MYOCD (Wang et al., 2002).

Previous reports could show that TCF- and MRTF-binding are mutually exclusive since the cofactors bind to the same region of the SRF-DNA-binding domain as depicted in figure 7 (Hill et al., 1994; Wang et al., 2004).

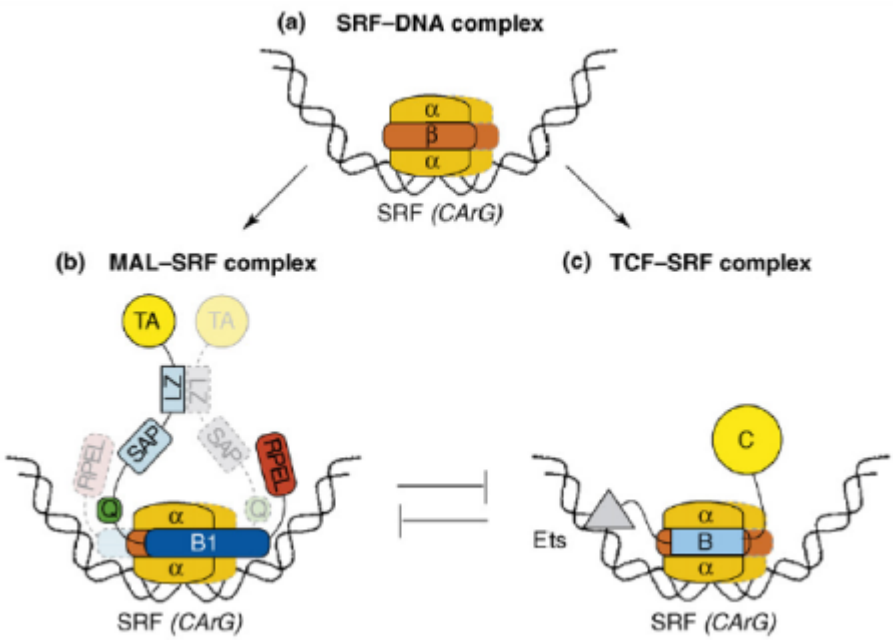

Figure 7 – Model of mutually exclusive binding of MAL and TCFs to SRF (Posern et al., 2006)

1.1.6 Functions of *SRF*

One of the first published functions of *SRF* is the transcriptional regulation of immediate early genes as a response after stimulation with mitotic signals. This reaction is drastically reduced in *Srf*-/- ES cells (Schratt et al., 2001). So far over 200 genes have been identified, that contain one or more CArG boxes in their promoter region. These genes are, in addition to immediate early genes, also actin-cytoskeletal and muscle-specific genes, whose expression is directly regulated by *SRF* and its partner proteins (Chai et al., 2004; Sun et al., 2006; Miano et al., 2007).

Since *SRF* induces immediate early gene expression after stimulation with serum (Poser et al., 2000), it was hypothesized that *SRF* is directly involved in cellular proliferation. Indeed, an impairment of SRF activity led to an inhibition of cell cycle progression in somatic cells (Gauthier-Rouviere et al., 1991; Soulez, Gauthier-Rouviere et al., 1996). However, *Srf*-/- mouse embryos grow and develop up to E6.0 and embryonic stem cells proliferate with no significant change in proliferation rate (Schratt et al., 2002). Alberti et al. (2005) and Knöll et al. (2006) showed that brain-specific conditional *Srf* knockout mice do not display altered cell proliferation. Therefore, it seems that *Srf* is not required for the ES cell cycle. It might be that compensatory mechanism are activated when *Srf* is knocked out, which could be a reason for the different observations.

Another discussed function of *Srf* is its role in cell survival: Schratt et al. (2004) showed that *Srf* promotes cell survival by regulating the expression of anti-apoptotic genes such as *Bcl2*. On the other hand, Bertolotto et al. (2000) provided evidence for *SRF* to be a switch between cell survival and death pathways. Cell type-specific regulatory mechanisms could also be a reason for these contradictory observations, since Schratt et al. used murine ES cells and Bertolotto et al. investigated human Jurkat T cells.

SRF is not only required for the activation of muscle-specific genes but also for the differentiation of C2 myogenic cells (Soulez, Gauthier-Rouviere et al., 1996; Soulez, Tuil et al., 1996). *SRF* plays a critical role in early embryonal development in

mammals. After constitutive deletion of both *Srf* alleles in mouse embryos, no mesodermal cells or mesodermal marker gene expression can be detected (Arsenian et al., 1998). VEGF-induced angiogenesis was impaired in HUVECs treated with SRF siRNA, which reveals *SRF* to be a downstream mediator for this process (Chai et al., 2004).

SRF has a distinct role in contractile and cytoskeletal architecture. Schratt et al. (2004) illustrated that *Srf* plays a vital role in focal adhesion assembly and actin cytoskeletal organization in ES cells. *Srf* deficiency leads to an arrest of neuronal migration by affecting gelsolin and cofilin (Alberti et al., 2005). Knöll et al. (2006) showed that *Srf* is also required for a cytoskeletal dynamics of growth cones, neurite outgrowth, axon guidance, correct target recognition and synapse formation.

SRF plays an important role in muscle cell biology. *SRF* is required for proliferation, differentiation and expression of specific markers in skeletal muscle (Soulez et al., 1996). SRF and RhoA selectively control the expression of MyoD, suggesting a direct or indirect role of *SRF* in muscle determination (Carnac et al., 1998). Many *SRF* target genes are differentially expressed during normal cardiac development, which implies that *SRF* may be involved in the genetic regulation of cardiac structure and function. Zhang, Azhar et al. showed in 2001 that over-expression of wild type *Srf* in hearts of young mice resulted in cardiac hypertrophy, cardiomyopathy and early mortality. Another study of the same group demonstrated that animals, which expressed a mutant form of *Srf* that is unable to bind DNA or transactivate transcription developed early cardiomyopathy and dies prematurely. Hearts from these mice had elevated amounts of total *Srf* mRNA and protein, but reduced DNA-binding ability. *Srf*-dependent gene expression was also altered (Zhang, Chai et al., 2001). Ablation of Srf in the developing cardiovascular system resulted in defective cytoskeletal assembly in the aorta and myofibrillogenesis in the heart (Miano et al., 2004). Li et al. demonstrated in 2005 that ablation of Srf in developing skeletal muscle resulted in perinatal lethality. A smooth-muscle specific ablation of Srf showed impaired contraction, defective peristalsis and died within 2 weeks after ablation of SRF (Angstenberger et al., 2007). Niu et al. could show in 2005 that conditional cardiac-specific ablation of Srf blocked cardiogenesis.

1.1.7 *SRF* target genes

ACTA2 (also known as *smooth muscle α-actin*) is a member of the actin protein family. Actins are highly conserved cytoskeletal proteins. Six tissue-specific actin isoforms are known in vertebrates (Vandekerckhove et al., 1978). ACTA2 is the single most abundant protein in SMCs, it makes up 40% of total cellular protein and about 70% of total actin (Fatigati et al., 1984). It is a major protein in the actin filaments of the contractile apparatus in vascular SMCs (for review see Small et al., 1998). The *ACTA2* gene contains two CArG boxes within the promoter region and is an SRF target gene (Saga et al., 1999; Shimizu et al., 1995; Mack et al., 1999).

CNN1 (or *smooth muscle calponin*) encodes the smooth muscle-specific form of the Calponin protein (Gimona et al., 1990), of which three isoforms are known (Takahashi et al., 1988). All Calponins are actin regulatory proteins, CNN1 stabilizes actin filaments (Takahashi et al., 1988). Its expression is activated by *Srf*, although there is no CArG box within the promoter region, but within the first intron (Landerholm et al., 1999; Miano et al., 2000).

The TAGLN (=transgelin or SM22α) protein is found in all myogenic cell lineages (Solway et al., 1995). It is the most dominant form of *SM22* genes (Lees-Miller et al., 1987), but its biological and physiological functions still remain unclear. There are two CArG boxes in the promoter region of *Tagln* and it is also an *Srf* target gene (Li et al., 1996; Li et al., 1997).

1.2 Cell cycle of eukaryotic cells

The eukaryotic cell cycle describes the process from one cell division to the next one. The replication of a cell can be divided in two phases: the interphase and the mitotic phase (M phase).

The interphase describes the stages between the mitotic divisions and can itself be separated in G_1, S and G_2 phase. The nuclear and cytoplasmic division take place in M phase.

1.2.1 Phases of the cell cycle

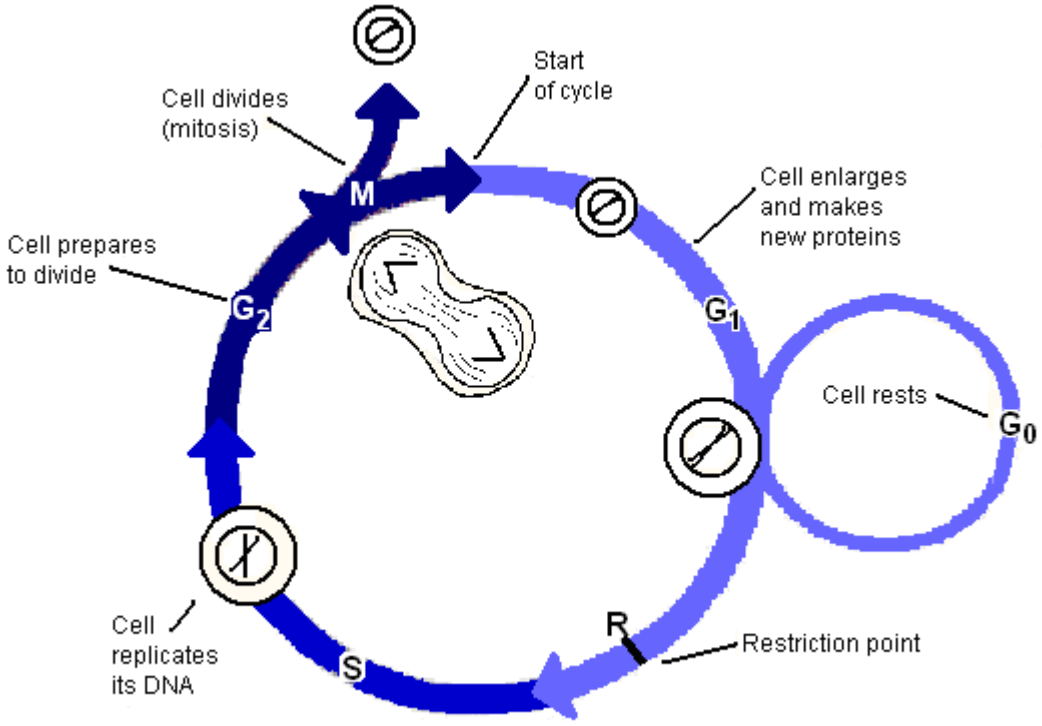

Figure 8 – Schematic drawing of cell cycle (adapted from http://www.breastcancersource.com)

This figure illustrates the cell cycle. The interphase consisting of the G_1, S and G_2 phase and the M phase, which stands for the nuclear and cytoplasmic division. The R point (restriction point) represents the point of no return, cells will enter S phase and finish the cell division even if the conditions for proliferation get worse.

The interphase is split up in G_1, S and G_2 phase. The cell is growing and cytoplasm and organelles are supplemented in G_1 phase, a set of one-chromatid-chromosomes is present in this phase (Pardee et al., 1978). In the absence of growth factors, the

cell is in G_0 phase, which is characterised by the absence of CCNs (cyclins) and CDKs (cyclin-dependent kinases) (see 1.2.4 Senescence). When growth factors are present, CCND and CCNE are expressed and the cell can re-enter the cell cycle even after a long time period in G_0 phase. DNA replication and histone production take place in the S phase, whereby S stands for synthesis (of DNA). The S phase is completed with a two-chromatid chromosome (Howard, 1951). The G_2 phase is characterized by melting of the endoplasmatic reticulum, thereby preparing the cells for mitosis. The end of the interphase is reached at the end of the G_2 phase, when cells enter mitosis (Pardee et al., 1978).

The M phase can be separated in the karyokinesis or mitosis, the division of the chromosomes, and the cytokinesis, the separation of the cytoplasm. Mitosis can be divided into prophase, prometaphase, metaphase, anaphase and telophase (Baserga, 1985).

1.2.2 Regulation of cell cycle

The cell cycle is regulated by CCNs and CDKs. CCNs are the regulatory subunits and the CDKs are the catalytic component of the heterodimer (Nigg, 1995). The specific activation or inhibition and degradation of proteins by CDKs leads to a directional and ordered progression through the cell cycle, which makes it impossible to “reverse” it (Morgan, 1995).

CCNDs and CCNEs are the main players in the G_1/S transition. CCND-CDK4/6 is slowly increasing during G_1 phase. CCND expression is induced upon stimulation by growth factors, hormones, amino acids and other triggers of proliferation. The active CCND-CDK4/6 complex can then phosphorylate the RB1 protein, which subsequently dissociates from E2F1. One of the first genes that is transcribed by the activated E2F1 is CCNE, which builds a complex with CDK2. The CCNE-CDK2 complex also phosphorylates RB1. Therefore, this positive feedback-loop leads to more CCNE and thereby further promoting S phase gene expression. Another function of CCND1-CDK4/6 and CCNE-CDK2 is the phosphorylation and consequent degradation of CDK inhibitors like CDKN1A and CDKN1B (Matsushime, 1991).

Another S-phase protein, whose gene is transcribed by E2F1, is CCNA, which is thereby slowly increasing during G_1 phase. CCNA builds a complex with CDK2 that triggers DNA synthesis (Pagano et al., 1992). CCNA-CDK2 phosphorylates E2F1 in order to down-regulate E2F1, thereby allowing S-phase progression. CCNA-CDK2 and CCNE-CDK2 complexes then phosphorylate proteins that are required for building of the DNA replication fork (Baserga, 1985; Pagano et al., 1992). When all DNA is replicated, the CCNB-CDK1 complex is activated, which is also called MPF (mitosis promoting factor) (Labbe et al., 1989). CCNB-CDK1 is already synthesized during S and G_2 phase but is activated in late G_2 phase by a phosphatase that removes an inhibitory phosphate group (Dunphy, 1994). CCNB-CDK1 promotes entry to mitosis from G_2 phase by an activating phosphorylation of proteins like condensins, lamins and myosin. CCNB-CDK1 phosphorylates also the Golgi matrix, which leads to its fragmentation. This is all preparation for the anaphase, where the separation of the sister chromosomes takes place. When all requirements for entry into anaphase are fulfilled, the APC (anaphase promoting complex) is activated. APC first polyubiquitinates CCNA (Geley et al., 2001) and later CCNB (King et al., 1995; King et al., 1996), which marks these complexes for degradation (Sudakin et al., 1995). APC is an E3 ubiquitin ligase and is composed of several proteins. It targets Securin for degradation (Cohen-Fix et al., 1996); thereby releasing saparase, which then cleaves cohesins. Cohesins hold the sister chromatids together, so after cleavage the chromatids are separated and can then move to opposite ends. This is the onset of anaphase. APC is active until the end of M phase and beginning of G_1 phase. It is inactivated by CCND-CDK4/6 in early G_1 phase and the cell cycle can now start over again.

1.2.3 Checkpoints

The cell monitors the cell cycle progress and regulates it. There are several checkpoints within the cell cycle. At these points, the cell checks if all requirements are fulfilled to proceed to the next phase. If they are not fulfilled, repair genes are activated and the cell is arrested and – if repair proves insufficient – eventually undergoes apoptosis (Nigg, 1995; Morgan, 1995). This mechanism ensures that damaged or incomplete DNA is not passed onto daughter cells (Nigg, 2001).

- G_1 checkpoint
  If the DNA of cells is damaged in early to mid G_1 phase they can be arrested in G_1 in response to different signals, like activation of TP53 (Little, 1968; Kastan et al., 1991), overexpression of CDK inhibitors like CDKN1A (Harper et al., 1995), CDKN1B (Toyoshima et al., 1994) or CDKN2A (Krishnamurthy et al., 2004), telomere shortening (Bodnar et al., 1998) and others. CCNA-CDK2 is also an important player in G_1/S transition, since it is required for the inactivation of E2F1 and DNA-synthesis (Krek et al., 1995).

- G_2 checkpoint
  G_2 arrest can be induced by inhibition of CCNB-CDC2 protein kinase (Herzinger et al., 1995). This is achieved by binding of CDKN1A to the kinase, thereby inhibiting its activity (Dulic et al., 1998).

- Spindle checkpoint
  At this checkpoint the cell is ensuring in anaphase of mitosis that all centromeres are connected to the spindle apparatus and that the chromosomes are arranged correctly in the equatorial plate (for review see Rudner et al., 1996) before telophase can start. The previously described APC and CCNB-CDK1 complexes play important roles in this process (King et al., 1995; Masui et al., 1971).

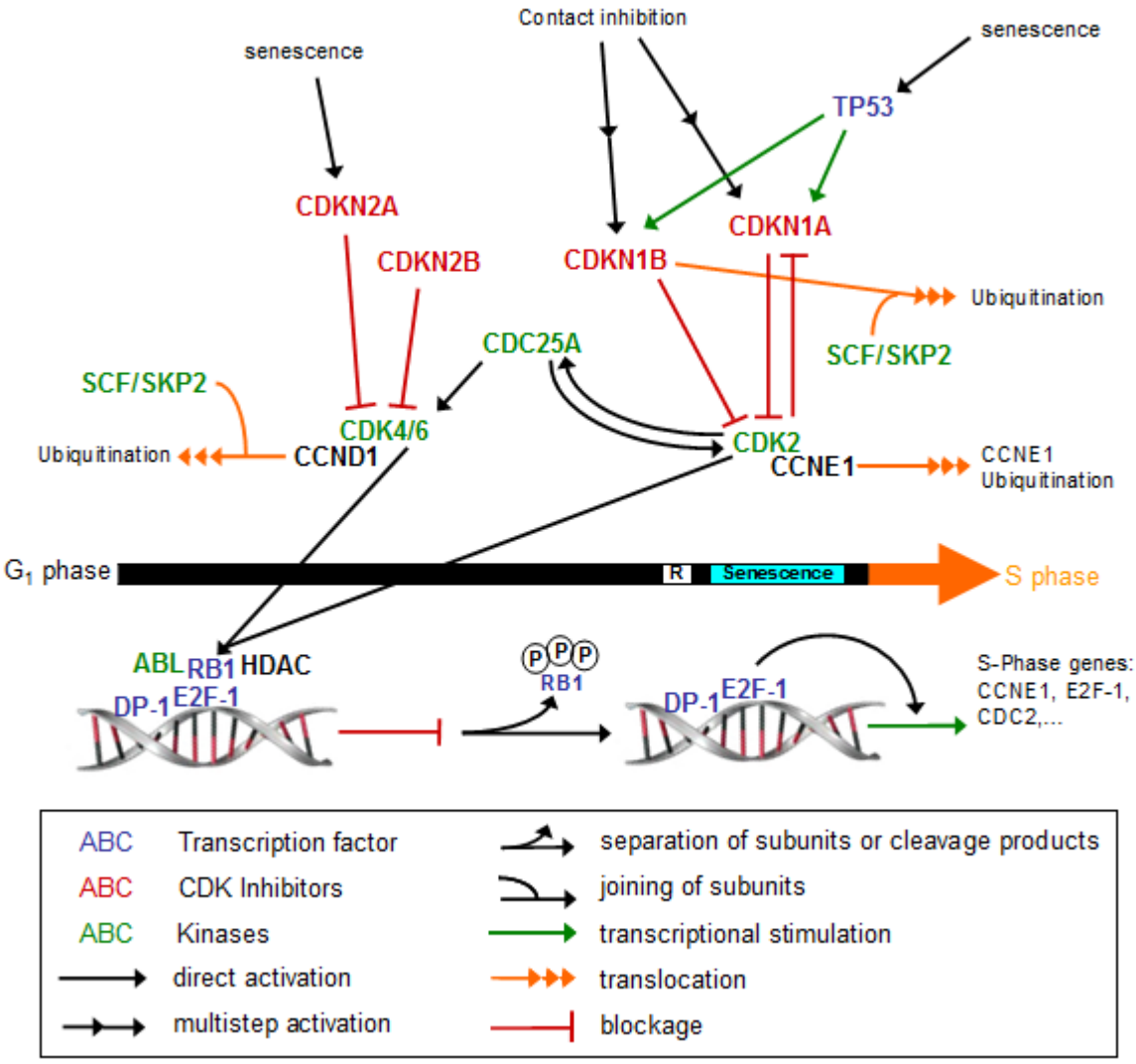

Figure 9 – Section of the G_1/S transition-pathway showing most of the important proteins involved in this transition

Figure 9 shows several proteins that are important for the G_1/S transition. By analyzing protein levels and their phosphorylation status, the cell cycle status can be determined.

1.2.4 Senescence

Cells that are irreversibly arrested in late G_1 phase are defined as being senescent. Hayflick and Moorhead first described this state and hypothesized the existence of cellular factors, whose deprivation in the course of repeated cell divisions would limit the proliferation of normal cells (Hayflick et al., 1961). Senescent cells cannot resume proliferation in response to any known physiological stimuli and many cells do not respond to apoptotic stimuli (for review see Campisi et al., 2007). Senescence is often a biochemical alternative to the self-destruction of such a damaged cell by apoptosis (Kastan, 1997). This type of arrest is caused by the upregulation of CDK inhibitors, which can be induced by different events, for example aberrant proliferative signals, DNA damaging, intracellular stress like strong mitogenic signaling and others (for reviews see Blagosklonny, 2006; Gil et al., 2006). The CDK inhibitors hinder the phosphorylation of RB1 by CDKs and thereby prevent the progress from G_1 to S phase. Dependent upon to the mechanism inducing the senescent phenotype, there are different proteins involved. Senescence can be determined using β-galactosidase (=β-gal) activity staining at pH 6 (Dimri et al., 1995). Cells are incubated over night with a staining solution containing X-Gal at pH 6. Cells, which develop a blue color that is visible under the light microscope, are considered senescent. The percentage of senescent cells can be determined when β-gal staining is combined with a DAPI counterstaining for total cell number.

The interplay between TP53 and CDKN1A plays an important role in the induction of senescence (for review see Vousden et al., 2002). TP53 is a nuclear protein and transcription factor that is a major regulator of cell fate. In a normal cell, the TP53 levels are very low, an increase of TP53 leads first to growth arrest and at higher expression levels to the induction of apoptosis (Harris et al., 2005; Laptenko et al., 2006). This decision is regulated by affinities of TP53 to its response elements (Szak et al., 2001; Aylon et al., 2007). TP53 levels are determined mainly over its rate of degradation. MDM2 ubiquitinates TP53, marking TP53 for degradation. Therefore, reduced MDM2 levels lead to an increase of TP53 (for review see Momand et al., 2000). One of the first genes activated after a TP53 increase is CDKN1A and increased level of this CDK inhibitor can lead to senescence. CDKN1A binds to CCNE-CDK2 complexes, which are thereby inactivated and cannot phosphorylate

RB1; consequently, progress to S phase is blocked. This cell cycle arrest is induced by the activation of the TP53-CDKN1A axis (El-Deiry et al., 1994; Wagner et al., 1994; Knudsen et al., 1997). CDKN1B has a similar, but somewhat broader function than CDKN1A. CDKN1B is transactivated by BRCA1 (Zhang et al., 1998). It can be phosphorylated at tyrosine residues and in its phosphorylated form it binds to CCND-CDKN4/6, which is thereby stabilized and can translocate into the nucleus (Kardinal et al., 2006). Free and unphosphorylated CDKN1B, which is exported back into the cytoplasm, is degraded by KPC (Kamura et al., 2004). The higher affinity of CDKN1B to CCND-CDK4/6 leads to more unbound and activated CCDE-CDK2, thereby promoting G_1/S transition (Polyak et al., 1994). Trimeric CCNE-CDK2 phosphorylates CDKN1B, which is thereby marked for degradation by SKP2 (Montagnoli et al., 1999). Elevated CDKN1B levels are able to induce a senescent phenotype (Alexander et al., 2001). After phosphorylation by a CDK, SCF complexes ubiquitinate CDKN1B leading to its proteasomal degradation (Pagano et al., 1995). SKP2 is part of the SCF^{SKP2} complex that degrades CDKN1B. Shin et al. showed in 2008 that downregulation of SKP2 by siRNAs was already sufficient to induce senescence in SK-OV-3 cells.

Since senescence can be induced by different cellular mechanism, there is no universal protein marker to detect senescence. Dimri et al. showed in 1995 that β-gal activity staining at pH6 is a potential, but not general marker for senescence.

β-galactosidase is a hydrolase, which is involved in the removal of galactose residues from glycoproteins, sphingolipids and keratan sulphates. The enzyme is localized in lysosomes and its activity is optimal at acid pH 3-5 and is species-, organ-, substrate- and buffer-dependent (Krishna et al., 1999)

Senescence-associated β-gal is lysosomal β-gal, which is active at pH 6 and represents probably the residual activity of the enzyme at sub-optimal pH in cells that have accumulated more enzymes because of increased lysosomal mass (Kurz et al., 2000; Krishna et al., 1999; Lee et al., 2006). Its activity at pH 6 might arise due to interconversion of the β-galactosidase enzyme (Kuo et al., 1978; Krishna et al., 1999). Lee et al. showed in 2006 that the levels of lysosomal β-gal protein increase during senescence around 4-fold in senescent cells. They could also show that

senescence-associated β-gal is expressed from the *GLB1* gene, which encodes for lysosomal β-D-galactosidase. Senescent cells, which have a defective *GLB1* gene, and senescent cells, where *GLB1* mRNA is suppressed by shRNAs show no β-gal activity at pH6. So senescence-associated β-gal activity originates from the *GBL1* gene, but it is not required for senescence.

Dimri et al. analyzed in 1995 cells from all three embryonic layers and could proof an increased β-gal activity in senescent cells. Proliferative cells also express β-gal, but this is only active at pH4 and not pH6. Quiescent and immortalized cells show also no β-gal activity at pH6. They found also two exceptions: adult melanocytes and sebaceous and eccrine gland cells showed also in proliferative cells a β-gal activity at pH, whereas senescence fibroblasts from two mouse strains showed no β-gal activity at pH6 (Dimri et al., 1995).

Therefore, it seems that there are three different kinds of cells:

- Cells, which show a β-gal activity at pH4 in the proliferative state and when they undergo senescence, β-gal activity at pH6 is detectable (Dimri et al., 1995; Chen et al., 2000; Lee et al., 2006).
- Cells, where β-gal is always active, independent of the pH. So here, the β-gal staining cannot be used as a marker for senescence (Dimri et al., 1995; Yang et al., 2005).
- Immortalized cells and cells with a defective *GBL1* gene show no β-gal activity (Lee et al., 2006).

Senescence-associated β-gal activity staining at pH 6 has been shown to be not a reliable marker for aging and in vitro studies (for review see Cristofalo, 2005), but it seems to be a reliable marker for senescence in cell culture. Exceptions are obvious, since either no staining or always staining is observed.

1.3 Smooth muscle cells (SMCs)

1.3.1 Origin of smooth muscle cells

The fertilized egg, the zygote, and the cells from the 8-cell-stage are totipotent, so they can differentiate into any cell type. The blastocyst (≈ 64 cells) can be divided into the trophectoderm, which will form the placenta and the extra-embryonic tissue, and the inner cell mass. During gastrulation the inner cell mass is divided into germ cells and the somatic cells. The somatic cells are composed of the three germ layers:
- the ectoderm, which will form neuronal and epidermal cells
- the mesoderm that differentiates into muscle and connective tissue and
- the endoderm, which will make gut epithelial cells.

The formation and development by which the three germ layers develop into the internal organs is called organogenesis. The circular system and heart undergo organogenesis early, since abundant oxygen must be delivered to every cell.

Vascular smooth muscle cells originate from various embryonic mesodermal progenitors (for review see Gittenberger-de Groot et al., 1999). Cells from the neurectoderm and from multiple mesodermal sources can differentiate into smooth muscle cells (Rosenquist et al., 1990). First layers of cells around the endothelial cell-lined tubes express SM α-actin and can transdifferentiate from the endothelium (DeRuiter et al., 1997). Whether this mechanism is more general or only specific for the dorsal aorta has not been studied yet.

Coronary SMCs originate from the epicardial lining (Glukhova et al., 1990). The complete coronary vasculature seems to originate from the epicardial lining and it has not been shown that the endothelial cells contribute to the SMC population by trans-differentiation (Glukhova et al., 1990; Dettman et al., 1998)

1.3.2 Structure and functions of smooth muscle cells

Smooth muscle cells have a characteristic form, which is elongated, thin and spindle-shaped. They are a type of non-striated muscle and surround hollow organs and the lumen of the body, such as blood vessels. Smooth muscle cells in blood vessels are generally arranged in sheets of bundles that are connected by gap junctions (Owens et al., 2004). They are usually 15-20 µm long and have an average diameter ranging from 5-8 µm (for review see Sinanan et al., 2006).

Smooth muscle contracts slower, but to a greater extent than skeletal muscle. The contraction of smooth muscle can normally not be controlled by will. The muscle can remain in the contracted state over a long time period without energy demand, fatigue or action potentials. Malfunctions and diseases of muscle cells are more present in smooth muscle cells than in skeletal muscle cells and a big issue is that smooth muscle cells do not regenerate as efficiently as skeletal muscle cells (for review see Sinanan et al., 2006).

1.3.3 Arterial and venous SMCs

Smooth muscle cells can be divided into the classes of vessels of which they were derived: arterial and venous smooth muscle cells. Arteries carry oxygen-rich blood from the heart to the rest of the body, whereas veins carry blood from the capillaries back to the heart. In this dissertation, human coronary artery smooth muscle cells and porcine venous smooth muscle cells have been used.

Both types of SMC are usually derived from the tunica intima and tunica media (see figure 10) of the artery or vein, respectively. Coronary artery SMCs are derived from human coronary arteries. They are often used for the investigations of coronary artery diseases since they are a good cellular model (Owens, 1996). Veins have in contrast to arteries valves in the larger veins. These valves prevent the backflow of the blood, since the heart pressure is not sufficient. Primary SMC cultures isolated from veins or arteries share many common features, like similarities in morphology

and responses to mitogens and chemo-attractants (Yang et al., 1998; Liu B et al., 2004).

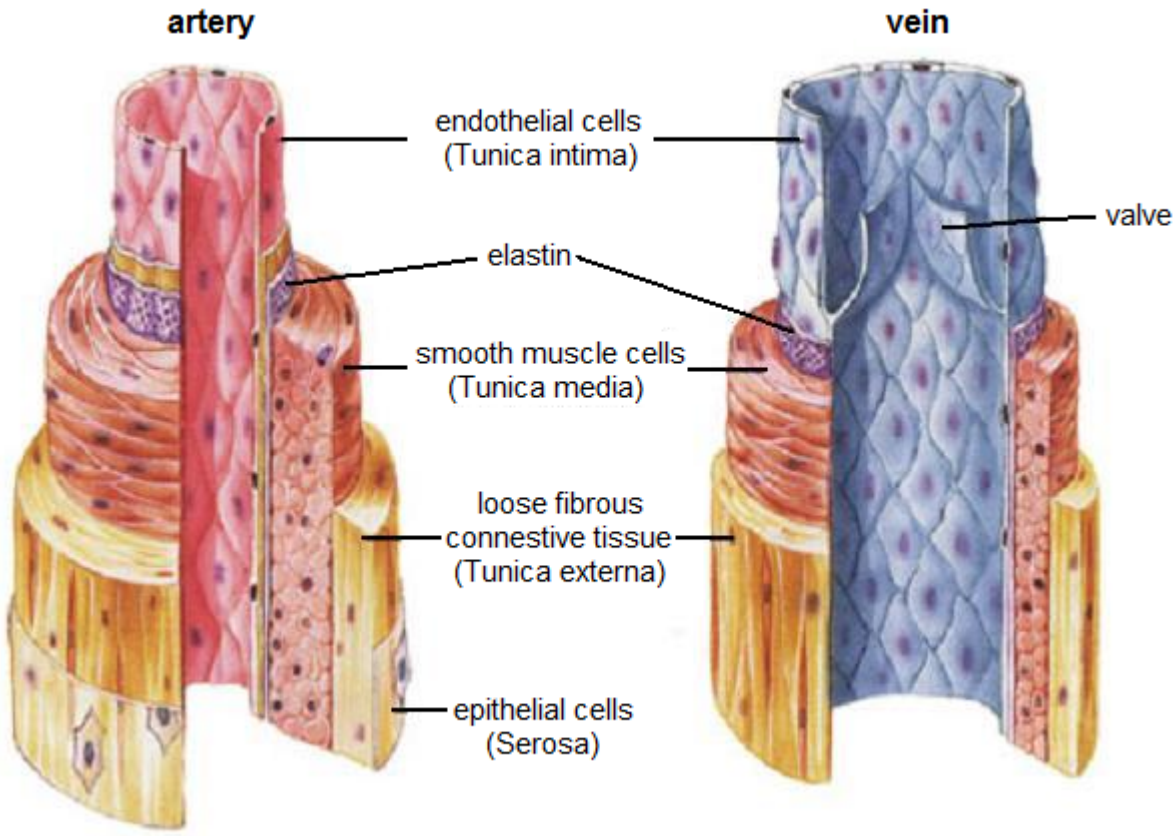

Figure 10 – Comparison of artery and vein (modified – Fox, 1993)

1.3.4 Contraction of smooth muscle cells

The specialty of smooth muscle cells is their ability to contract, which determines largely their function. Vascular SMCs contribute to the maintenance of blood pressure. In general, all SMCs serve to guide medium transport and by means of controlled contractions induce peristaltic movements (for review see Rensen, 2007). The contraction is caused by the sliding of myosin and actin filaments over each other. The energy that is required for this is provided by hydrolysis of ATP. Movement of the fibers along each other happens when heads on the myosin fibers form cross bridges with the actin fibers. These heads tilt and drag the actin fiber a small distance. The heads then release the actin fiber and adopt their original conformation. They can then rebind to another part of the actin molecule and drag it

along further. This process is called cross-bridge-cycling and is the same for all muscles (Reedy et al., 1965; Huxley et al., 1971). Myosin light chain kinase (MLCK) inhibition prevents cross-bridge-cycling, which leads to relaxation of the muscle. Vasodilators such as endothelium-derived relaxing factor or nitric oxide dilate blood vessels, because they stimulate the production of cAMP or cGMP, which then bind to MLCK and thereby inhibit MLCK (Huxley et al., 1954).

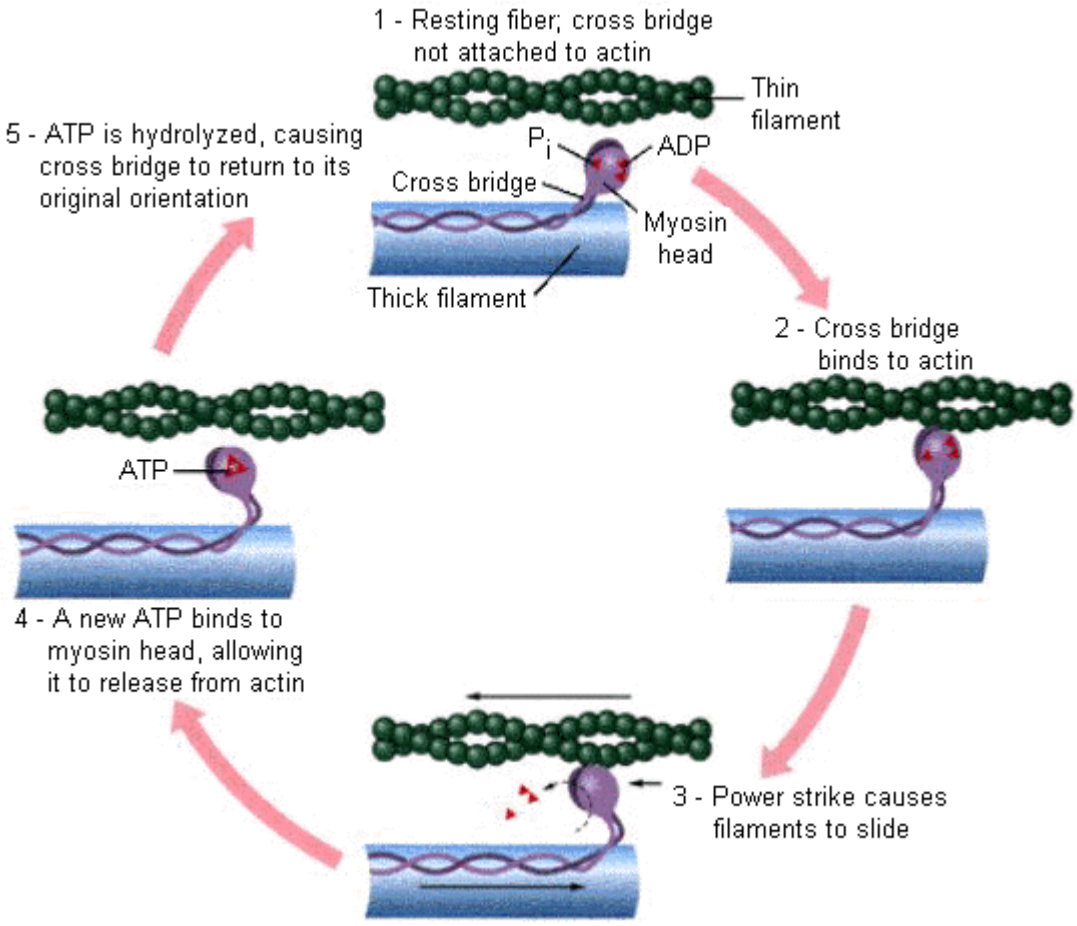

Figure 11 – Cross-bridge-cycling (modified Fox, 1993)

1.3.5 Phenotypic modulation

Smooth muscle cells can switch between a contractile and a synthetic phenotype. The capability of shuttling between these phenotypes is called phenotypic modulation. In the contractile phenotype, the cells are able to contract, which is not possible when the cells are in the synthetic phenotype. The differences are also visible in morphology and can be detected by expression levels of SMC marker genes, proliferative potential and migration properties (for review see Rensen et al., 2007).

Contractile SMCs have an elongated and spindle-shaped morphology, whereas synthetic SMCs are less elongated and have a cobblestone shape, which is referred to as epitheloid or rhomboid (Hao et al., 2003). Contractile SMCs contain thick myosin-containing filaments, whereas synthetic SMCs hold a high number of organelles involved in protein synthesis of secretory proteins (Chamley-Campbell et al., 1981). Synthetic SMCs have a higher migratory activity and exhibit higher growth rates than contractile SMCs (Hao et al., 2003). When SMCs are kept in culture, they tend to revert to the synthetic phenotype, but the extracellular matrix and medium supplements play also an important role for the phenotype (for review see Moiseeva, 2001). Fibronectin leads to a synthetic phenotype, whereas laminin promotes the switching into the contractile phenotype (Thyberg et al., 1997). Concentration gradients and alternatively spliced isoforms of SRF have specific effects on SMC gene transcription and consequently may contribute to SMC diversity (Belaguli et al., 1999).

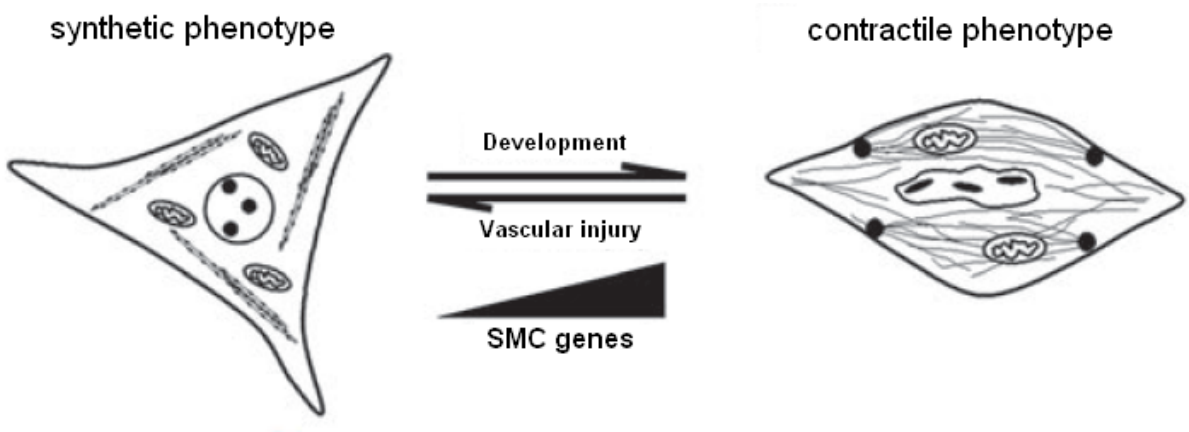

Figure 12 – Schematic model of phenotypic modulation (modified McDonald et al., 2006)

1.3.6 Malfunctions of SMCs

Malfunction of SMCs can lead to severe diseases. Atherosclerosis is a specific form of atheriosclerosis, which describes a hardening of an artery. It affects mainly arterial blood vessels and is a chronic inflammatory response in the walls of the arteries to the plaques within the arteries. Intimal smooth muscle proliferation plays a key event in the development of atherosclerosis. The vein that is implanted during bypass surgery is prone to atherosclerosis (Motwani et al., 1998). This might lead to restenosis. Restenosis means the re-occurrence of stenosis that usually occurs in an artery (Schwartz et al., 1992). It describes an abnormal narrowing in the blood vessel (Wagner et al., 1982).

These coronary artery diseases describe the limitation of blood flow to the heart muscle (=myocardium) (Mullany, 2003), which leads to buildup of deposits of cholesterol and other substances in the wall of the coronary arteries that transport the blood to the myocardium. These so-called plaques lead to reduction of blood supply in the myocardium and can therefore lead to a heart attack or chest pain (Mullany, 2003; American HA, 2004). A bypass surgery is then necessary to restore the blood circulation in the heart. During this heart operation blood vessels are used to “bypass” the clogged coronary arteries (American HA, 2004), which can provide the blood flow in the heart. The most commonly used blood vessel for this bypass are the Arteria thoracica interna (also called Arteria mammaria interna) or veins from the lower leg, for example the vena saphena magna.

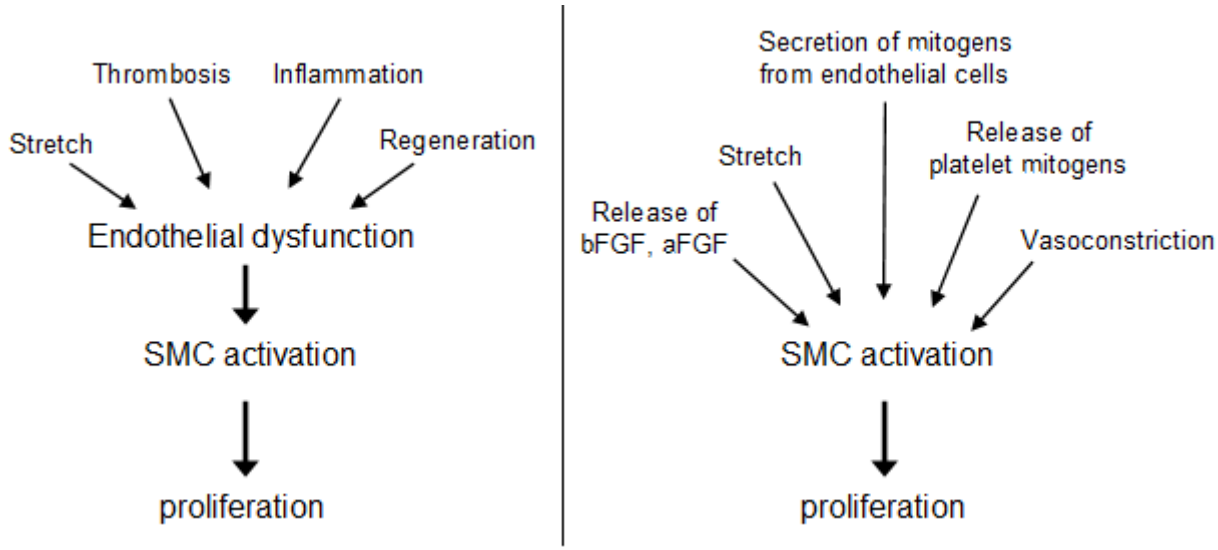

Figure 13 – Several mechanisms contribute to SMC proliferation after a bypass surgery (modified Casscells et al., 1994)

Walker et al. showed in 2009 that siRNA-mediated down-regulation of adhesion molecules in endothelial veins might be a useful approach to inhibit the initial leukocyte adhesion and transmigration of endothelial cells. A cocktail consisting of three siRNAs against three different endothelial adhesion molecules was very efficient in reduction of leukocyte attachment. This combined with an antiproliferative siRNA might be a useful approach to improve bypass compatibility.

Since there is a very high functional conservation between *Homo sapiens* to *Sus scrofa*, the pig is often used for bypass surgery and cardiologic studies. *Sus scrofa* is a well-known model for this, because the heart and all responses to stress, surgery or therapeutics are very similar to the ones observed in *Homo sapiens*.

1.4 RNA Interference

RNA Interference (RNAi) was discovered in *Caenorhabditis elegans* in 1998 by Fire and colleagues and it has become an important tool for cell and molecular biology, because RNAi can be used for specific inhibition of genes (Fire et al., 1998; Kreutzer, 2004). Long double-stranded RNAs (dsRNAs) are processed to short interfering RNAs (siRNAs), which target homologous mRNA for degradation. siRNAs are complementary nucleotide strands with a length of 21-23 nucleotides each strand that form a duplex (Tang, 2004). The advantage of this technique is that the siRNAs do not interact with the DNA itself, but rather interfere with the translation process of gene expression (Kreutzer, 2004).

Carmichael discussed in 2003 that long dsRNAs are frequently formed in eukaryotic cells, which are then transferred into the cytoplasm and are then able to trigger RNAi. A ribonuclease protein complex named DICER, which is part of the RNase III family of nucleases, cuts the dsRNA into siRNAs (Elbashir et al., 2001).

Since the discovery of RNA interference, many RNAi-related research tools have been developed and RNA interference has become a standard technology for loss-of-function approaches to analyze gene function.

1.4.1 Design of siRNAs

Chemically synthesized siRNAs can be designed for customized down-regulation of gene activity. Synthetic siRNAs are convenient to obtain and can be widely used. After transfection, siRNAs enter the RNA interference-induced silencing complex (=RISC), which then degrades complementary mRNA (see 1.4.3 Mechanism of RNA interference). The limitation of using siRNAs is the transient effect of silencing. Since mammalian cells do not have the mechanisms to amplify and propagate siRNAs, the downregulation is restricted by the rate of cell division. Therefore, it is not applicable for functional assays that need long-term read-out.

There are several methods to introduce siRNAs into mammalian cells, but not only the delivery but also many other factors determine the strength and duration of the silencing response: potency of siRNAs and protein half-life time, overall efficiency of transfection and confluency of cells.

The characteristics of the siRNA, especially the thermodynamic properties, are an important issue for the efficiency. An efficient siRNA shows mostly a low internal stability of the sense 3'-end, which is possibly involved in duplex unwinding and strand retention by RISC (Khvorova et al., 2003; Reynolds et al., 2004). The concentration of delivered siRNAs is another factor. A relatively inefficient siRNA can also silence its target mRNA when large amounts are delivered, but this high concentration will probably lead to numerous undesired side effects (Semizarov et al., 2003). Very long dsRNAs, which are known to trigger an interferon response or activate RNA-dependent protein kinases, can lead to non-sequence specific effects or even to apoptosis (Samuel, 2003; Agrawal, 2004). Some siRNAs might also activate toll-like receptors, which can lead to immune responses particularly in antigen-presenting cells (Heidel, 2004).

1.4.2 Transfection of siRNAs

Transfection is defined as the introduction of nucleic acids into cells by non-viral methods. The techniques can be divided into either physical methods, for example electroporation and direct microinjection, or chemical methods, which utilize reagents like DEAE-dextran, Calcium phosphate or artificial liposomes. In this dissertation Cellfectin® was chosen, which belongs to the class of artificial liposomes. It is a 1:1.5 (M/M) liposome formulation of the cationic lipid N, N^{I}, N^{II}, N^{III}-tetramethyl-N, N^{I}, N^{II}, N^{III}-tetrapalmityl-spermine (TM-TPS) and the neutral lipid dioleoyl phosphatidyl-ethanolamine (DOPE) in membrane-filtered water.

The cationic lipid component TM-TPS shows at physiological pH an overall net positive charge. Thereby, it associates with the negatively charged nucleic acids, which leads the compaction of the nucleic acid in a liposome / nucleic acid complex. DOPE is the neutral lipid component in this mixture and it is considered as a

“fusogenic” lipid (Felgner et al., 1994), since it is required to build the lipoplex, which encloses the siRNAs.

The uptake of the complex into the cell may occur by endocytosis or fusion with the plasma membrane via the lipid moieties of the liposome (for review see Gao et al., 1995). The complexes then are often trapped in endosomes and lysosomes after entering the cell. DOPE facilitates the endosomal disruption (Farhood et al., 1995), which sets free the complexes and the nucleic acids can enter the RNAi machinery.

1.4.3 Mechanism of RNA interference

After entering the cytoplasm, the siRNA enters the RISC, which then leads to the degradation of mRNAs with sequence complementary to the antisense strand of the siRNA (Kreutzer 2004, Carmichael, 2003).

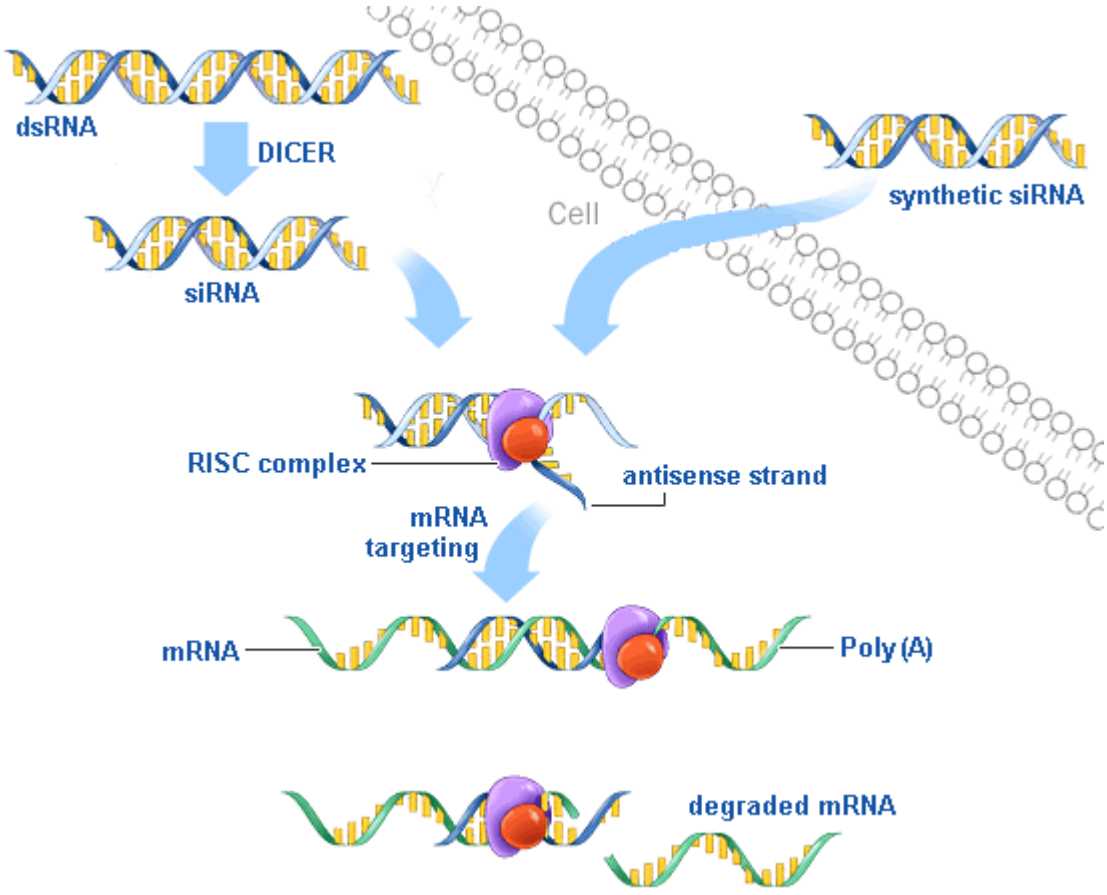

Figure 14 – Basic steps of RNAi (modified, Ting et al., 2005)

1) Initiation of RNA interference
   The dsRNAs are cleaved into siRNAs by Dicer, an RNase III enzyme. Dicer digests dsRNAs into siRNAs with a 3'-overhang of 2 to 3 nucleotides, presenting 5'-phosphate and 3'-hydroxyl termini (Elbashir et al., 2001).

2) Assembly of siRNA with the RNA-induced silencing complex (RISC)
   An ATP-dependent helicase, which is part of the RISC, unwinds the siRNAs (Zhang et al., 2002). The assembly itself is not ATP-dependent (Nykänen et al., 2001). The separation of the strands is called activation of RISC (Reynolds, 2004) and the incorporated strand is used to identify complementary mRNA sequences (Rossi, 2004).

3) Target cleavage
   When the RISC recognizes a complementary mRNA, the mRNA is cleaved exactly ten nucleotides upstream of the nucleotide paired with the 5' end of the guide siRNA strand (Rossi, 2004). The cellular enzyme Ago2, which does not require ATP, cleaves the mRNA (Liu J et al., 2004). Therefore, translation is prevented and no protein can be synthesized (Tang, 2004; Rossi, 2004).

1.4.4 Applications for siRNAs

Applications for siRNAs in medicine are unlimited, since all cells have the ability to use the RNAi machinery. Therefore, all genes can be potential targets for therapeutic approaches. Song et al. demonstrated in 2003 the therapeutic usage of siRNAs against hepatitis in a mouse model and the FDA approved first clinical trials using RNAi in 2004. There are several successful studies regarding siRNA usage in very different fields: Landen et al. showed in 2005 that siRNAs against *EphA2* drastically reduced ovarian tumors. The progress of Huntington's disease was halted after treatment with siRNAs (Diaz-Hernandez et al., 2005). An siRNA that targets VEGF and is directly injected into the eye is already in Phase II of clinical trials. It improves vision of retinae suffering from age-related macular degeneration (Tolentino et al., 2004).

2 Aims of this work

About 20 % of bypasses develop restenosis a few days after the surgery, due to stress. Restenosis is caused by increased proliferation of vascular smooth muscle cells. The function of *SRF* in cellular proliferation has been discussed extensively and controversially. However, *SRF* does seem to play a key role in proliferation.

Experiments of a former PhD student, Dr. Daniela Werth, showed that down-regulation of SRF in human SMCs led to an inhibition of proliferation and block in cell cycle. BrdU stainings showed an increase in G_1 cells and reduced number in S phase after *SRF* depletion. Senescence could be shown by β-gal activity stainings.

Based on these results, the aim of this work was to characterize the role of *SRF* in cellular proliferation in human and porcine SMCs. Analyses of cell cycle genes and genes, which are known to induce senescence, should define which genes are important for the siSRF797-triggered senescence.

Sus scrofa is a standard model for bypass surgery and cardiac approaches. Therefore, the antiproliferative effect of *SRF* can be tested in vivo and might show a diminished risk of restenosis.

3 Materials

3.1 Chemicals and reagents

1st antibody: mouse-α-GAPDH	HyTest Ltd. (Turku, Finland); Cat. 5G4; Lot: 03/02 – G4 – C5 diluted 1 : 20,000
1st antibody: mouse-α-hs Retinoblastoma protein 1	BD Pharmingen (Erembodegem, Belgium); Cat. 554136, Lot: 66458 diluted 1 : 1,000
1st antibody: mouse-α-hs-p21: monoclonal	Oncogene Science, Bayer HealthCare LLC (Cambridge, USA); Cat. OP64-100µg; Lot: D16013-9 diluted 1 : 1,000
1st antibody: mouse-α-hs-underphosphory-lated Retinoblastoma protein 1,	BD Pharmingen (Erembodegem, Belgium); Cat. 554164, Lot: 0000045180 diluted 1 : 1,000
1st antibody: mouse-α-tubulin Ab-4 (Cocktail)	Neomarkers (Fremont, USA); Cat. MS-719-PO; Lot: 719P307 dilution 1 : 10,000
1st antibody: mouse-α-p53	Santa Cruz Biotechnology, Inc. (Santa Cruz, USA); Cat. sc-263 dilution 1 : 1,000
1st antibody: rabbit-α-p21/WAP (C-19)	Santa Cruz Biotechnology, Inc. (Santa Cruz, USA); Cat. sc-397 dilution 1 : 1,000
1st antibody: rabbit-α-p27Kip (C-19)	Santa Cruz Biotechnology, Inc. (Santa Cruz, USA); Cat. sc-528; Lot: E1906 dilution 1 : 1,000
1st antibody: rabbit-α-SRF (G-20)	Santa Cruz Biotechnology, Inc. (Santa Cruz, USA); Cat. sc- 335; Lot: L015 dilution 1 : 1,000

2nd antibody: α-mouse IgG, HRP linked	Amersham Pharmacia Biotech (Buckinghamshire, England); Cat. NA 931; Lot: 348867 dilution 1 : 10,000
2nd antibody: α-rabbit IgG, HRP linked	Amersham Pharmacia Biotech (Buckinghamshire, England); Cat. NA 934; Lot: 340346 dilution 1 : 10,000
ABgene buffer IV with 15 mM $MgCl_2$	ABgene (Hamburg, Germany)
AbiPrism Template Suppression Reagent	PE Applied Biosystems (Foster City, USA)
Acetic acid	AppliChem (Darmstadt, Germany)
Acetone	Merck KGaA (Darmstadt, Germany)
Agarose	Gibco / Invitrogen (Paisley, Scotland)
Ammonium peroxodisulfate (APS)	Merck KGaA (Darmstadt, Germany)
BigDye Terminator v1.1 RR Mix	PE Applied Biosystems (Foster City, USA)
Boric acid	AppliChem (Darmstadt, Germany)
Bromphenole-blue	AppliChem (Darmstadt, Germany)
Calcium chloride dihydrate	Merck KGaA (Darmstadt, Germany)
Cellfectin	Invitrogen (Carlsbad, USA)
Chaps	AppliChem (Darmstadt, Germany)
Collagenase Type I	Sigma Aldrich Chemie GmbH (Steinheim, Germany); Cat. C0130
D-Glucose	AppliChem (Darmstadt, Germany)
DAPI (4',6-diamidino-2-phenylindole)	AppliChem (Darmstadt, Germany)
N,N-Dimethylformamide	Sigma Aldrich Chemie GmbH (Steinheim, Germany)
Dimethyl sulfoxide	AppliChem (Darmstadt, Germany)
Dithiothreitol (DTT)	AppliChem (Darmstadt, Germany)
dNTPs	Promega GmbH (Mannheim, Germany)
Dumont #7, Standard tip, curved, 0.17mm x 0.1mm, Inox, 11 cm	Fine Science Tools (Heidelberg, Germany)
EDTA (ethylenediaminetetraacetic acid)	AppliChem (Darmstadt, Germany)
Ethanol p.a.	Merck KGaA (Darmstadt, Germany)
Ethidium bromide	AppliChem (Darmstadt, Germany)

FBS (Fetal bovine serum)	Gibco / Invitrogen (Paisley, Scotland)
Feeding needles: Gauge 16, length 75mm, tip diameter 3.00 mm, curved	Fine Science Tools (Heidelberg, Germany)
Feeding needles: Gauge 18, length 50mm, tip diameter 2.25 mm, curved	Fine Science Tools (Heidelberg, Germany)
Forceps Semken, length 13 cm, curved	Fine Science Tools (Heidelberg, Germany)
Formaldehyde (37 %)	Roth GmbH (Karlsruhe, Germany)
Gelatin from porcine skin, Type A	Sigma Aldrich Chemie GmbH (Steinheim, Germany)
Gentamycin	AppliChem (Darmstadt, Germany)
Glutaraldehyde (50 %)	Sigma Aldrich Chemie GmbH (Steinheim, Germany)
Glycerol 87 %	AppliChem (Darmstadt, Germany)
Glycerol p.a.	Merck KGaA (Darmstadt, Germany)
Halsted-Mosquito, curved, length 12.5 cm	Fine Science Tools (Heidelberg, Germany)
Human CASMCs	PromoCell (Heidelberg, Germany); Cat. C12511; Lot: 5060807.6
Hams F-12 Medium	Invitrogen (Carlsbad, USA); Cat. 21765; Lot: 388374
Immobilon Western Chemiluminescent HRP Substrate	Millipore Corp. (Chelmsford, USA); Cat. WBKLS0100
i-Propanol – extra pure –	Merck KGaA (Darmstadt, Germany)
Magnesium chloride hexahydrate	Merck KGaA (Darmstadt, Germany)
β-Mercaptoethanol	AppliChem (Darmstadt, Germany)
Methanol p.a.	Merck KGaA (Darmstadt, Germany)
Micro Serrefine, light bend, 26 mm	Fine Science Tools (Heidelberg, Germany)
Minipräp Kit	Qiagen (Hilden, Germany)
M-MLV RT 5x buffer	Promega GmbH (Mannheim, Germany)
M-MLV RT, RNase H(-) Point Mutant	Promega GmbH (Mannheim, Germany)
MOWIOL	Merck KGaA (Darmstadt, Germany)
Nonfat dried milk powder	AppliChem (Darmstadt, Germany)
Polyacrylamide (40 %) - Mix 19:1	AppliChem (Darmstadt, Germany)

PageRuler Prestained Protein Ladder	Fermentas GmbH (St. Leon-Rot, Germany); Cat. SM0671; Lot: 00012835
PBS (Phosphate-buffered saline)	Gibco / Invitrogen (Paisley, Scotland); Cat. H15-002; Lot: H00206-1021
Potassium chloride	AppliChem (Darmstadt, Germany)
Potassium hexacyanoferrate (III)	Merck KGaA (Darmstadt, Germany)
Potassium hexacyanoferrate (II) trihydrate	Merck KGaA (Darmstadt, Germany)
mono-potassium phosphate	AppliChem (Darmstadt, Germany)
n-propyl gallate	Sigma Aldrich Chemie GmbH (Steinheim, Germany)
Protein Assay Reagent	Bio-Rad Laboratories GmbH (Munich, Germany)
Purified BSA 100x, 10 mg/ml	New England Biolabs Inc. (Ipswich, USA)
QIAquick Gel extraction Kit	Qiagen (Hilden, Germany)
Random Hexamers	Purimex (Grebenstein, Germany)
Ribonuclease Inhibitor	Fermentas GmbH (St. Leon-Rot, Germany)
RNase A	Roche Diagnostics GmbH (Mannheim, Germany)
RNeasy Kit	Qiagen (Hilden, Germany)
RPMI 1640 medium (+GlutaMAX + 25mM HEPES)	Gibco / Invitrogen (Paisley, Scotland); Cat. 72400; Lot: 14179
Senescence β-Galactosidase Staining Kit	Cell Signaling Technology, Inc. (Danvers, USA)
SMC Basal medium	PromoCell (Heidelberg, Germany); Cat. C-22262; Lot: 6110702
Sodium acetate trihydrate	AppliChem (Darmstadt, Germany)
Sodium acid	AppliChem (Darmstadt, Germany)
Sodium chloride	Sigma Aldrich Chemie GmbH (Steinheim, Germany)
tri-sodium-citrate-dihydrate	AppliChem (Darmstadt, Germany)
Sodium dihydrogen phoshphate monohydrate	Merck KGaA (Darmstadt, Germany)
Sodium dodecyl sulfate (SDS)	AppliChem (Darmstadt, Germany)
Sodium hydrogen carbonate	Merck KGaA (Darmstadt, Germany)
Sodium hydroxide	AppliChem (Darmstadt, Germany)

Surgical scissors, standard pattern, 12 cm	Fine Science Tools (Heidelberg, Germany)
SybrGreen – PCR Core Reagent	PE Applied Biosystems (Foster City, USA)
TaqPolymerase	ABgene (Hamburg, Germany)
Tetramethylethylenediamine (TEMED)	AppliChem (Darmstadt, Germany)
Trichloroacetic acid	AppliChem (Darmstadt, Germany)
Trizma base, minimum 99,9 % titration	Sigma Aldrich Chemie GmbH (Steinheim, Germany)
Trypsin-EDTA (1x)	Gibco / Invitrogen (Paisley, Scotland)
Tryptone	AppliChem (Darmstadt, Germany)
Tween 20	AppliChem (Darmstadt, Germany)
Urea	AppliChem (Darmstadt, Germany)
Waymouth Medium	Invitrogen (Carlsbad, USA); Cat. 31220; Lot: 9165
X-Gal	AppliChem (Darmstadt, Germany)

3.2 Consumable material

2.0 ml Cryogenic vial	Corning Inc. (New York, USA)
CEA RP new radiography films	CEA AB (Strängnäs, Sweden)
Clear seal diamont sheets for TaqMan plates	ABgene (Hamburg, Germany)
Conical tubes - 15 ml	Becton Dickinson (LePont De Claix, France)
Conical tubes - 50 ml	Becton Dickinson (LePont De Claix, France)
Cover slips, round - 12 mm diameter	Roth GmbH (Karlsruhe, Germany)
Disposable cuvettes - 1.5 ml semi-micro	Brand GmbH (Wertheim, Germany)
Gel blotting paper	Schleicher & Schuell (Dossel, Germany)
Glas pipettes - 1 ml, 2 ml, 5 ml, 10 ml, 25 ml, 50 ml	Hirschmann Laborgeräte (Eberstadt, Germany)
Immobilon-P Transfer Membrane	Millipore Corporation (Chelmsford, USA)
Microscope slides -SuperFrost-76x26 mm	Roth GmbH (Karlsruhe, Germany)
Pipet tips	Eppendorf AG (Hamburg, Germany)
Precision cuvettes	Hellma (Müllheim, Germany)
TaqMan plates	ABgene (Hamburg, Germany)
Tissue culture dish, 100x20mm style	Becton Dickinson (LePont De Claix, France)
Tissue culture plate, 6 well, flat bottom with low evaporation lid	Becton Dickinson (LePont De Claix, France)
Toppits – transparent film	Melitta Haushaltsprodukte GmbH & Co. KG (Minden, Germany)
Tubes - 0.5 ml, 1 ml, 1.5 ml, 2 ml	Eppendorf AG (Hamburg, Germany)

3.3 Buffers and stock solutions

Fixative Solution	2 % formaldehyde 0.2 % glutaraldehyde PBS
Freezing medium	40 % SMC medium 40 % FBS 20 % DMSO
Mowiol	5 % Mowiol in PBS – stir over night add 25 % glycerol – stir over night centrifuge at 4000 rpm for 15 minutes add a spatula tip n-propyl gallate to supernatant centrifuge again for 15 minutes at 4000 rpm aliquot supernatant and store at -20 °C
2x protein loading buffer	125 mM Tris (pH 7.5) 2.5 % SDS 0.1 % bromphenol blue 20 % glycerol 5 % β-mercaptoethanol
6x protein loading buffer	300 mM Tris (pH 6.8) 600 mM β-mercaptoethanol 6 % SDS 60 % glycerol spatula tip of bromphenol blue
RNA Hybridization buffer	25 mM Tris (pH 7.5) 100 mM NaCl

10x SDS-PAGE buffer	0.25 M Tris (pH 7.5) 15 % glycerol for 1x, add 0.1 % SDS
Separation gel (5-15 %)	0.5 M Tris (pH 8.8) 5-15 % acrylamide (40 %) 0.1 % SDS 0.07 % APS 0.01 % TEMED
SMC medium	15 % FBS 28.3 % SMC basal medium 28.3 % Waymouth medium 28.3 % F-12
Solution A	137 mM NaCl 5.4 mM KCl 4.2 mM $NaHCO_3$ 5 mM D-Glucose
Stacking gel	0.25 M Tris (pH 6.8) 5 % acrylamide 0.1 % SDS 0.07 % APS 0.01 % TEMED
Staining Solution ready	Staining Solution 5 mM $K_4[Fe(CN)_6]$ 5 mM $K_3[Fe(CN)_6]$ 1 g/l X-Gal (20 g/l in DMF)

Staining Solution for β-galactosidase activity staining

Staining Solution 1	Staining Solution 2
40 mM $Na_3C_6H_5O_7 \cdot 2H_2O$	40 mM $NaH_2PO_4 \cdot H_2O$
150 mM NaCl	150 mM NaCl
2 mM $MgCl_2 \cdot 6H_2O$	2 mM $MgCl_2 \cdot 6H_2O$

→ mix Staining Solutions 1 and 2 until pH6

Stripping buffer	62.5 mM Tris (pH 6.7) 2 % SDS 0.7 % β-mercaptoethanol H_2O
50xTAE buffer	2 M Tris 50 mM EDTA 1 M acetic acid adjust to pH 8.5
10xTBE buffer	1 M Tris 1 M boric acid 20 mM EDTA
Transfection medium	50 % Hams F-12 medium 50 % Waymouth medium
10 x Transfer buffer	0.25 M Tris (pH 7.5) 15 % glycerol
10xTST	100 mM Tris (pH 7.5) 1 M NaCl 1 % Tween20 10 mM EDTA (pH 8)
Urea buffer	9 M urea 4 % CHAPS 1 % DTT

3.4 Laboratory equipment and technical devices

Abi Prism, 310 Genetic Analyzer	Applied Biosystems (Weiterstadt, Germany)
Abi Prism, 7000 Sequence Detection System	Applied Biosystems (Weiterstadt, Germany)
Biofuge pico	Heraeus Instruments (Langenselbold, Germany)
Centrifuge 5417 C	Eppendorf AG (Hamburg, Germany)
Centrifuge Super T 21	Sorvall Products, L.P. (Newtown, USA)
DNA Speed Vac, DNA110	Savant Instruments (Holbrook, USA)
Easy Cast Electrophoresis System	Owl Scientific, Inc. (Woburn, USA)
Freezer: UF80-450 S	Colora Messtechnik GmbH (Lorch, Germany)
GeneAmp PCR System 9700	Applied Biosystems (Weiterstadt, Germany)
Heating plate with magnetic stirring MR 3001	Heidolph (Kelkheim, Germany)
Incubator CB 150	Binder GmbH (Tuttlingen, Germany)
Innova 4230	New Brunswick Scientific (Edison, USA)
Microscope	Zeiss (Oberkochen, Germany)
Milli-Q, Biocel	Millipore (Schwalbach, Germany)
Mini Trans-Blot System	Bio-Rad Laboratories (Hercules, USA)
Mini-PROTEAN 3 System	Bio-Rad Laboratories (Hercules, USA)
Neubauer Improved, Depth 0.100 mm, 0.0025 mm^2	Brand GmbH (Wertheim, Germany)
Personal densitometer SI	Molecular Dynamics (Sunnyvale, USA)
Pipet boy: pipetus akku	Hirschmann Laborgeräte (Eberstadt, Germany)
Rotator	GFL (Burgwedel, Germany)
Tecnoflow 3F120 - II GS	Integra Biosciences (Fernwald, Germany)
Thermomixer 5436	Eppendorf AG (Hamburg, Germany)
Thermomixer comfort	Eppendorf AG (Hamburg, Germany)
Ultrospec 3000 UV/Visible Spectrophotometer	Amersham Pharmacia Biotech (Buckinghamshire, England)
Vortex genie 2	Scientific Industries, Inc. (Bohemia, USA)

3.5 Oligonucleotides

All oligonucleotides listed here were ordered from Purimex (Grebenstein, Germany).

3.5.1 Primers for real-time RT-PCR

Primers for human samples

hsACTA2

hsACTA2-fw	5’ – CCT TGG TGT GTG ACA ATG GC – 3’
hsACTA2-rev	5’ – AAA CAG CCC TGG GAG CAT C – 3’

hsCDKN1A

hsCDKN1A-fw	5’ – TGG AGA CTC TCA GGG TCG AAA – 3’
hsCDKN1A-rev	5’ – CGG CGT TTG GAG TGG TAG AA – 3’

hsCDKN1B

hsCDKN1B-fw	5’ – GGC TCG CCT CTT CCA TGT – 3’
hsCDKN1B-rev	5’ – CGG TGG ACC ACG AAG AGT TAA – 3’

hsCNN1

hsCNN1-fw	5’ – GGA CAC ACG CGG TTT GGT – 3’
hsCNN1-rev	5’ – GCT CTC ATT ACA AAC GCC ACT G – 3’

hsGAPDH

hsGAPDH-fw	5’ – GAA GGT GAA GGT CGG AGT C – 3’
hsGAPDH-rev	5’ – GAA GAT GGT GAT GGG ATT TC – 3’

hsSKP2

hsSKP2-fw	5’ – ATG GAC CAA CCA TTG GCT GA – 3’
hsSKP2-rev	5’ – GAC AGT ATG CCG TGG AGG GT – 3’

hsSRF

hsSRF-fw	5’ – TTG CCA CCC GAA AAC TGC – 3’
hsSRF-rev	5’ – AGA GTC TGG CGA GTT GAG GC – 3’

hsTAGLN

hsTAGLN-fw	5’ – CGT GGA GAT CCC AAC TGG TT – 3’
hsTAGLN-rev	5’ – TGC AGC TGG CTC TCT GTG AA – 3’

hsTP53

hsTP53-fw	5’ – CAC CCT TCA GAT CCG TGG G – 3’
hsTP53-rev	5’ – TGA GTT CCA AGG CCT CAT TCA – 3’

Primers for porcine samples:

ssACTA2 (same as hsACTA2)

ssACTA2-fw	5’ – CCT TGG TGT GTG ACA ATG GC – 3’
ssACTA2-rev	5’ – AAA CAG CCC TGG GAG CAT C – 3’

ssCNN1 (same as hsCNN1)

ssCNN1-fw	5’ – GGA CAC ACG CGG TTT GGT – 3’
ssCNN1-rev	5’ – GCT CTC ATT ACA AAC GCC ACT G – 3’

ssGAPDH

ssGAPDH-fw	5’ – GGG TCA TCA TCT CTG CCC CT – 3’
ssGAPDH-rev	5’ – CTC ATG GTT CAC GCC CAT C – 3’

ssSRF (same as hsSRF)

ssSRF-fw	5’ – TTG CCA CCC GAA AAC TGC – 3’
ssSRF-rev	5’ – AGA GTC TGG CGA GTT GAG GC – 3’

ssTAGLN (same as hsTAGLN)

ssTAGLN-fw	5’ – CGT GGA GAT CCC AAC TGG TT – 3’
ssTAGLN-rev	5’ – TGC AGC TGG CTC TCT GTG AA – 3’

3.5.2 Primer for RT-PCR and sequencing

Forward primer

PS4	5’ – GAT TCC TCG CTG ACT GCC C – 3’
FSq2-2	5’ – TGA GCG CCA TGT TAC CGA G – 3’
FSeq3	5’ – AGC CTG AGC GAG ATG GAG CT – 3’
Seq fw	5’ – TTC ATC GAC AAC AAG CTG CG – 3’
TM fw	5’ – TTG CCA CCC GAA AAC TGC – 3’

Reverse primer

Seq rev	5’ – GCC CAT TTC TTT GGC TGG A – 3’
TM rev	5’ – AGA GTC TGG CGA GTT GAG GC – 3’
SeqFrv	5’ – CGC AGC TTG TTG TCG ATG AA – 3’
Seq 8	5’ – AAT AAG TGG TGC CGT CCC TTG – 3’

3.5.3 siRNAs

siCDKN1B

siCDKN1B – sense	5’ – GGA GCA AUG CGC AGG AAU AUU – 3’
siCDKN1B – antisense	5’ – UAU UCC UGC GCA UUG CUC CUU – 3’

siGL2

siGL2 – sense	5’ – CGU ACG CGG AAU ACU UCG AdTdT – 3’
siGL2 – antisense	5’ – UCG AAG UAU UCC GCG UAC GdTdT – 3’

siSKP2

siSKP2 – sense	5’ – UCU UAG CGG CUA CAG AAA GdTdT – 3’
siSKP2 – antisense	5’ – CUU UCU GUA GCC GCU AAG AdTdT – 3’

siSRF797

siSRF797 – sense	5’ – GAU GGA GUU CAU CGA CAA CAA – 3’
siSRF797 – antisense	5’ – GUU GUC GAU GAA CUC CAU CUU – 3’

siSRF820

siSRF820 – sense	5’ – GCU GCG GCG CUA CAC GAC CdTdT – 3’
siSRF820 – antisense	5’ – GGU CGU GUA GCG CCG CAG CdTdT – 3’

3.6 Cells

human CASMCs	Cambrex (Verviers, Belgium) Lot: 3F0246
human CASMCs	PromoCell GmbH (Heidelberg, Germany) Cat. C-12511; Lot: 5060807.6
2-3 cm long piece of a porcine vein (Vena Saphena)	Courtesy of Dr. Wendel; THG surgery; University of Tuebingen (Tuebingen, Germany)

4 Methods

4.1 Cell culture

4.1.1 Isolation of primary porcine SMCs

A 2-3 cm long piece of a vein was incubated for 20 minutes in RPMI 1640 medium, which contained 0.5 % Gentamycin. Then the outside of the vein was wiped off with 70 % ethanol. The vein was rinsed twice with 25 ml Solution A and then with 5 ml of 1 % collagenase in PBS. Then the vein was filled with 1 % collagenase in PBS. To humidify the outside, it was covered with a few ml SMC medium followed by incubation at 37 °C and 5 % CO_2 for 2 hours. After incubation, the vein was opened and the eluate was collected in a 15 ml Falcon tube. It was rinsed with 10 ml PBS, which was merged with the first eluate. This suspension was centrifuged for 5 minutes at 220 g and the supernatant was discarded. The pellet was resuspended in 500 µl SMC medium, which was added into a well that already contained 2 ml of pre-warmed medium. The cells were incubated at 37 °C and 5 % CO_2 over night and are rinsed the next day with 2 ml SMC medium.

4.1.2 Thawing and freezing of cells

Frozen cells were thawed and resuspended in 10 ml SMC medium and brought into a 10-cm dish. The cells were then cultured in Petri dishes with SMC medium and split when the confluence has reached about 80 %.

The freezing procedure was to trypsinize the cells, and mix 0.5 ml cell suspension with 0.5 ml freezing medium. The cryo vials have then been put into an isopropanol cooling device and after 2 days in a -80 °C freezer, they were put into liquid nitrogen for long-time storage.

4.1.3 siRNA hybridization

The siRNA strands were diluted with RNA hybridization buffer to the designated concentration (20µM). To hybridize siRNAs, the siRNA solution was heated up to 95 °C in a heating block and switched then to 37 °C. It was let cooled down slowly to 37 °C and then to room temperature. Stock solutions have been stored at -20 °C.

4.1.4 Transfection

The lipofection of cells with siRNAs is a technique that is used for transient transfections. The siRNAs are brought into the cell, enter there the RISC, and induce therefore a downregulation of the target protein. Two cover slips were put into a 10 cm dish, which was then coated with 0.2 % gelatin (for 30 minutes at room temperature). Cells were seeded with a density of $5x10^5$ cells into a 10 cm dish and let adhere for 24 hours. The transfection was performed with Cellfectin®.

For each transfection, 70 µl Cellfectin® were diluted 1:8 in TF medium. 113.7 µl siRNA with a concentration of 20 µM were diluted with TF medium to a concentration of 4 µM. The diluted Cellfectin® and siRNA solutions were then mixed and incubated for 20 minutes at room temperature. During this time liposome-siRNA-complexes were formed. The supernatant of the cells was removed and the cells were washed with PBS. 4 ml TF medium was added to the cells and then the Transfection mixture was applied to the cells. The incubation time was 5 hours at 37 °C and 5 % CO_2. The supernatant was then replaced by SMC medium.

4.1.5 Harvest of cells

Three days after transfection, the cover slips were removed before the harvest to use these for stainings. The other cells were trypsinized; the enzymes were stopped by addition of SMC medium and centrifuged. The pellet was then resuspended in PBS, again centrifuged and then the cell pellet was lysed in 600 µl RLT buffer. The cell lysates were prepared due to the manufacturer's protocol for RNeasy Mini Prep Kit – Protocol using a microcentrifuge. The flow-through of the first passage through the RNeasy mini spin column (Step 4 in manufacturer's protocol) was used for protein precipitation with acetone. 2 volumes of acetone were added to 1 volume of flow-through and were incubated over night at -80 °C. The protein purification and determination are explained in 4.2.1 Protein determination.

4.1.6 Senescence β-galactosidase activity staining

The cover slips that were removed before harvest of the other cells were put in a 24-well plate to perform a senescence-associated β-gal activity staining at pH 6 (Dimri et al., 1995) (see also 1.2.4 Senescence). The cells were washed twice with PBS and then fixed with Fixative Solution for 10 minutes at room temperature. After fixation,

the cells were again washed twice with PBS and 500 µl of Staining Solution mix was put onto the cover slips. The plate was then incubated at 37 °C over night. The next day cells were washed twice with PBS and then stained for 30 minutes with DAPI (2 µg/ml in PBS) in the dark. After another washing step with PBS, the cover slips were dried and the mounted with Mowiol. Cells that showed a β-gal activity at pH6 developed a blue color, which was seen in the Brightfield channel. Non-senescent cells show a very light blue background staining. Senescent cells develop a dark blue color. Intensities between were scored as non-senescent.

4.2 Protein analysis

4.2.1 Protein determination

The precipitated proteins were centrifuged for 30 min at 14,000 rpm at 4 °C. The supernatant was discarded and the pellet was resuspended in 50 µl Urea buffer. The used Protein Assay is based on the method of Bradford for determination of protein concentrations. It uses the color shift from 465 nm to 595 nm, when the Protein Assay Reagent dye binds to proteins. Standards with the concentrations 2 µg/µl, 4 µg/µl, 6 µg/µl, 8 µg/µl and 10 µg/µl BSA were prepared and the absorbance was measured using the Ultrospec 3000 UV/Visible Spectrophotometer. These data points were used to calculate a regression line. The absorbance of the samples was the measured and the concentrations were calculated using the equation of the regression line.

4.2.2 SDS-PAGE

SDS-PAGE is a technique to separate proteins due to their length and not charge or charge/mass ratio. An SDS gel with the desired acrylamide concentration was prepared: The solution for the separation gel was prepared (see 3.4 Buffers and stock solutions) and the equipment was filled to about 70%. The acrylamide solution was layered with isopropanol to even it out. When the gel was polymerized, the isopropanol was dumped and the solution for the stacking gel was prepared (for recipe see 3.4 Buffers and stock solutions). The remaining space of the equipment was then filled and a comb was inserted to get chambers. After polymerization of the stacking gel, the comb was removed and the equipment was put into the electrophoresis chamber, which was filled with SDS-PAGE buffer. The chambers were then loaded with 10-15 µg of proteins and an electrophoresis was performed. The conditions for collecting were 50 V and 400 mA for 20 minutes and the following separation was performed at 150 V and 400 mA for 1 hour.

4.2.3 Blotting and protein detection

The proteins can be transferred from the gel onto a PVDF membrane and then be analyzed with antibodies. The transfer was performed at 100 V and 400 mA for 1 hour. If the membrane was dried, it was put briefly in methanol and then washed

3 times with 1xTST. The membrane was first blocked in 10 % milk in 1xTST buffer for 30 minutes. The first antibody was diluted 1:1,000 in 10 % milk and incubated at 4 °C over night. The loading control tubulin was diluted 1:10,000 and GAPDH 1:20,000. The membrane was then washed for 3 times for 15 minutes with 1xTST buffer. The secondary antibodies, which were all HRP linked, were diluted 1:10,000 in 1xTST and incubated for 1 h at RT. After this incubation, the membrane was again washed 3 times with 1xTST for 15 minutes. Then the Immobilon Western, which is a chemiluminescent HRP substrate, was prepared due to manufacturer's protocol. The membrane was then incubated with this substrate for 5 minutes. The chemiluminescent detection catalyzes the oxidation of luminol by peroxide. Oxidized luminol emits light as it decays to its ground state and this light can be visualized when the membrane is exposed to an X-ray film.

4.2.4 Antibody crossreactions

All antibodies have been purchased (see 3.1 Chemicals and reagents) and showed no crossreaction. Some antibodies showed more bands than the depicted ones in the results, but the band shown is the specific one. Other bands did not have the correct molecular weight and did not change upon treatment.

The antibodies against SRF, SKP2 and CDKN1B have been verified, since siRNAs against these proteins have been used. For SRF see 5.3.1 SRF mRNA and protein are significantly downregulated after transfection with siSRF797 in human and porcine SMCs. The verification for antibody against SKP2 is depicted in 5.5.1 Transfection of siSKP2 in human smooth muscle cells and for CDKN1B: 5.6.1 Transfection of siCDKN1B and cotransfection of siSRF797 and siCDKN1B in human SMCs.

4.2.5 Stripping

The membrane has to be stripped to get rid off the former used antibodies. Therefore, it was possible to detect other proteins or to make a loading control with the same membrane. The membrane was placed into stripping buffer and was incubated on a shaker for 30 minutes at 50 °C and washed afterwards twice with 1xTST for 10 minutes.

4.2.6 Loading control

To check if the protein loading was comparable in each sample, the membrane was detected with either GAPDH or tubulin as a loading control. The membrane was then analyzed the same way as describes above in 4.2.3.

4.2.7 Quantification of Western films

The Western Blot films were scanned and analyzed via Personal Densitometer SI measurement and ImageQuant5.1 Software. The values of either untransfected or siGL2-treated cells were set to 1. In most cases X-ray films with very low exposure times have been used for quantification to ensure, that the measurement is in the linear range of the instrument. Since these bands are very weak and are almost not visible after scanning in, films with a longer exposure time are shown in the results.

4.3 RNA analysis

4.3.1 RNA determination

The RNA concentration was determined via optical density (OD) measurement. One unit of OD at the wavelength of 260 nm (OD_{260}) corresponds to 40 µg/ml RNA, when using a quartz cuvette with a deposit thickness of 1 cm. Therefore, the OD_{260} value of the sample can be used to calculate the concentration of the sample using the rule of three.

4.3.2 cDNA synthesis

1 µg RNA was filled up to 8 µl with H_2O. 5 µl random hexamers with a concentration of 100 µM are added to the RNA and incubated at first for 10 minutes at 70 °C and then for 10 minutes on ice.

For the cDNA synthesis, a master mix was prepared.

Per sample:

4 µl MMLV-Puffer (5x)

2 µl 10mM dNTPs

0.5 µl MMLV-RT Polymerase

0.5 µl RNase Inhibitor

7 µl Mastermix were added to each sample and then incubated at RT for 10 minutes. The samples were then put into a shaker at 42 °C for 45 minutes and then at 99 °C for 3 minutes. Afterwards the samples were put on ice and for real-time RT-PCR 30 µl H_2O or for RT-PCR 20 µl H_2O have been added to each sample.

4.3.3 Real-time RT-PCR

For the real-time RT-PCR, mastermixes were prepared:

per gene:

0.5 µl 10 µM gene specific forward primer

0.5 µl 10 µM gene specific reverse primer

7.5 µl SybrGreen mix

3.5 µl H_2O

Into one well of a 96 well-plate 3 µl of the cDNA and 12 µl of the mastermix are pipetted. Triplicates were made to check for variances. The plate was sealed and either analyzed straight away or stored at -20 °C for later analysis.

ABI Prism Program:

Stage 1: 50 °C - 2 min
Stage 2: 95 °C - 10 min
Stage 3: 95 °C - 15 sec
60 °C - 1 min - 40 repeats
Stage 4 (=Dissociation stage): 95 °C - 15 sec
60 °C - 20 sec
95 °C - 15 sec

At first, the dissociation curve was checked for showing only a single peak and for all samples, the peak height, which indicates the intensity, should be similar. All samples for the same gene have been analyzed together in the amplification plot. Each gene was analyzed separately.

4.3.4 RT - PCR

The mastermix for the RT-PCR was set up:

per reaction:
1 µl dNTPs (10mM)
1.5 µl Primer fw (10µM)
1.5 µl Primer rev (10µM)
5 µl 10xTaq Buffer

Sample 1 (cDNA): 9 µl mastermix + 2.5 µl Taq Polymerase + 4 µl cDNA + 34.5 µl H_2O
Control 1 (RNA): 9 µl mastermix + 2.5 µl Taq Polymerase + 2 µl RNA + 34.5 µl H_2O
Control 2 (H_2O): 9 µl mastermix + 2.5 µl Taq Polymerase + 38.5 µl H_2O

PCR program:
94 °C - 2 min
30 cycles: 94 °C - 30 sec
57 °C - 1 min

72 °C - 2 min

72 °C - 7 min

4.3.5 Agarose gel separation of PCR products

The PCR products were loaded on a 1% or 1.5% agarose gel, to check, if there were amplicons with the right size that could be extracted and sequenced.

4.3.6 Gel extraction

The DNA fragment was excised from the agarose gel with a scalpel. The extraction was performed due to the manufacturer's protocol for QIAquick Gel Extraction Kit Protocol using a microcentrifuge. The DNA was eluted in 40 µl H_2O. Gel extracts were stored at -20 °C.

4.3.7 Sequencing of PCR products

The used method is based on Sanger's method (Sanger et al., 1977).

The mastermix for the PCR was prepared.

Per reaction:

1 - 2 µl gel extract

0.5 µl Primer (10µM)

2 µl BigDye

5.5 - 6.5 µl H_2O

Then the following PCR program was started:

96 °C - 1 Min.

30 Cycles: 96 °C - 10s

55 °C - 5s

60 °C - 4 min.

4 °C - ∞ min.

After the PCR, the DNA was precipitated by adding 1 µl of 3M sodium acetate (pH 5.5) + 25 µl ethanol to each sample and let stand at RT for 1.5 - 2 hours. Then it was centrifuged for 20 min at 13,000 rpm and the supernatant was discarded. The pellet was washed with 50 µl 70 % ethanol and centrifuged for 5 min at 13,000 rpm.

The supernatant was discarded and resuspended in 25 µl TSR buffer. The samples were heated for 2 min at 94 °C, put directly on ice and then into the sequencer. The Analysis software interprets the results, calling the bases for the fluorescence intensity at each data point.

4.4 Statistical analysis

4.4.1 Definition of independent analysis

Three batches of human smooth muscle cells have been ordered, one from Cambrex and two from PromoCell. The two vials from PromoCell are from the same lot. The vial was thawed and cells have been expanded until passage 4 or 5 and were then frozen in several vials. For each experiment, one vial was thawed and cells have been transfected in passage 7 or 8.

Porcine smooth muscle cells were isolated from a 2-3 cm long piece of vein (see 4.1.1 Isolation of primary porcine SMCs). Cells were expanded and a part was frozen in passage 4 or 5 and another part was used for transfection in passage 7 or 8. For most experiments with porcine cells, new cells have been isolated and only in a few cases, thawed vials were frozen and used for experiments.

4.4.2 Significance test

For statistical analyses, values of control-treated cells or loading controls have been set to 1. The figure description of figures including statistical analysis indicates what treatment was used for normalization. These values were used to perform a two-tailed Student's t-test using Microsoft Office Excel 2003. p-values higher than 0.05 were declared as non-significant, whereas p-values smaller than 0.05 indicate a significant change. p-values below 0.01 or 0.001 represent a higher significance.

5 Results

5.1 Sequencing of cDNA for *Sus scrofa SRF*

The first step was to sequence cDNA encoding for porcine *SRF* to check if the siSRF797 recognition sequence is also present in *Sus scrofa*. An alignment of several mammalian *SRF* mRNAs was used to design primers for RT-PCR. Porcine cells were isolated from Vena saphena magna (courtesy of Dr. Wendel, University of Tuebingen) as described in 4.1.1. mRNA was isolated and transcribed into cDNA, which was used for the RT-PCR. Agarose gel electrophoresis was used for purification of the PCR products and to check the amplicon sizes.

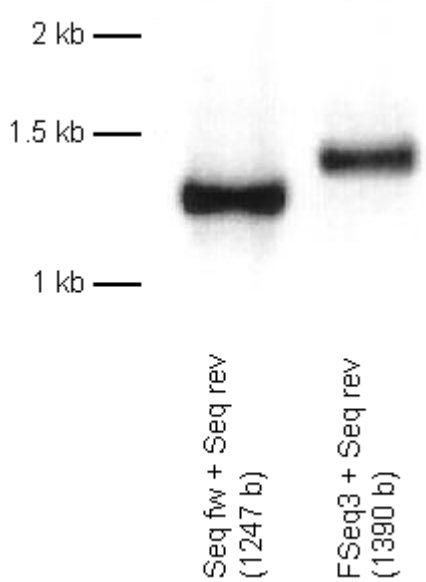

Figure 15 – 1% Agarose-gel with PCR products
The PCR products were loaded onto a 1% gel for purification purposes and to check for amplicons of the calculated size, which would then be used for sequencing.

Figure 15 shows amplicons with the calculated size. Bands that had the expected size, which was calculated based on the human sequence, have been extracted and purified for a PCR with fluorescein-labelled dideoxynucleotide triphosphates and the same primers that have been used in the previous RT-PCR. The product of this PCR was then analyzed using the 310 Genetic Analyzer (Abi Prism), which is an automated single-capillary genetic analyzer. The data was analyzed using the

integrated Sequencing Analysis Software from Applied Biosystems. A segment of the raw data of the sequencer is depicted in figure 16.

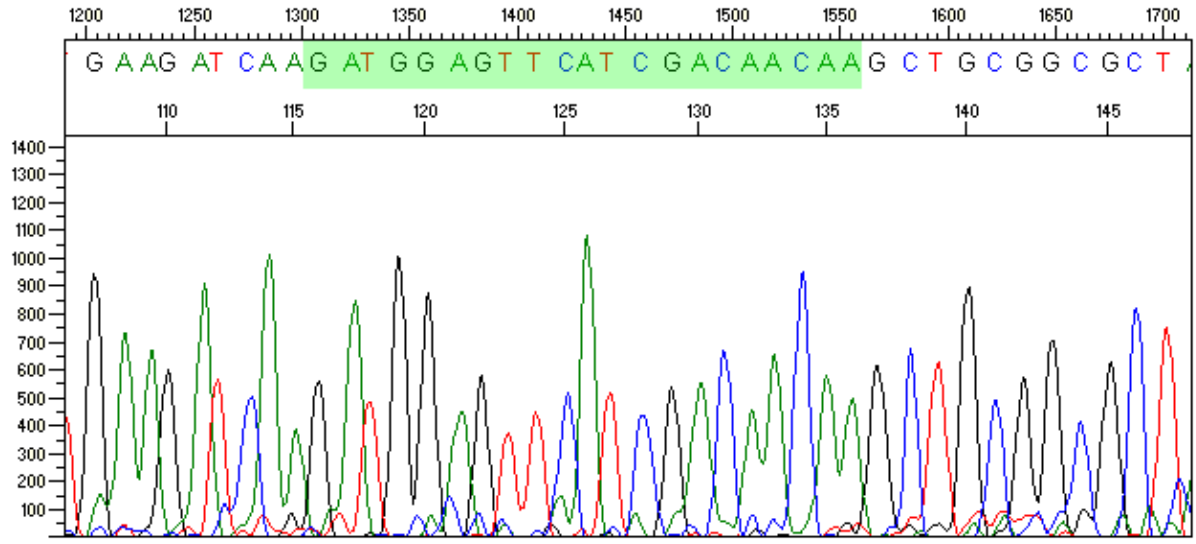

Figure 16 – Segment of raw data after sequencing of porcine *SRF* cDNA
The purified PCR product with the fluorescein-labelled ddNTPs was analyzed by the sequencing software. A segment of the raw data of the sequencer analysis is shown here. The siSRF797 recognition site is marked in green.

It was possible to sequence 1227 nucleotides of the porcine *SRF* cDNA. The human *SRF* mRNA has 1530 nucleotides. Taking this as a correspondence, about 80% of the porcine *SRF* have been sequenced. It was not possible to find primers, that were able to bind more upstream in the 5'-region. It could be due to the fact, that it is a very G/C-rich region or might be due to unspecific primers. The part, which could be sequenced, is depicted in figure 17.

Figure 17 depicts the sequenced cDNA of *Sus scrofa SRF*. When compared to the human SRF, this represents about 80% of the encoding region and figure 17 would show the cDNA sequence, starting from nucleotide 304 – 1530. An alignment of human and porcine cDNA is shown in figure 18.

porcine cDNA:

AGCCTGAGCG AGATGGAGAT CGGTATGGTG GTCGGTGGGC CCGAGGCGTC GGCAGCGGCC
ACCGGGGGCT ACGGGCCGGT GAGCGGCGCG GTGAGCGGGG CCAAGCCGGG TAAGAAGACC
CGGGGCCGCG TGAAGATCAA GATGGAGTTC ATCGACAACA AGCTGCGGCG CTACACGACC
TTCAGCAAGA GGAAGACGGG CATCATGAAG AAGGCCTATG AGCTGTCCAC GCTGACAGGG
ACACAGGTGC TGTTGCTGGT GGCCAGTGAG ACAGGCCATG TGTATACCTT TGCCACCCGC
AAACTGCAGC CCATGATCAC CAGTGAGACT GGCAAGGCAC TGATTCAGAC CTGCCTCAAC
TCGCCAGACT CTCCACCCCG CTCAGACCCT ACCACAGACC AGAGAATGAG TGCCACGGGC
TTTGAAGAGA CAGACCTCAC CTACCAGGTG TCGGAGTCCG ACAGCAGTGG GGAGACCAAG
GATACACCGA AACCTGCGTT TACCATCACC AACCTGCCGG GTACCACCTC CACAATCCAG
ACAGCACCCA GCACCTCTAC CACCATGCAA GTCAGCAGCG GCCCCTCCTT TCCCATCACC
AACTACCTGG CACCAGTGTC TGCTAGTGTC AGCCCCAGCG CTGTCAGCAG TGCCAACGGA
ACTGTGCTGA AGAGTACGGG CAGCGGCCCC GTTTCCTCCG GGAGCCTCAT GCAGCTGCCT
ACTAGCTTCA CCCTCATGCC TGGTGGGGCA GTGGCCCAGC AGGTCCCAGT ACAGGCCATA
CAGGTGCACC AGGCCCCACA GCAAGCGTCT CCCTCTCGCG ACAGCAGCAC AGACCTCACG
CAGACCTCCT CCAGCGGGAC AGTGACACTG CCCGCCACCA TCATGACGTC GTCCGTGCCC
ACCACTGTGG GCGGCCACAT GATGTACCCC AGCCCCCACG CGGTGATGTA TGCACCCACC
TCGGGCCTGG CTGATGGCAG CCTCACCGTG CTCAATGCCT TCTCCCAGGC ACCATCCACC
ATGCAGGTGT CCCACAGCCA GGTCCAGGAG CAAGGTGGCG TCCCCCAGGT ATTCCTGACA
GCGCCATCTG GGACAGTGCA GATCCCCGTC TCGGCGGTTC AGCTTCACCA GATGGCTGTG
ATAGGGCAGC AGGCCGGGAG CAGCAGCAAC CTCACCGAAA TACAGGTGGT AAACCTGGAC
GCCGCCCACA GCACCAAGAG TGACTGA

Figure 17 – Part of the porcine *SRF* cDNA. The siSRF797 recognition site is marked in green
This figure depicts the 1227 nt, which were possible to sequence of the porcine *SRF* cDNA. The 5'-part is lacking due to unspecific primers or the high G/C-content.

The following alignment shows the human and porcine cDNA sequences of *SRF*. Stars indicate homology; missing stars indicate a difference in nucleotides. x depicts the missing 5'-part of the porcine *SRF* sequence. The MADS box is marked in orange and the siSRF797 recognition site is highlighted in light green.

Alignment of *Homo sapiens* (hs) and *Sus scrofa* (ss) *SRF* cDNA.

```
ss      xxxxxxxxxx xxxxxxxxxx xxxxxxxxxx xxxxxxxxxx xxxxxxxxxx xxxxxxxxxx
hs      ATGTTACCGA CCCAAGCTGG GGCCGCGGCG GCTCTGGGCC GGGGCTCGGC CCTGGGGGGC

ss      xxxxxxxxxx xxxxxxxxxx xxxxxxxxxx xxxxxxxxxx xxxxxxxxxx xxxxxxxxxx
hs      AGCCTGAACC GGACCCCGAC GGGGCGGCCG GGCGGCGGCG GCGGGACACG CGGGGCTAAC

ss      xxxxxxxxxx xxxxxxxxxx xxxxxxxxxx xxxxxxxxxx xxxxxxxxxx xxxxxxxxxx
hs      GGGGGCCGGG TCCCCGGGAA TGGCGCGGGG CTCGGGCCCG GCCGCCTGGA GCGGGAGGCT

ss      xxxxxxxxxx xxxxxxxxxx xxxxxxxxxx xxxxxxxxxx xxxxxxxxxx xxxxxxxxxx
hs      GCGGCAGCGG CGGCAACCAC CCCGGCGCCC ACCGCGGGGG CCCTCTACAG CGGCAGCGAG

ss      xxxxxxxxxx xxxxxxxxxx xxxxxxxxxx xxxxxxxxxx xxxxxxxxxx xxxxxxxxxx
hs      GGCGACTCGG AGTCGGGCGA GGAGGAGGAG CTGGGCGCCG AGCGGCGCGG CCTGAAGCGG

ss      AGCCTGAGCG AGATGGAGCT CGGTGTGGTG GTCGGTGGGC CCGAGGCGGC GGCGGCGGCC
hs      AGCCTGAGCG AGATGGAGAT CGGTATGGTG GTCGGTGGGC CCGAGGCGTC GGCAGCGGCC
        ********** ******** * **** ***** ********** ******** * *** ******

ss      ACGGGGGGCT ACGGGCCGGT GAGTGGCGCG GTGAGCGGGG CCAAGCCGGG TAAGAAGACT
hs      ACCGGGGGCT ACGGGCCGGT GAGCGGCGCG GTGAGCGGGG CCAAGCCGGG TAAGAAGACC
        ** ******* ********** *** ****** ********** ********** *********
ss      CGGGGCCGCG TGAAGATCAA GATGGAGTTC ATCGACAACA AGCTGCGGCG CTACACGACC
hs      CGGGGCCGCG TGAAGATCAA GATGGAGTTC ATCGACAACA AGCTGCGGCG CTACACGACC
        *********  **********  **********  **********  **********  **********

ss      TTCAGCAAGA GGAAGACGGG CATCATGAAG AAGGCCTATG AGCTGTCCAC GCTGACAGGG
hs      TTCAGCAAGA GGAAGACGGG CATCATGAAG AAGGCCTATG AGCTGTCCAC GCTGACAGGG
        ********** ********** ********** ********** ********** **********

ss      ACACAGGTGC TGTTGCTGGT GGCCAGTGAG ACAGGCCATG TGTATACCTT TGCCACCCGC
hs      ACACAGGTGC TGTTGCTGGT GGCCAGTGAG ACAGGCCATG TGTATACCTT TGCCACCCGA
        ********** ********** ********** ********** ********** ****-----

ss      AAACTGCAGC CCATGATCAC CAGTGAGACT GGCAAGGCAC TGATTCAGAC CTGCCTCAAC
hs      AAACTGCAGC CCATGATCAC CAGTGAGACC GGCAAGGCAC TGATTCAGAC CTGCCTCAAC
        ********** ********** *********  ********** ********** **********

ss      TCGCCAGACT CTCCACCCCG CTCAGACCCT ACCACAGACC AGAGAATGAG TGCCACGGGC
hs      TCGCCAGACT CTCCACCCCG TTCAGACCCC ACAACAGACC AGAGAATGAG TGCCACTGGC
        ********** **********  ********  ** ******* ********** ****** ***

ss      TTTGAAGAGA CAGACCTCAC CTACCAGGTG TCGGAGTCCG ACAGCAGTGG GGAGACCAAG
hs      TTTGAAGAGA CAGATCTCAC CTACCAGGTG TCGGAGTCTG ACAGCAGTGG GGAGACCAAG
        ********** **** ***** ********** ******** * ********** **********

ss      GATACACCGA AACCTGCGTT TACCATCACC AACCTGCCGG GTACCACCTC CACAATCCAG
hs      GACACACTGA AGCCGGCGTT CACAGTCACC AACCTGCCGG GTACAACCTC CACCATCCAA
        ** **** ** * ** *****  **  ***** ********** **** ***** *** *****

ss      ACAGCACCCA GCACCTCTAC CACCATGCAA GTCAGCAGCG GCCCCTCCTT TCCCATCACC
hs      ACAGCACCTA GCACCTCTAC CACCATGCAA GTCAGCAGCG GCCCCTCCTT TCCCATCACC
        ******** * ********** ********** ********** ********** **********
```

```
ss      AACTACCTGG CACCAGTGTC TGCTAGTGTC AGCCCCAGCG CTGTCAGCAG TGCCAACGGA
hs      AACTACCTGG CACCAGTGTC TGCTAGTGTC AGCCCCAGTG CTGTCAGCAG TGCCAATGGG
        ********** ********** ********** ******** * ********** ****** **

ss      ACTGTGCTGA AGAGTACGGG CAGCGGCCCC GTTTCCTCCG GGAGCCTCAT GCAGCTGCCT
hs      ACTGTGCTGA AGAGTACAGG CAGCGGCCCT GTCTCCTCTG GGGGCCTTAT GCAGCTGCCT
        ********** ******* ** *********  ** ***** * ** **** ** **********

ss      ACTAGCTTCA CCCTCATGCC TGGTGGGGCA GTGGCCCAGC AGGTCCCAGT ACAGGCCATA
hs      ACCAGCTTCA CCCTCATGCC TGGTGGGGCA GTGGCCCAGC AGGTCCCAGT GCAGGCCATT
        ** ******* ********** ********** ********** **********  ********

ss      CAGGTGCACC AGGCCCCACA GCAAGCGTCT CCCTCTCGCG ACAGCAGCAC AGACCTCACG
hs      CAAGTGCACC AGGCCCCACA GCAAGCGTCT CCCTCCCGTG ACAGCAGCAC AGACCTCACG
        ** ******* ********** ********** ***** ** * ********** **********

ss      CAGACCTCCT CCAGCGGGAC AGTGACACTG CCCGCCACCA TCATGACGTC GTCCGTGCCC
hs      CAGACCTCCT CCAGCGGGAC AGTGACGCTG CCCGCCACCA TCATGACGTC ATCCGTGCCC
        ********** ********** ****** *** ********** **********  *********

ss      ACCACTGTGG GCGGCCACAT GATGTACCCC AGCCCCCACG CGGTGATGTA TGCACCCACC
hs      ACAACTGTGG GTGGCCACAT GATGTACCCT AGCCCGCATG CGGTGATGTA TGCCCCCACC
        ** ******* * ******** *********  ***** ** * ********** *** ******

ss      TCGGGCCTGG CTGATGGCAG CCTCACCGTG CTCAATGCCT TCTCCCAGGC ACCATCCACC
hs      TCGGGCCTGG GTGATGGCAG CCTCACCGTG CTGAATGCCT TCTCCCAGGC ACCATCCACC
        **********  ********* ********** ** ******* ********** **********

ss      ATGCAGGTGT CCCACAGCCA GGTCCAGGAG CAAGGTGGCG TCCCCCAGGT ATTCCTGACA
hs      ATGCAGGTGT CACACAGCCA GGTCCAGGAG CCAGGTGGCG TCCCCCAGGT GTTCCTGACA
        ********** * ******** ********** * ******** **********  *********

ss      GCGCCATCTG GGACAGTGCA GATCCCCGTC TCGGCGGTTC AGCTTCACCA GATGGCTGTG
hs      GCATCATCTG GGACAGTGCA GATCCCTGTT TCAGCAGTTC AGCTCCACCA GATGGCTGTG
        **  ****** ********** ****** **  ** ** **** **** ***** **********

ss      ATAGGGCAGC AGGCCGGGAG CAGCAGCAAC CTCACCGAAA TACAGGTGGT AAACCTGGAC
hs      ATAGGGCAGC AGGCCGGGAG CAGCAGCAAC CTCACCGAGC TACAGGTGGT GAACCTGGAC
        ********** ********** ********** ********  **********  *********

ss      GACGCCGCCC ACAGCACCAA GAGTGACTGA
hs      GACACCGCCC ACAGCACCAA GAGTGAATGA
        **  ****** ********** ****** ***
```

Figure 18 – Alignment of human (hs) and porcine (ss) cDNA. The MADS box is depicted in orange and the siSRF797 recognition site in light green.

Sequencing data from cDNA from porcine SMCs was aligned with human cDNA data. Stars represent homology, missing stars indicate differences in bases. The lacking 5'-part of porcine *SRF* cDNA is marked by x. The MADS box is marked in orange and the siSRF797 recognition site is highlighted in green. The alignment shows that there is a high homology between *Homo sapiens* and *Sus scrofa*. The MADS box is completely conserved.

It was possible to sequence 1227 bases of the porcine *SRF*, which are 80% of the total sequence, when human *SRF* is taken as reference. The porcine 5'-part could not be sequenced, maybe because of the high G/C-content or no complementary primers.

66 out of the 1227 bases differ to the human sequence, which is a 95% conservation. The alignment reveals that the complete MADS box (highlighted in orange) and thereby also the siSRF797 recognition site (marked in green) are completely homologous.

The sequenced cDNA was then translated into amino acid using software of the ExPASy proteomics server of the Swiss Institute of Bioinformatics (http://www.expasy.org/ tools/dna.html).

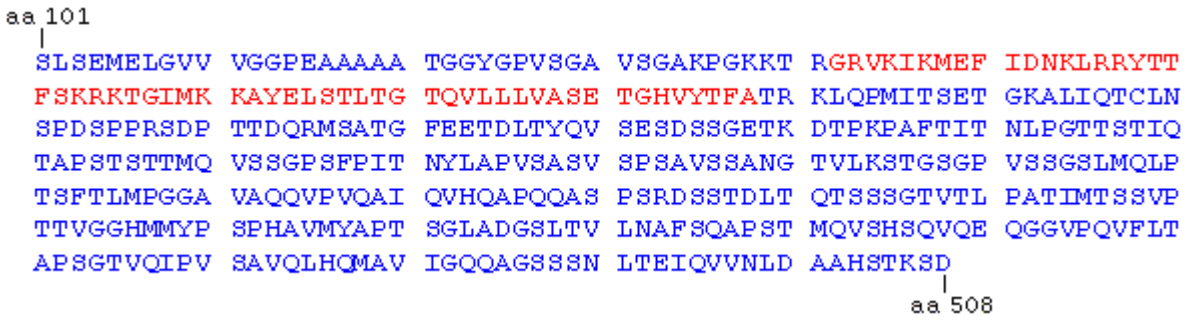

Figure 19 – Part of porcine SRF protein with highlighted MADS box (red)
This figure depicts a part of the porcine SRF protein. Using the human SRF protein as a reference, amino acids 101-508 of the porcine SRF protein are shown. The MADS box, which is highly conserved, is highlighted in red.

Figure 19 shows a segment of the translated protein sequence for *Sus scrofa* SRF. Based on the information on human *SRF* about 100 amino acids are lacking at the 5' end. Therefore, amino acids 101-508 could be translated from the porcine *SRF* cDNA. The MADS box is highlighted in red. It is highly conserved between *Homo sapiens, Sus scrofa* and others mammals.

An alignment of human *SRF* protein and the predicted porcine *SRF* protein is shown in figure 20. The MADS box is marked in blue and the siSRF797 recognition site is labelled. Green amino acids stand for a silent alteration, so a different nucleotide codon that encodes for the same amino acids. The red amino acids highlight amino acid alterations, so a change in the codon that leads to a different amino acid. The x represent the missing 5' part of *Sus scrofa SRF*, which was not possible to sequence due to a very high G/C content or no primer binding.

```
ss    xxxxxxxxxx xxxxxxxxxx xxxxxxxxxx xxxxxxxxxx xxxxxxxxxx xxxxxxxxxx
hs    MLPTQAGAAA ALGRGSALGG SLNRTPTGRP GGGGGTRGAN GGRVPGNGAG LGPGRLEREA

ss    xxxxxxxxxx xxxxxxxxxx xxxxxxxxxx xxxxxxxxxx SLSEMELGVV VGGPEAAAAA
hs    AAAAATTPAP TAGALYSGSE GDSESGEEEE LGAERRGLKR SLSEMEIGMV VGGPEASAAA
                                      siSRF797
ss    TGGYGPVSGA VSGAKPGKKT RGRVKIKMEF IDNKLRRYTT FSKRKTGIMK KAYELSTLTG
hs    TGGYGPVSGA VSGAKPGKKT RGRVKIKMEF IDNKLRRYTT FSKRKTGIMK KAYELSTLTG

ss    TQVLLLVASE TGHVYTFATR KLQPMITSET GKALIQTCLN SPDSPPRSDP TTDQRMSATG
hs    TQVLLLVASE TGHVYTFATR KLQPMITSET GKALIQTCLN SPDSPPRSDP TTDQRMSATG

ss    FEETDLTYQV SESDSSGETK DTPKPAFTIT NLPGTTSTIQ TAPSTSTTMQ VSSGPSFPIT
hs    FEETDLTYQV SESDSSGETK DTLKPAFTVT NLPGTTSTIQ TAPSTSTTMQ VSSGPSFPIT

ss    NYLAPVSASV SPSAVSSANG TVLKSTGSGP VSSGSLMQLP TSFTLMPGGA VAQQVPVQAI
hs    NYLAPVSASV SPSAVSSANG TVLKSTGSGP VSSGGLMQLP TSFTLMPGGA VAQQVPVQAI

ss    QVHQAPQQAS PSRDSSTDLT QTSSSGTVTL PATIMTSSVP TTVGGHMMYP SPHAVMYAPT
hs    QVHQAPQQAS PSRDSSTDLT QTSSSGTVTL PATIMTSSVP TTVGGHMMYP SPHAVMYAPT

ss    SGLADGSLTV LNAFSQAPST MQVSHSQVQE QGGVPQVFLT APSGTVQIPV SAVQLHQMAV
hs    SGLGDGSLTV LNAFSQAPST MQVSHSQVQE PGGVPQVFLT ASSGTVQIPV SAVQLHQMAV

ss    IGQQAGSSSN LTEIQVVNLD AAHSTKSD
hs    IGQQAGSSSN LTELQVVNLD TAHSTKSE
```

Figure 20 – Alignment of human (hs) and porcine (ss) SRF protein
This figure shows an alignment of human and porcine SRF protein. The MADS box is depicted in blue and the siSRF797 recognition site is labeled. Red amino acids represent alterations in amino acids, whereas green amino acids represent silent alterations. The part that was not possible to sequence is shown by the x in the Sus scrofa (ss) sequence.

This alignment shows that 12 out of the 408 amino acids that could be revealed of the porcine SRF are changed when comparing it to human SRF protein. This stands for 97 % conservation when compared to the human sequence. Therefore, the siSRF797 is very likely to work in most mammalian cells due to the high conservation of SRF.

5.2 Testing of siRNAs on human smooth muscle cells

5.2.1 Test of different siRNAs against *SRF* and verification of siGL2 as neutral control siRNA using human smooth muscle cells

Two different siRNA against *SRF* (siSRF797 and siSRF820) have been tested on human smooth muscle cells (SMCs) for their efficiency. Cells have been purchased from Cambrex or PromoCell (see 3.6). Both siRNAs recognize a sequence within the MADS box of *SRF*, which is highly conserved among all mammals, and should therefore be functional in a variety of mammalian cells. In addition, an siRNA against Luciferase (siGL2) was tested as a control, since cells that have been transfected with a non-functional siRNA are a better control than untreated cells. Cells have been harvested three days after transfection and mRNA was isolated, transcribed into cDNA that was then used for real-time RT-PCR analysis.

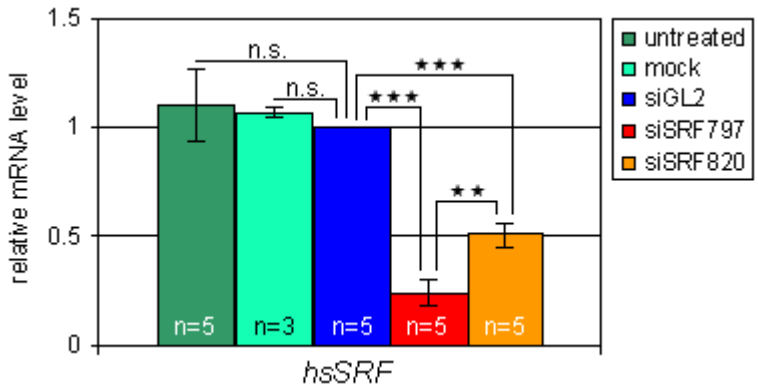

Figure 21 – relative mRNA levels of *SRF* in human SMCs
Relative mRNA of *SRF* isolated from human SMCs three days after transfection. The values have been normalized to GAPDH and values of siGL2-treated cells have been set to 1. Untreated and siGL2-treated cells do not show a significant difference. Both siRNAs against SRF, siSRF797 and siSRF820, show a significant reduction, whereas siSRF797 shows a stronger downregulation than siSRF820. n = number of independent experiments, mean values ± SEM are shown, significance: two-tailed Student's t-test; $p>0.05$ = n.s.; $p<0.01$ = **; $p<0.001$ = ***

Figure 21 shows relative mRNA levels of *SRF* in differently treated human SMCs. The three left panels show the controls, untreated-, mock- and siGL2-treated cells, which do not show any difference. Untreated cells are cells treated as transfected cells, without the transfection agent and without siRNAs. Mock-treatment of cells included the transfection agent, but no siRNA. Since no difference was observed using control-treatments, siGL2 was used as control siRNA in further experiments. The two panels on the right depict the significant downregulation of *SRF* upon siSRF transfection. siSRF797-transfection leads to a stronger downregulation than siSRF820 and was therefore used for further experiments.

5.2.2 Transfection procedure does not induce an interferon response

Published reports (Sledz et al., 2003; Hornung et al., 2005) demonstrate that the transfection procedure itself can lead to an interferon response and thereby cause undesirable off-target effects. It is possible to detect markers for this induction on mRNA level via real-time RT-PCR. Therefore, it is necessary to compare transfected cells with untreated cells, since any kind of transfection can result in an interferon response. *OAS1* (*2',5'-oligoadenylate synthetase 1*) and *STAT1* (*signal transducer and activator of transcription 1*) are such marker genes since they play a role in the induction of interferon-dependent responses (for review see Samuel, 2001). Former colleagues confirmed the OAS1 and STAT1 primers and showed a highly significant increase upon transfection of PolyIC, thereby inducing an interferon response (Thomas et al., 2005). mRNA was isolated three days after transfection of human SMCs and real-time RT-PCR analysis was performed.

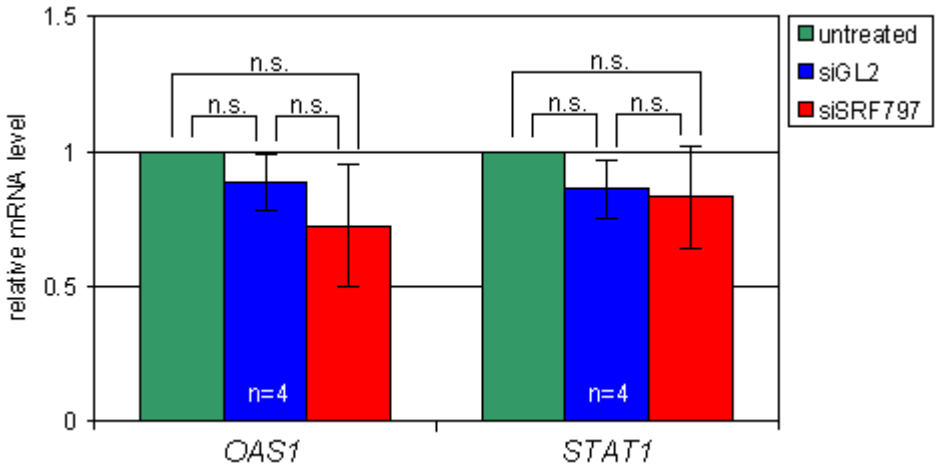

Figure 22 – Relative mRNA levels of markers for interferon response
Relative levels of *OAS1* and *STAT1* mRNA that was isolated from hsSMCs three days after transfection. The values have been normalized to *GAPDH* and untreated cells have been set to 1. Both marker genes for an interferon response do not show a significant change after transfection of siGL2 or siSRF797. n = number of independent experiments, mean values ± SEM are shown, significance: two-tailed Student's t-test; $p>0.05$ = n.s.

Real-time RT-PCR experiments showed no significant induction of interferon-specific markers upon transfection either with siSRF797 or with siGL2 when compared to untransfected cells. If there were an induction, these markers would be upregulated 10 – 10,000 fold. However, no significant change can be detected in this experimental setup. Thus, target-unrelated effects due to an interferon response can be excluded.

5.3 Effectiveness of siSRF797-transfection in human and porcine smooth muscle cells

5.3.1 *SRF* mRNA and protein are significantly downregulated after transfection with siSRF797 in human and porcine SMCs

After ensuring that the transfection procedure does not lead to undesired side-effects, the effectiveness of the siRNA was then tested on human and porcine SMCs (see 3.6). The cells have been harvested three days after transfection and RNA and proteins have been isolated. The RNA was transcribed into cDNA for real-time RT-PCR analysis. The results were normalized to GAPDH. Protein levels were analyzed by immunoblotting and GAPDH or tubulin served as loading controls. Immunoblots were quantified using Personal Densitometer SI and ImageQuant5.1 Software.

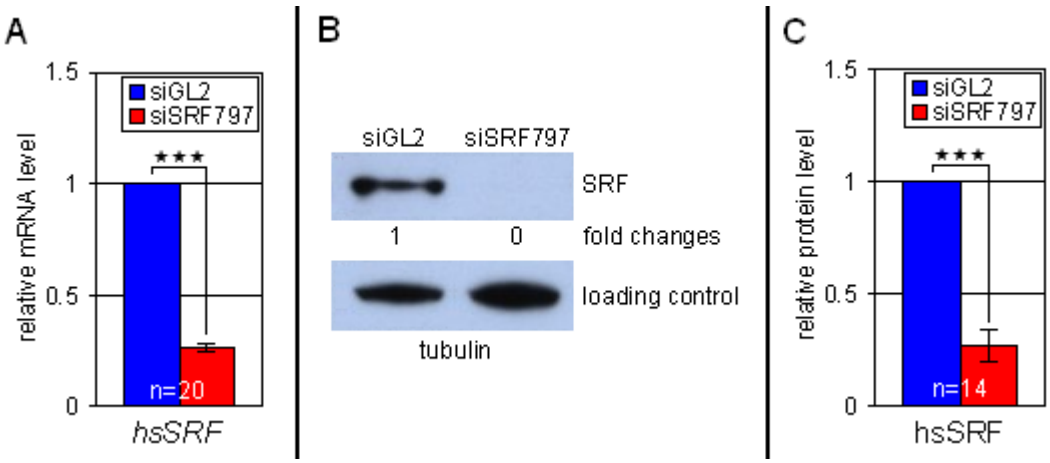

Figure 23 – mRNA and protein levels of *SRF* in human SMCs
A shows the summary of all real-time RT-PCR analyses, which show a significant downregulation of *SRF* three days after transfection in hsSMCs. All data was normalized to *GAPDH*. **B** depicts a representative immunoblot of SRF and tubulin as loading control. **C** shows a summary of quantifications of all immunoblots. GAPDH or tubulin was used as loading control. This shows that also SRF protein is strongly downregulated after transfection with siSRF797 in hsSMCs. n = number of independent experiments, mean values ± SEM are shown, significance: two-tailed Student's t-test; $p<0.001$ = ***

Figure 23 shows a summary of all analyses for *SRF* on mRNA level (**A**) and protein level (**C**) with a representative immunoblot (**B**). On mRNA as well as on the protein level a highly significant downregulation to about 25% can be observed after transfection with siSRF797 when compared to siGL2-transfected human control SMCs.

The same setup has been used to analyze the siRNA efficiency on porcine SMCs. mRNA and proteins have been isolated three days after transfection. cDNA, which was synthesized from the RNA, has been used for real-time RT-PCR analysis; proteins have been analyzed via immunoblotting.

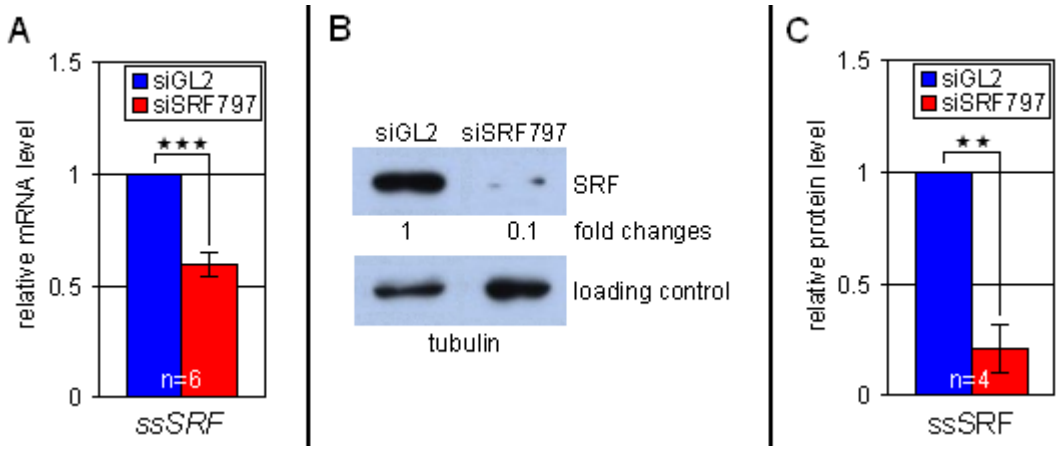

Figure 24 – mRNA and protein levels of *SRF* in porcine SMCs
A depicts the summary of the real-time RT-PCR data. A significant downregulation of *SRF* to 55% is observed, when cells were harvested three days after transfection. *GAPDH* was used for normalization. **B** shows a representative immunoblot of SRF and the loading control tubulin. **C** summarizes all quantifications of immunoblots for SRF. A downregulation to 20% on protein level can be achieved when compared to siGL2-transfected porcine SMCs. Either GAPDH or tubulin served as loading control. n = number of independent experiments, mean values ± SEM are shown, significance: two-tailed Student's t-test; p<0.01 = **; p<0.001 = ***

All real-time RT-PCR analyses are summarized in (**A)**. A significant downregulation of *SRF* mRNA to 55% can be observed after transfection with siSRF797 in porcine SMCs when compared to siGL2-transfected cells. (**B)** shows a representative immunoblot of SRF and the loading control tubulin. A summary of all immunoblot quantifications for SRF in porcine SMCs is shown in (**C)**. SRF protein levels are downregulated to 20%, which is highly significant.

This data demonstrates that siSRF797 is a very potent siRNA against *SRF* that leads to a strong decrease in *SRF* mRNA and protein in human as well as in porcine smooth muscle cells.

5.3.2 *SRF* target genes are also affected after siSRF797 treatment

To check if also *SRF* target genes are downregulated after the transfection of cells with siSRF797, three different target genes (Sun et al., 2006) have been analyzed, namely *ACTA2*, *CNN1* and *TAGLN*. All three genes are not only *SRF* target genes; they are also marker genes for the contractile form of smooth muscle cells.

Human and porcine SMCs have been harvested three days after transfection and RNA was isolated. It was transcribed into cDNA, which was used for real-time RT-PCR analysis using specific primers. The results were normalized to *GAPDH*.

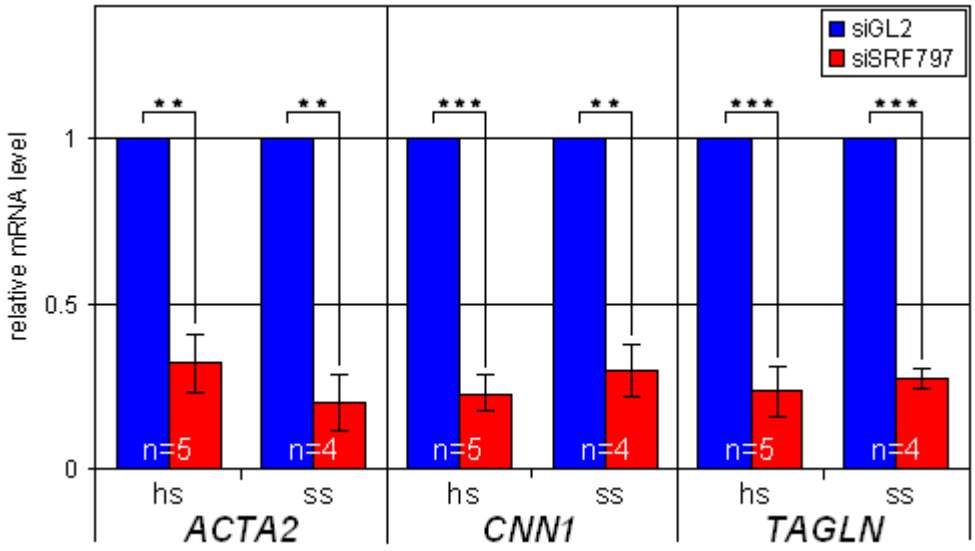

Figure 25 – Downregulation of *SRF* target genes in human and porcine SMCs after depletion of *SRF*

This figure summarizes the real-time RT-PCR data obtained from RNA isolated three days after transfection. A significant downregulation of *SRF* target genes to all three genes to 20-30% can be observed in human as well as in porcine SMCs after transfection with siSRF797 when compared with siGL2-transfected cells. *GAPDH* was used for normalization. n = number of independent experiments, mean values ± SEM are shown, significance: two-tailed Student's t-test; $p<0.01$ = **; $p<0.001$ = ***

Figure 25 shows a summary of real-time RT-PCR analyses of the *SRF* target genes *ACTA2*, *CNN1* and *TAGLN* three days after transfection of human and porcine SMCs with siSRF797 and siGL2, respectively. All three target genes are significantly downregulated on mRNA level to 20 – 30% after transfection with siSRF797 in human as well as in porcine SMC. So not only *SRF* expression, but also expression of *SRF* target genes is affected after transfection with siSRF797 on mRNA level.

5.4 Induction of senescence after downregulation of SRF

5.4.1 *SRF* depletion induces senescence in human and porcine SMCs

Previous papers showed that SRF activity is required for cell cycle progression (Gauthier-Rouviere et al., 1991; Poser et al., 2000; Soulez et al., 1996). Therefore, it was interesting to see, if the cell cycle progression of SMCs was also affected after downregulation of *SRF*. Stainings for senescence, which is an irreversible block in G_1, have been performed. Senescent cells can be visualized by β-gal activity staining at pH 6. If the cells show a blue color reaction at this pH, they are considered senescent (Dimri et al., 1995). Cells have been transfected with siSRF797 and the control siRNA, siGL2. Cover slips have been stained three days after transfection over night. The next day a counterstaining with DAPI was performed to be able to count total cell number. β-gal active cells show a blue staining in Brightfield microscopy; proliferative cells show a slight light blue background staining. Total cells have been counted via DAPI staining.

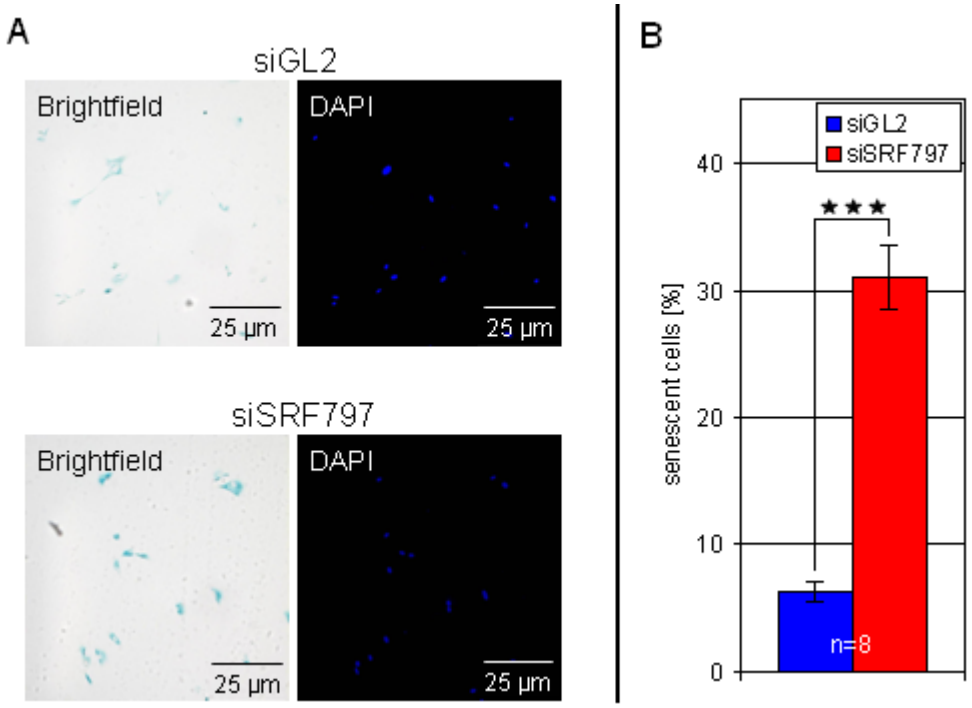

Figure 26 – Senescence staining and quantification of human SMCs after siSRF797-transfection

A shows representative microscopy pictures (Brightfield or DAPI) of human SMCs, either transfected with siSRF797 or siGL2. Senescent cells develop a blue color and have been counted using Brightfield pictures and total cell numbers were determined by DAPI counting. **B** shows the summary of the analyzed data and a highly significant upregulation in senescence after siSRF797-transfection can be observed. n = number of independent experiments, mean values ± SEM are shown, significance: unpaired, two-tailed Student's t-test; $p<0.001$ = ***

The same experiment has been performed with porcine SMCs:

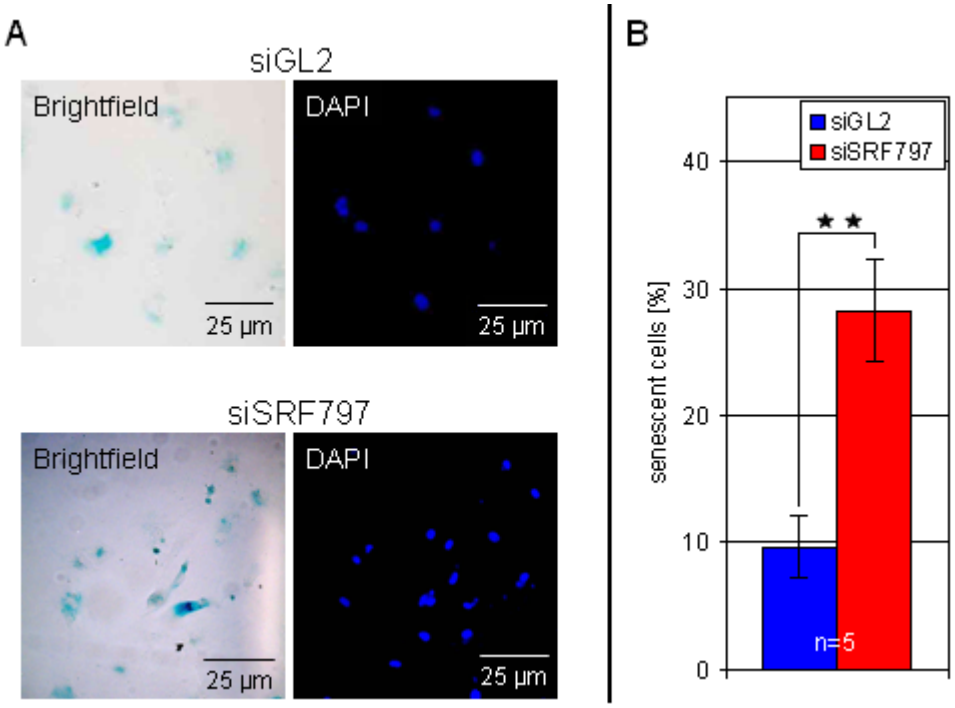

Figure 27 – Senescence staining and quantification of porcine SMCs after *SRF* downregulation
On the left hand side representative microscopy pictures from transfected porcine SMCs are shown. The Brightfield images have been used to count senescent cells (blue staining) and the DAPI images were used to count total cell number. **B** depicts a quantification of the analyzed images and a significant upregulation can be observed, when SMCs have been transfected with siSRF797. n = number of independent experiments, mean values ± SEM are shown, significance: unpaired, two-tailed Student's t-test; $p<0.01$ = **

Figure 26 and 27 show representative stainings for β-gal activity and their quantifications. Figure 26 depicts the results for human SMCs and figure 27 the results for the porcine SMCs. (**A**) displays in figures 26 and 27 representative microscopy pictures. Senescence associated β-gal active cells can be counted via the blue staining in the Brightfield channel. The total cell number can be determined via the DAPI channel. (**B**) shows in figures 26 and 27 the quantification of all stainings from 8, respectively 5, independent experiment.

In human as well as in porcine SMCs, the percentage of senescent cells is significantly increased after siSRF797-transfection when compared to the control siGL2-treated cells. The number of senescent cells is 4-fold increased for human SMCs (see figure 26), respectively 3-fold for porcine SMCs (see figure 27).

5.4.2 Analysis of cell cycle-specific genes in human SMCs after reduction of SRF with siRNAs

After the finding that downregulation of *SRF* leads to a senescent phenotype in human and porcine SMCs, an analysis of several cell cycle-specific genes was performed to identify regulatory proteins that induce the senescent phenotype. Human SMCs have been harvested three days after transfection with siSRF797 or siGL2. RNA and proteins have been isolated.

CDKN1B is a member of the Cip/Kip family of CDK inhibitors and previous studies showed that an increase in *CDKN1B* can lead to a G_1 arrest and cause a senescent phenotype. Toyoshima et al. identified in 1994 CDKN1B protein as inhibitor of CCND1-CDK4 in mouse fibroblasts and human cell lines. Lwin et al. showed in 2007 in human lymphoma cell, that CDKN1B upregulation leads to cell cycle arrest. Therefore, the levels of *CDKN1B* have been checked to see if also in this experimental setup an increase of *CDKN1B* might be the inducer of senescence.

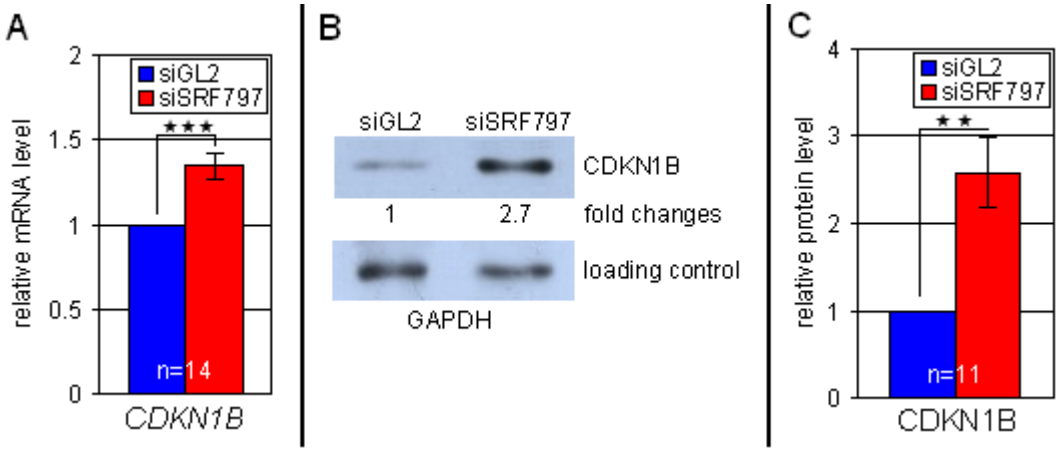

Figure 28 – Data for CDKN1B mRNA and protein levels in human SMCs after transfection
A summarizes the real-time RT-PCR data and a highly significant upregulation of *CDKN1B* mRNA can be observed. All values have been normalized to *GAPDH*. **B**+**C** Immunoblotting showed that also the protein levels were strongly increased. A representative immunoblot is depicted in **B** and the quantification is shown in **C**, where 2.5-fold, significant increase can be observed. The loading control GAPDH or tubulin was used for normalization. n = number of independent experiments, mean values ± SEM are shown, significance: two-tailed Student's t-test; $p<0.01$ = **; $p<0.001$ = ***

Figure 28 sums up all data for *CDKN1B*. It shows a significant upregulation on both mRNA (**A**) and protein level (**B**+**C**) upon transfection of siSRF797 when compared to siGL2-transfected cells. However, the increase in *CDKN1B* transcript levels was with 1.4-fold not very substantial. CDKN1B binds to CyclinE-CDK2 that therefore cannot phosphorylate RB1 and thereby leads to a G_1 arrest.

SKP2 is a component of the ubiquitin protein ligase complex SCF^{SKP2}. It ubiquitinates CDKN1B, which is then consequently degraded and cells can progress from G_1 to S phase. A downregulation of *SKP2* by siRNAs lead to a G_1 arrest in SK-OV-3 cells (Shin et al., 2008) and therefore it was interesting to check if the increase on CDKN1B might be due to a downregulation of SKP2.

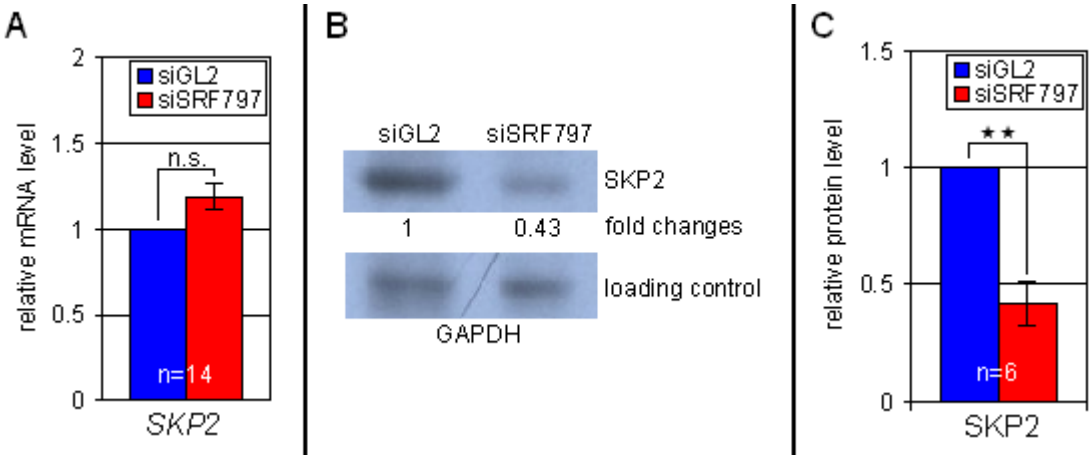

Figure 29 – Summary of all results obtained for *SKP2* in transfected human SMCs
A shows the real-time RT-PCR data and a slight, but not significant upregulation of *SKP* mRNA can be observed. *GAPDH* was used for normalization. **B** depicts a representative immunoblot of SKP2 and a 2-fold decrease in SKP2 protein is detected. **C** summarizes all quantified immunoblots of SKP2 and a significant 2-fold downregulation is detected. GAPDH or tubulin served as loading controls for normalization. n = number of independent experiments, mean values ± SEM are shown, significance: two-tailed Student's t-test; $p>0.05$ = n.s.; $p<0.01$ = **

Figure 29 shows a summary of all data that has been attained for *SKP2*. On mRNA level there is no significant change in *SKP2* detectable as shown in (**A**). Immunoblotting has been performed to check protein levels. A representative immunoblot is depicted in (**B**) and a 2-fold downregulation of SKP2 protein can be seen. All immunoblots have been quantified and a summary of these is shown in (**C**). A highly significant downregulation in SKP2 protein levels is detected.

Senescence is often induced by stabilization of TP53 protein, which transactivates CDKN1A, thereby building the so called TP53-CDKN1A axis and induction of cell cycle arrest (El-Deiry et al., 1994). Therefore, the levels of these genes have been analyzed. Cells have been harvested three days after transfected. RNA and proteins have been isolated and analyzed.

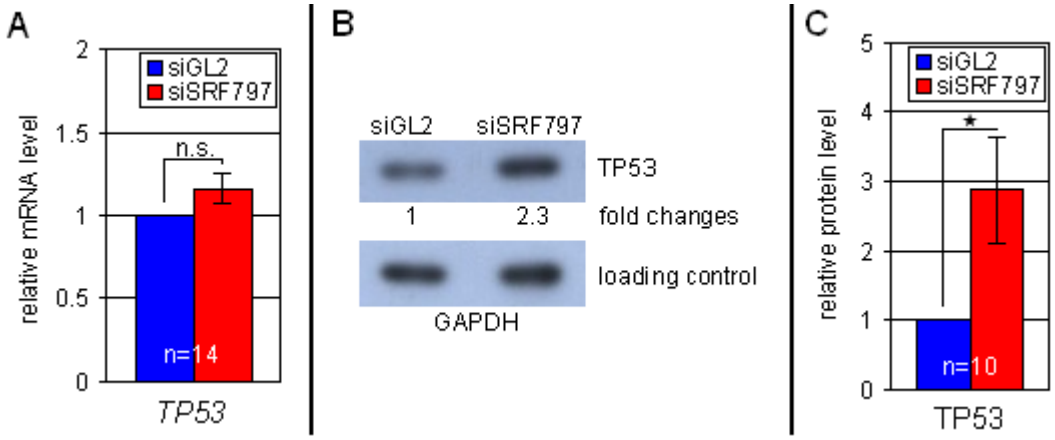

Figure 30 – *TP53* levels in human SMCs after downregulation of *SRF*
A summarizes the real-time RT-PCR data. No significant change on RNA level can be observed. All values have been normalized to *GAPDH.* **B** shows representative immunoblots for TP53 and GAPDH as loading control. A strong increase on TP53 protein can be observed. **C** depicts a summary of all quantified immunoblots of TP53 and a significant upregulation of TP53 protein can be determined. GAPDH or tubulin has been used for normalization. n = number of independent experiments, mean values ± SEM are shown, significance: two-tailed Student's t-test; $p>0.05$ = n.s.; $p<0.05$ = *

Figure 30 sums up all data for *TP53*. It shows a significant upregulation on protein level (**C**) upon transfection of siSRF797 when compared to siGL2-transfected cells. (**B**) depicts a representative immunoblot for TP53. The mRNA levels of *TP53* are not significantly changed (**A**), but it is known that *TP53* is posttranslationally regulated by modulating its degradation (Kastan et al., 1991).

TP53 transactivates CDKN1A and can thereby induce a senescent phenotype (El-Deiry et al., 1993). *CDKN1A* is CDK inhibitor that belongs to the Cip/Kip family of CDK inhibitors. It shows a high similarity to *CDKN1B* and it inhibits also the activity of CDK2-CyclinE.

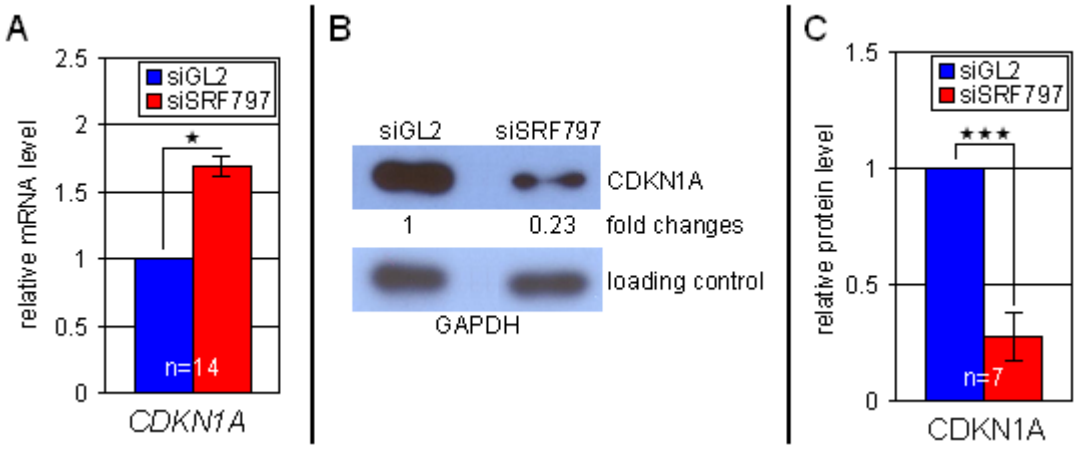

Figure 31 – Data for *CDKN1A* mRNA and protein levels in human SMCs after transfection
A summarizes the real-time RT-PCR data and shows a significant upregulation of *CDKN1A* mRNA. *GAPDH* was used for normalization. **B** depicts a representative immunoblot, **C** shows a quantification of all blots, were a downregulation to 30% can be observed. Blots have been normalized to GAPDH or tubulin. n = number of independent experiments, mean values ± SEM are shown, significance: two-tailed Student's t-test; $p<0.05$ = *; $p<0.001$ = ***

Figure 31 shows that *CDKN1A* mRNA is significantly upregulated whereas CDKN1A protein is strong and significantly downregulated. The mRNA is 1.7-fold upregulated, which is significant (**A**). A representative immunoblot for CDKN1B is depicted in (**B**). (**C**) shows a quantification of all immunoblots and a highly significant downregulation to 25% can be observed. Immunoblots were quantified using Personal Densitometer SI and ImageQuant5.1 Software.

5.5 Downregulation of *SKP2* as possible inducer of senescence

Previous reports showed that a downregulation of SKP2 protein was able to induce a G_1 arrest (Lwin et al., 2007; Shin et al., 2008). Since SKP2 protein was also downregulated after transfection of primary human SMCs with siSRF797, it was tested, if a downregulation of *SKP2* is also sufficient to induce a senescent phenotype in these cells.

5.5.1 Transfection of siSKP2 in human smooth muscle cells

An siRNA against *SKP2* was designed and tested. Human SMCs have been transfected with siSKP2 and siGL2 was again used as control. RNA and proteins have been isolated three days after transfection and real-time RT-PCR and immunoblot analyses have been performed.

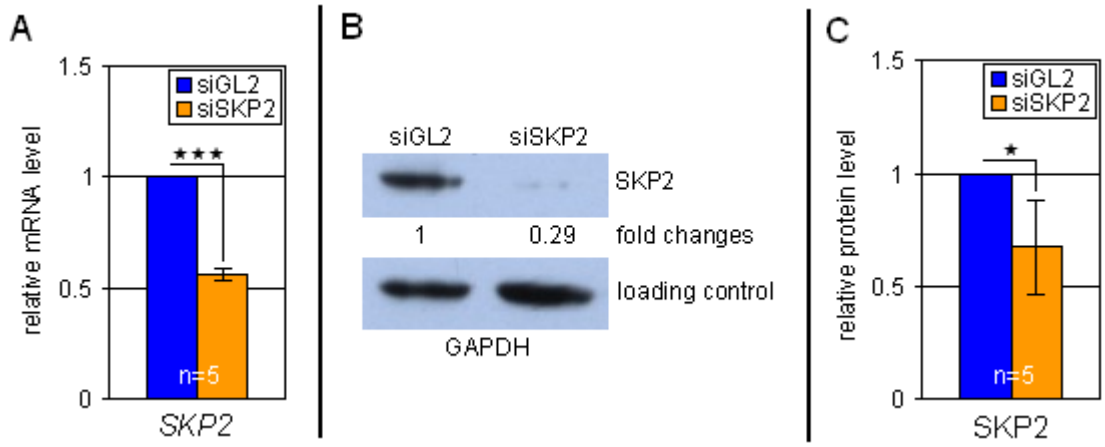

Figure 32 – siSKP2-transfection leads to a decrease of *SKP2* mRNA and protein
Human SMCs have been transfected with siSKP2 and siGL2 as control. mRNA and proteins were harvested three days after transfection. mRNA data was normalized to *GAPDH*. The siSKP2-transfection leads to a strong decrease in *SKP2* mRNA (**A**), but only a trend can be observed on protein levels (**C**). (**B**) depicts an immunoblot, in which a strong downregulation could be detected. n = number of independent experiments, mean values ± SEM are shown, significance: two-tailed Student's t-test; p>0.05 = n.s.; p<0.001 = ***

Figure 32 shows that transfection with siSKP2 leads to 2-fold downregulation of *SKP2* mRNA (**A**). (**B**) depicts an immunoblot, where a strong downregulation was detected. This is not representative, since sometimes only very little decrease of SKP2 could be detected. Therefore, the quantification (**C**) shows only a slight, but significant downregulation and high error bars.

5.5.2 Downregulation of *SKP2* leads to an induction of senescence in human SMCs

After verification of the efficiency of the siRNA against SKP2, senescence stainings have been performed. Human SMCs have been transfected with siSKP2 and siGL2 as control. Cells were stained with senescence staining solution three days after transfection over night. A counterstaining with DAPI was performed on the next day to be able to count total cell number.

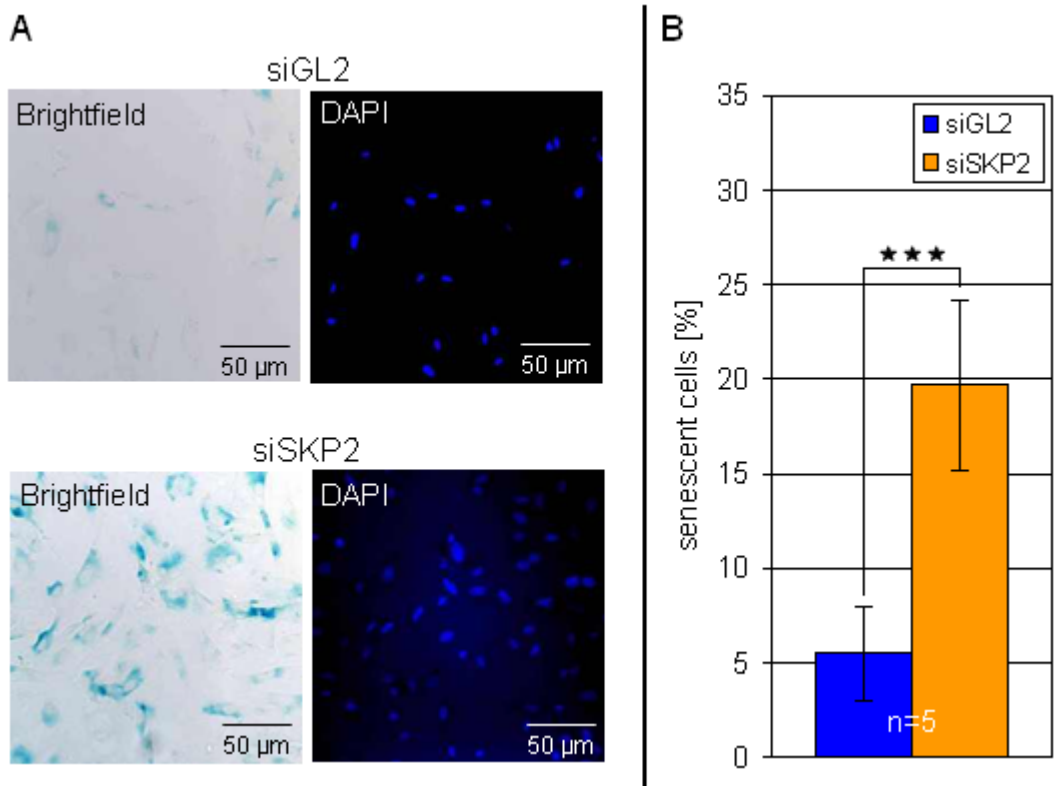

Figure 33 – Senescence staining and quantification of human SMCs after *SKP2* downregulation
A shows representative microscopy pictures (Brightfield and DAPI channels) of human SMCs, either transfected with siSKP2 or siGL2. Senescent cells have been counted using Brightfield pictures and total cell numbers were determined via DAPI counting. **B** depicts the summary of the analyzed data and a highly significant up-regulation in senescence after siSKP2-transfection can be observed. n = number of independent experiments, mean values ± SEM are shown, significance: unpaired, two-tailed Student's t-test; p<0.001 = ***

Figure 33 shows representative microscopy pictures (**A**). The Brightfield channel was used to count senescent cells and the DAPI channel was used to determine total cell numbers. (**B**) shows a quantification and summary of five independent experiments. A highly significant upregulation can be observed. Therefore, the downregulation of *SKP2* is sufficient to drive human SMCs into senescence.

5.5.3 Analysis of *SRF* and its target gene *TAGLN* after downregulation of *SKP2*

At first *SRF* and *TAGLN* levels have been checked, to ensure that *SRF* and its target genes are not affected after downregulation of *SKP2*. Human SMCs have been harvested three days after transfection and RNA and protein were isolated and analyzed via real-time RT-PCR, respectively immunoblotting.

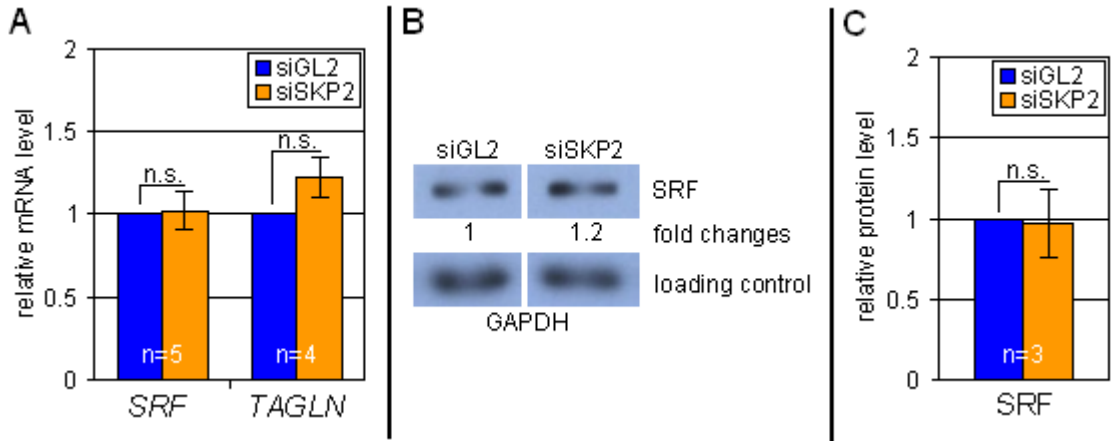

Figure 34 - Analysis of *SRF* and *TAGLN* levels after transfection of siSKP2
mRNA and proteins have been harvested three days after transfection of human SMCs. The values were normalized to *GAPDH. SRF* and *TAGLN* mRNA levels are not altered (**A**). Protein levels of SRF show also no change in expression levels. (**B**) depicts a representative immunoblot for SRF and a summary of all quantified immunoblots against SRF upon siSKP2-transfection is shown in (**C**). n = number of independent experiments, mean values ± SEM are shown, significance: two-tailed Student's t-test; p>0.05 = n.s.

Figure 34 shows all data obtained for *SRF* and *TAGLN* after siSKP2-transfection. siGL2 was used as control. *SRF* levels are not significantly changed after *SKP2* downregulation neither on mRNA level (**A**) nor on protein level (**C**). A representative immunoblot is shown in (**B**). The *SRF* target gene *TAGLN* is also not changed on mRNA level.

So unspecific off-target effects due to alterations of *SRF* levels can be excluded.

5.5.4 Analysis of *CDKN1B* and *TP53* levels after siSKP2-transfection

The hypothesis was that a downregulation of *SKP2* leads to an increase of CDKN1B and thereby to the induction of senescence. Therefore, the next step was to analyze *CDKN1B* levels after siSKP2-transfection. Cells have been transfected with the control siRNA siGL2 or siSKP2. mRNA and proteins have been isolated three days after transfection and analyzed by real-time RT-PCR or immunoblotting.

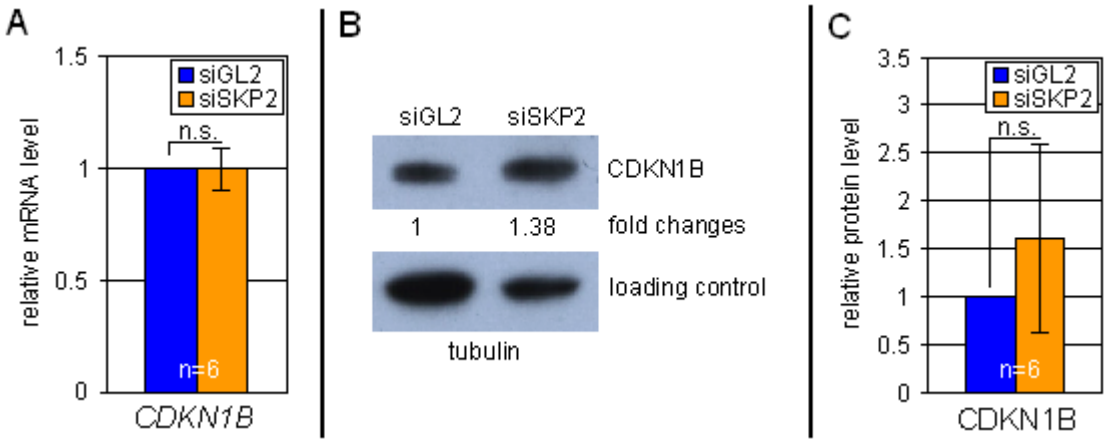

Figure 35 – Analysis of *CDKN1B* levels after transfection of siSKP2
Cells were harvested three days after transfection of human SMCs. mRNA and protein were isolated and analyzed. *CDKN1B* does not show any significant upregulation neither on mRNA level (A) nor on protein level (C). (B) depicts a representative immunoblot for CDKN1B, which shows a slight upregulation. All values were normalized to GAPDH. n = number of independent experiments, mean values ± SEM are shown, significance: two-tailed Student's t-test; $p>0.05$ = n.s.

CDKN1B mRNA levels show no change upon siSKP2-downregulation (**A**), whereas on protein level a slight, but not significant upregulation can be observed (**B**+**C**). This non-significant change of *CDKN1B* mRNA was expected, since SKP2 ubiquitinates CDKN1B protein, so that the mRNA level of *CDKN1B* should not be affected upon siSKP2-transfection.

The unaltered CDKN1B protein level is probably due to not sufficient downregulation of SKP2 protein (see 5.5.1 Transfection of siSKP2 in human smooth muscle cells). High variances of CDKN1B protein are another reason for the non-significant change on protein level. The very strong increase of *CDKN1B* upon siSRF797-transfection is not reached at all.

Expression of *TP53* as a marker for senescence and transactivator of CDKN1A and CDKN1B was also checked after *SKP2* downregulation. Cells have been harvested three days after transfection and mRNA and proteins were analyzed.

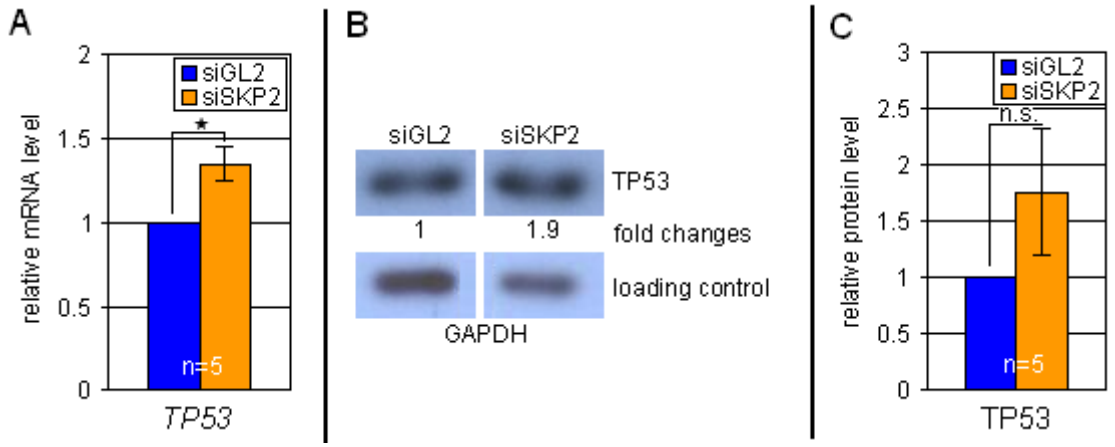

Figure 36 – Analysis of *TP53* levels after transfection of siSKP2
TP53 mRNA and protein levels of cells harvested three days after transfection of human SMCs. *TP53* mRNA level is slight, but significantly increased (A). The protein levels are not significantly changed, but show a tendency to be upregulated (C). An immunoblot, which shows an average upregulation of TP53, is depicted in (B). GAPDH served for normalization. n = number of independent experiments, mean values ± SEM are shown, significance: two-tailed Student's t-test; $p>0.05$ = n.s.; $p<0.05$ = *

TP53 is often a marker for senescence, but it the case of senescence upon siSKP2-transfection, it does not seem to play a role here. The *TP53* mRNA level is slight, but significantly increased, but the protein levels are not affected. Sometimes an upregulated was detected, one is shown in figure 36 B, but sometimes no change at all was observed. This discrepancy leads to the high error bars and non-significance. It seems therefore, that the senescence phenotype, which was observed upon SKP2-depletion, is not induced by TP53.

5.6 CDKN1B as main inducer of senescence upon downregulation of SRF

5.6.1 Transfection of siCDKN1B and cotransfection of siSRF797 and siCDKN1B in human SMCs

Since the downregulation of *SKP2* was sufficient to induce senescence in human SMCs, the cotransfection of siCDKN1B and siSRF797 might lead to a rescue. An siRNA against *CDKN1B* was designed and verified as shown in figure 37. Cells have been harvested three days after transfection and RNA and proteins were isolated and analyzed via real-time RT-PCR and immunoblotting.

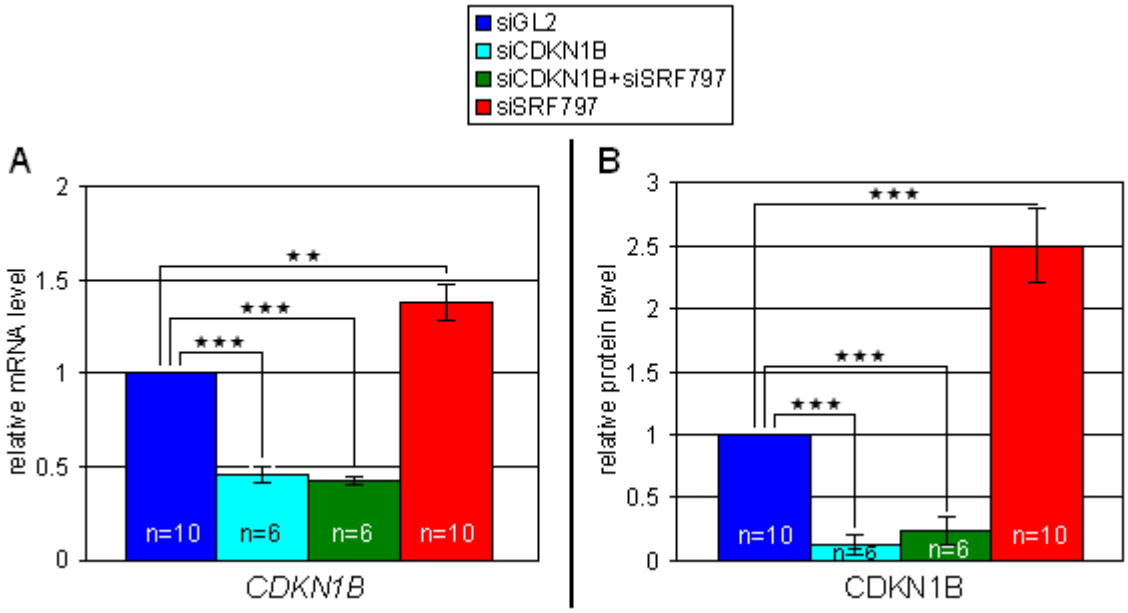

Figure 37 – relative mRNA and protein levels of *CDKN1B*

Figure **A** shows real-time RT-PCR data of hsSMCs three days after transfection. siCDKN1B-transfection showed a high and significant reduction, also when cells were cotransfected with siCDKN1B and siSRF797. The cotransfection is as sufficient as transfection of each siRNA on its own. All data was normalized to *GAPDH*. Figure **B** shows the efficiency of the siCDKN1B and the cotransfection with siSRF797 on protein level. Here is also a strong reduction of CDKN1B and SRF protein observable after transfection of the siRNA on their own or cotransfected. n = number of independent experiments, mean values ± SEM are shown, significance: two-tailed Student's t-test; $p<0.01$ = **; $p<0.001$= ***

Figure 37 shows that the siRNA against *CDKN1B* leads to a strong and significant downregulation of *CDKN1B* mRNA and protein, no matter if transfected alone or cotransfected with siSRF797. The cotransfection is very effective since *CDKN1B* and

SRF are equally downregulated when compared to transfection of only one siRNA, although the amount of siRNA was halved for cotransfection.

SRF levels were checked using the setup as before. mRNA and protein were isolated from human SMCs transfected three days before.

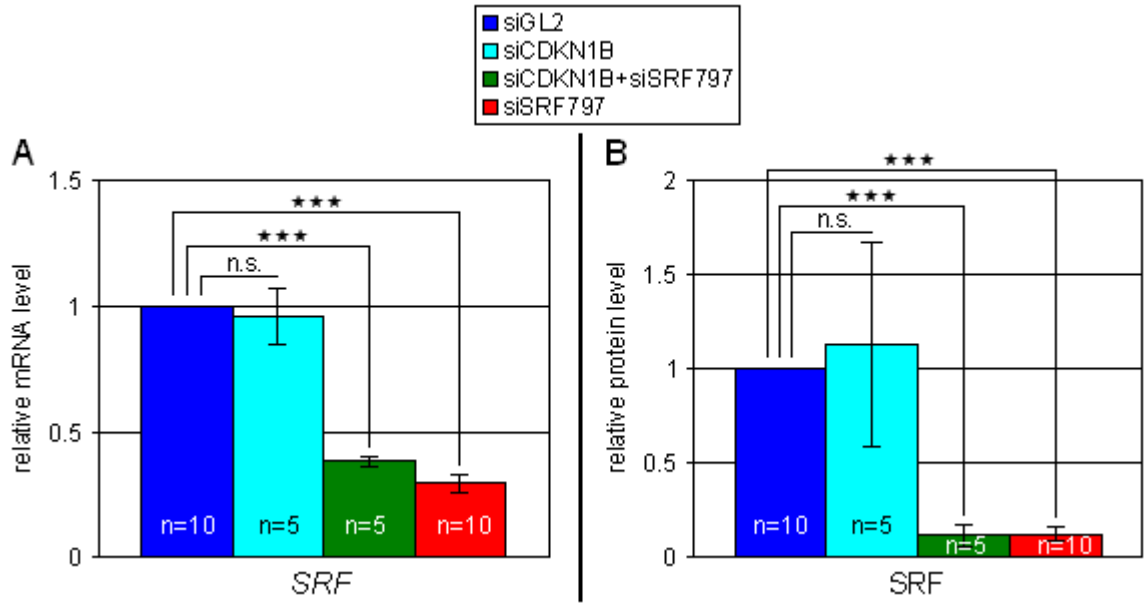

Figure 38 - relative mRNA and protein levels of *SRF*
All real-time RT-PCR data obtained is depicted in (**A**) and immunoblot analyses are summarized in (**B**). siCDKN1B-transfection did not have any effect on *SRF* levels neither on mRNA nor on protein level. The cotransfection of siCDKN1B+siSRF797 had the same efficiency when compared to siSRF797-transfected cells, although half of the siRNA concentrations were used. n = number of independent experiments, mean values ± SEM are shown, significance: two-tailed Student's t-test; $p>0.05$ = n.s.; $p<0.001$= ***

Figure 38 shows the summarized data of *SRF* mRNA and protein levels after different siRNA-transfections. siCDKN1B did not affect *SRF* in any way, whereas the cotransfection of siCDKN1B+siSRF797 shows the same efficiency in downregulation as compared to siSRF797-transfection alone.

The cotransfection was performed using half of the amount of siRNAs when compared to transfection of one siRNA, so that the total amount of siRNA was equal. Therefore, off-target effects due to high siRNA concentrations could be excluded. On the other hand, the reduced siRNA concentration might lead to a reduced senescent phenotype and other cell cycle genes might be not as prominently misregulated when compared to single-siRNA-transfection.

To analyze how effective the transfection was, although the siRNA amount was halved, the mRNA level of the SRF-target gene TAGLN were determined. Cells have been transfected with the control-siRNA siGL2, siCDKN1B and siSRF797 alone and siCDKN1B and siSRF797 together using half of the amount as when transfected alone. The mRNA was isolated three days after transfection and analyzed via real-time RT-PCR.

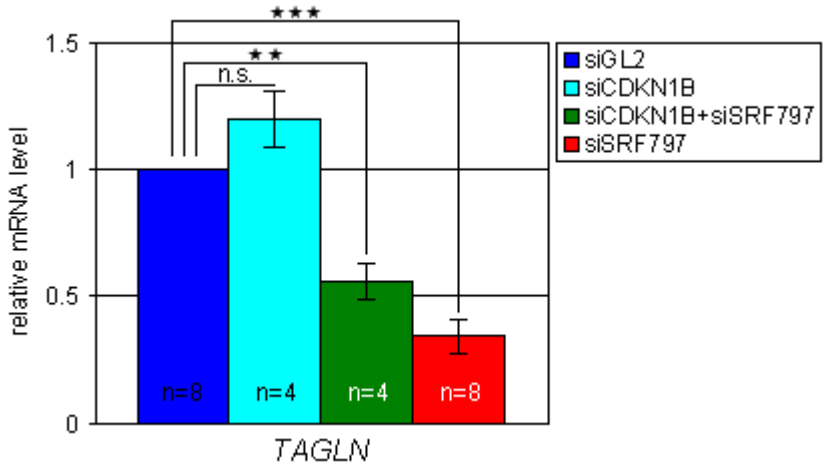

Figure 39 - relative mRNA of *TAGLN*

This figure shows the mRNA levels of the SRF target gene *TAGLN* three days after transfection. siCDKN1B+siSRF797 downregulated *TAGLN* to the same extent than siSRF797 alone (n.s.), whereas siCDKN1B-transfection did show any effected when compared to control siGL2-tranfected cells. All data was normalized to *GAPDH*. n = number of independent experiments, mean values ± SEM are shown, significance: two-tailed Student's t-test; $p>0.05$ = n.s.; $p<0.01$ = **; $p<0.001$= ***

The transfection of siCDKN1B did not affect the SRF-target gene *TAGLN* as expected. The transfection of siSRF797 alone showed again a very strong, expected decrease of *TAGLN* mRNA. For these transfections, the normal siRNA concentration was used (see 4.1.4 Transfection). The co-transfection was therefore performed using half of the amount of each siRNA. Figure 39 shows that the reduced amount had the same efficiency of downregulation of *TAGLN* mRNA as siSRF797-transfection alone ($p>0.05$).

5.6.2 Cotransfection of siSRF797 and siCDKN1B leads to a rescue of the senescent phenotype

After ensuring that the siRNA against *CDKN1B* and the cotransfection with siSRF797 worked, the cells have been stained for senescence three days after transfection. Cells have been stained as described in 4.1.6 Senescence-associated β-galactosidase activity staining. A counterstaining with DAPI was performed to determine total cell number.

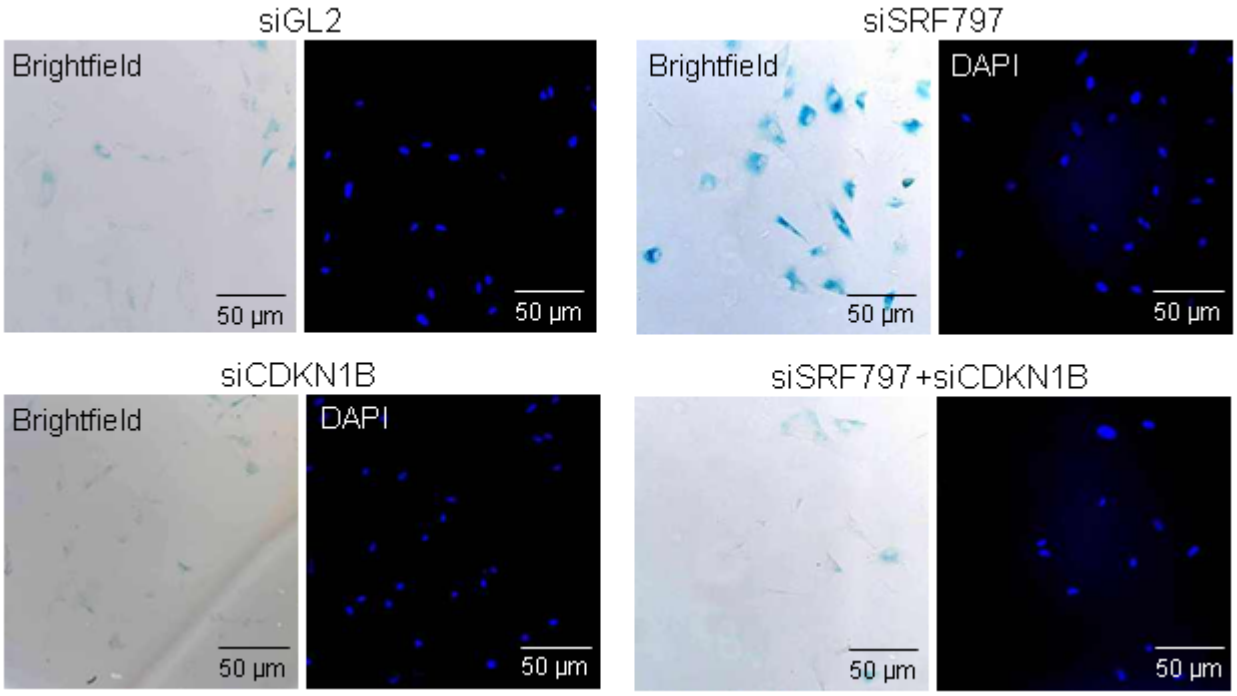

Figure 40 – Senescence staining of human SMCs after transfection with different siRNAs
This figure shows representative microscopy pictures of the differently transfected hsSMCs. Brightfield images have been used for countings of senescent cells and DAPI channel images have been used for counting of total cell numbers. A quantification of this experiment is shown in figure 41.

Figure 40 shows representative microscopy pictures of senescence staining of siGL2-, siSRF797-, siCDKN1B- or siCDKN1B+siSRF797-treated cells. Already upon visual inspection, it is clear that the cotransfection leads to a rescue. No differences can be seen between siGL2-, siCDKN1B- and siCDKN1B+siSRF797-transfected cells, whereas many dark blue (=senescent) cells can be observed after siSRF797-treatment. Figure 41 shows a quantification of these experiments.

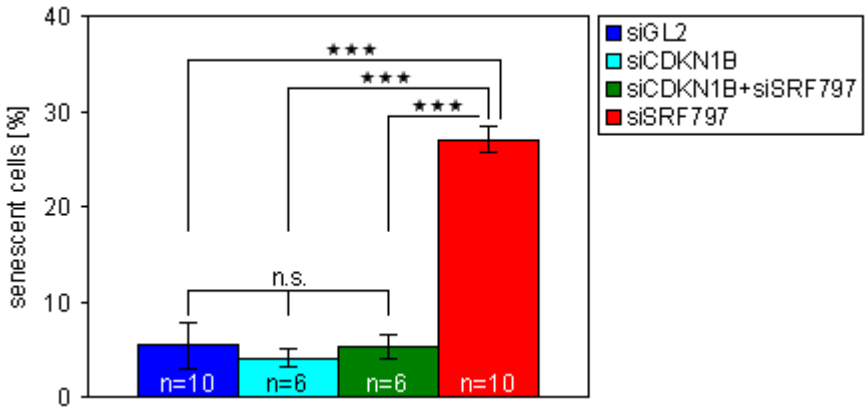

Figure 41 – Quantification of senescence stainings of human SMCs
This figure depicts the quantification of the senescence staining after siGL2-, siSRF797-, siSRF797+siCDKN1B- or siCDKN1B-transfection. The known induction of senescence after siSRF797-transfection can be again observed. Transfection of an siRNA against *CDKN1B* does not show a significant change when compared to siGL2-treated cells. Cotransfection of siSRF797 and siCDKN1B does not lead to significant change when compared to siGL2. n = number of independent experiments, mean values ± SEM are shown, significance: unpaired, two-tailed Student's t-test; $p>0.05$ = n.s.; $p<0.001$= ***

The quantification of the senescence stainings shows that a cotransfection of siSRF797 and siCDKN1B leads to a rescue, since no significant change is detectable when compared to siGL2- or siCDKN1B-treated cells. Transfection of siSRF797 alone shows the previously described strong and significant increase in senescent cells.

5.6.3 Analysis of *TP53* and *SKP2* levels after cotransfection of siSRF797+siCDKN1B

Since the senescent phenotype was rescued after the cotransfection of siSRF797 and siCDKN1B, the levels of cell cycle genes have also been checked. *SKP2* and *TP53*, which were the main inducers of senescence after siSRF797-transfection, have been analyzed. mRNA and proteins have been isolated three days after transfection and real-time RT-PCR and immunoblot analyses have been performed.

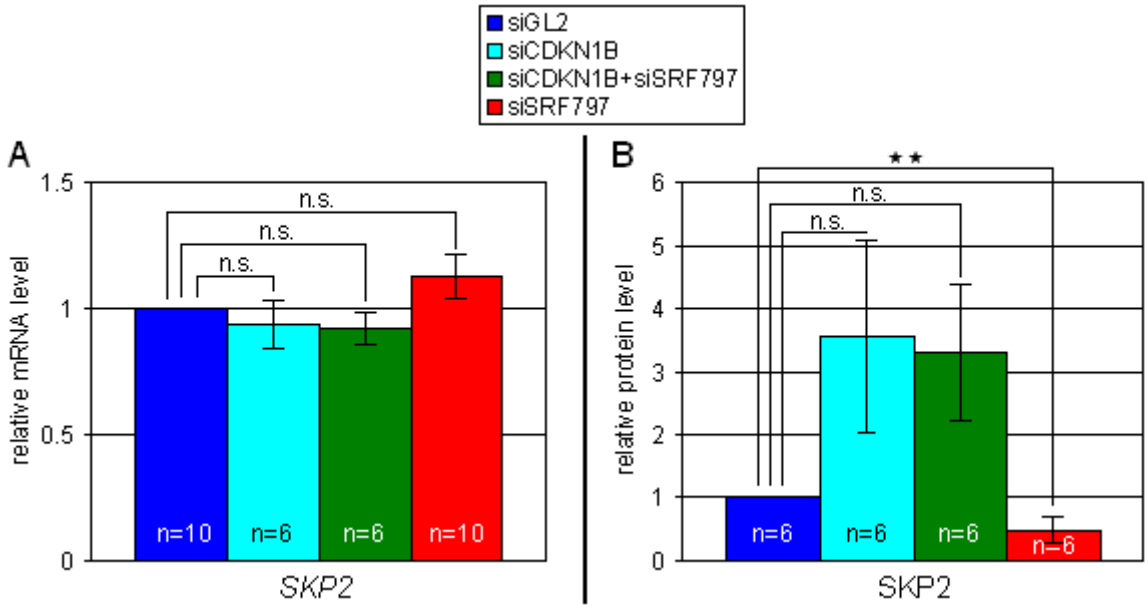

Figure 42 - relative mRNA and protein levels of SKP2
(**A**) depicts a summary of all data obtained for SKP2 mRNA levels. No transcriptional changes can be observed after any siRNA-transfection. (**B**) summarizes all immunoblot data. The slight but significant downregulation upon siSRF797-transfection can be detected. siCDKN1B and cotransfection of siCDKN1B+siSRF797 show a tendency to be upregulated, but it is not significant. All data was normalized to *GAPDH*. n = number of independent experiments, mean values ± SEM are shown, significance: two-tailed Student's t-test; $p>0.05$ = n.s.; $p<0.01$ = **

(**A**) shows a summary of all data obtained for *SKP2* mRNA levels after different siRNA-transfections. No significant changes can be detected. In (**B**) the immunoblots for SKP2 are summed up. siCDKN1B and siCDKN1B+siSRF797-transfection show a substantial, but not statistically significant upregulation of SKP2 protein. The results for siSRF797-transfection can be reproduced.

Since TP53 was upregulated after siSRF797- as well as after siSKP2 transfection, it was interesting to check if the cotransfection of siCDKN1B+siSRF797 has an effect on TP53 levels. Cells have been harvested three days after transfection. Isolated mRNA and protein levels were analyzed by real-time RT-PCR, respectively immunoblotting.

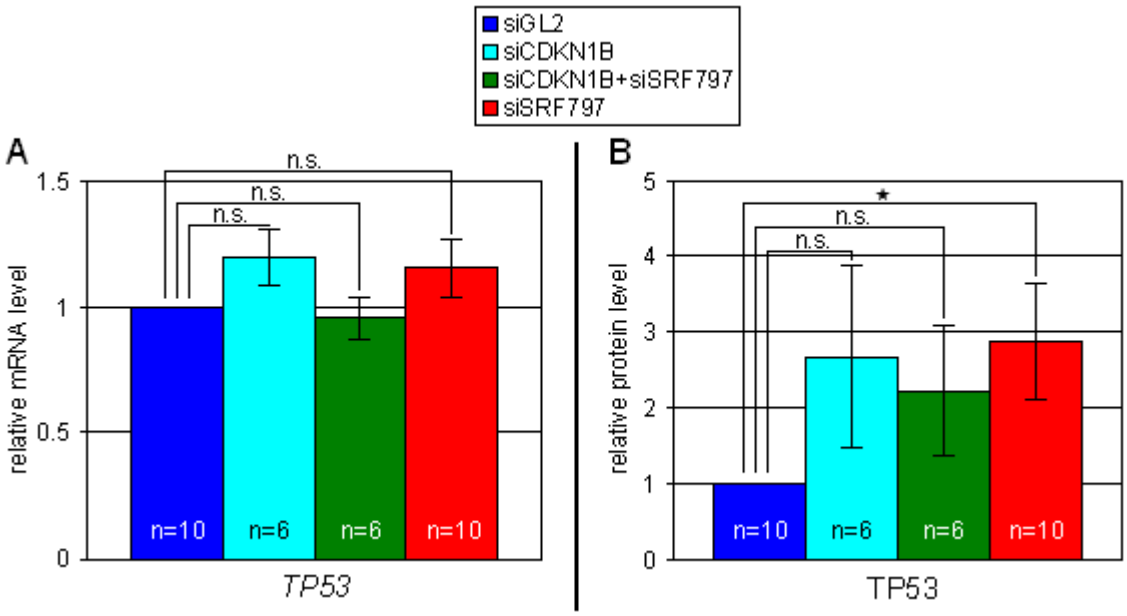

Figure 43 - relative mRNA and protein levels of TP53

(**A**) shows a summary of all real-time RT-PCR data of hsSMCs three days after transfection. None of the used siRNAs had an effect on *TP53* mRNA levels. (**B**) depicts the quantified immunoblots against TP53. The upregulation upon siSRF797-transfection can be observed again, whereas neither siCDKN1B nor siCDKN1B+siSRF797 show a significant alteration, but show a tendency to be upregulated. n = number of independent experiments, mean values ± SEM are shown, significance: two-tailed Student's t-test; $p>0.05$ = n.s.; $p<0.05$ = *

Cells cotransfected with siCDKN1B and siSRF797 do not show a change in expression of TP53 and SKP2, which was observed after siSRF797-transfection. The cotransfection rescues also the senescent phenotype (see figure 41). This finding point to a key role of CDKN1B- and SKP2 in siSRF797-triggered senescence.

6 Discussion

6.1 *Sus scrofa* as model organism for cardiologic studies

Sus scrofa is very often used as a model organism for cardiologic studies and bypass surgeries. It has a high homology to *Homo sapiens* and the heart is very similar in size and structure to the human heart, so that a lot of clinical trials or new techniques dealing with cardiac surgeries can be tested on *Sus scrofa* (for review see Schwartz et al., 2004).

The high homology could also be confirmed in this thesis via sequencing of *SRF*. The data shows that the whole MADS box and hence the recognition site for siSRF797 is completely conserved when compared to *Homo sapiens*. The downregulation after transfection is as efficient as in human SMCs. Therefore, the prerequisites for an siRNA application are fulfilled.

During bypass surgery the vein that will be used for the bypass, is kept in isotonic NaCl-solution. This time period could be used for the siRNA-transfection. This ex-vivo application and non-viral therapeutic might protect the bypass graft, since the antiproliferative effect of siSRF797 reduces the risk of hyperplasia and thereby restenosis. Another advantage of this technique is that the siRNA are only transfected into the bypass and they are degraded after a few days.

However, it should also be considered that the induction of senescence in these cells might even trigger sclerosis, since they are severely damaged and non-functional. The neighboring cells might react with an inflammatory response, which could lead to dying of the bypass graft (Motwani et al., 1998).

6.2 siSRF797 is a highly efficient and specific siRNA against *SRF* in different mammalian cells

After the validation of siGL2 as control and siSRF797 as most efficient siRNA against *SRF*, these siRNAs were used for further analyses. siSRF797-transfection led to a strong downregulation in human as well as in porcine primary SMCs. In addition, three *SRF* target genes, *ACTA2*, *CNN1* and *TAGLN*, showed a strong downregulation in both cell types after siSRF797-transfection.

The transfection procedure itself can induce an interferon response (Sledz et al., 2003; Hornung et al., 2005). However, the setup used in this thesis did not lead to an interferon response in human SMCs. The mRNA levels of OAS1 and STAT1 are markers for this and they did not show any change in expression levels. Therefore, off-target effects due to an interferon response could be excluded.

Other off-target effects could not be observed, since siSKP2- and siCDKN1B-transfection did not affect *SRF* mRNA and protein levels. A low siRNA concentration was used to reduce the risk, but there could still be undetected off-target effects.

Analyses of siSRF797-transfected cells showed a strong increase of TP53, which might be a problem. A further increase of TP53 might induce apoptosis (Szak et al., 2001) and then an siSRF797-application in bypass grafts would not be possible.

6.3 Downregulation of *SRF* triggers senescence in human and porcine SMCs

It has been shown that *SRF* plays an important role in many cellular processes. Gauthier-Rouviere et al. showed in 1991 that impaired SRF activity led to an inhibition of cell cycle progression in somatic cells, which already hints to SRF playing a role in cell cycle regulation. Schratt et al. showed in contrast that murine *Srf*-/- ES cells proliferate normally (2002). Compensatory mechanisms could be activated in knock-out cells and might explain the different results. Although a lot studies have been published about Srf knockout cells and mouse models, only few data exist about SRF and its role in cell cycle regulation in primary human vascular SMCs.

The first reports about *SRF* and a possible role in senescence were published in 1999 and 2001. Meyyappan et al could show in 1999 that SRF binding activity is reduced in senescent fibroblasts, which leads to a decreased expression of Egr-1 and c-fos. Ding et al. reported in 2001 that SRF is absent in the nuclei of senescent fibroblasts. This was confirmed by Han et al. in 2006. They detected the translocation of SRF in senescent HUVECs and the inactivation of *SRF* corresponds with the senescent phenotype. Whether the senescence leads to the inactivation of *SRF* or if the inactivation of *SRF* induces the senescence could not be resolved. This thesis shows that downregulation of *SRF* in human and porcine SMCs leads to the induction of senescence. Angstenberger et al. showed in 2007 that homozygous inactivation of *Srf* in murine colon-derived SMCs led also to an induction of senescence, which supports the results of this thesis, that *SRF* depletion results in senescence in this cell class.

This indicates that *SRF* seems to be a positive regulator of cell proliferation. Downregulation of *SRF* causes senescence in human and porcine SMCs. The translocation of SRF, which was observed by other groups, is probably a requirement for the establishment for senescence, not a consequence.

6.4 The *TP53-CDKN1A* axis and its possible role in siSRF797-triggered senescence

CDKN1A and *TP53* are known to build the so-called *CDKN1A-TP53* axis that has been described as essential for senescence (Noda et al., 1994). *TP53* is a transactivator of *CDKN1A* and can thereby induce a G_1 arrest due to increased CDKN1A protein levels. *TP53* mRNA showed no change in our experimental setup, whereas the protein level showed a high and significant upregulation upon siSRF797 transfection. This is probably due to the posttranslational control of TP53, since its protein level is determined by the rate of degradation and not transcription (Momand et al., 1992). The upregulation of *CDKN1A* mRNA, which was observed after siSRF797-transfection, is probably due to the transcriptional activation by TP53. The downregulation of CDKN1A protein is perplexing, but could be due to posttranslational degradation. Two publications report a similar observation: Human breast cancer cells and fibroblasts that were treated with iron chelators were arrested in G_1. These cells showed also an increased *CDKN1A* mRNA levels, but decreased protein levels (Fu et al., 2007; Le et al., 2003). Therefore, it might be that the high *CDKN1A* mRNA levels are due to the transactivation of TP53, but cannot be translated due to a mislocation in the nucleus.

The cotransfection of siCDKN1B+siSRF797 showed no senescent phenotype, so it was interesting if also *TP53* levels showed a different expression pattern. *TP53* was neither on mRNA nor protein level altered when compared to control cells, which fits to the non-senescent phenotype and point to a role for TP53 in siSRF797-triggered senescence.

Downregulation of *SKP2* led to a similar induction of senescence when compared to siSRF797-transfected cells in the β-galactosidase activity staining. *TP53* mRNA is slightly, but significantly upregulated, whereas the protein shows high variances in expression level. However, this slight alteration is probably not sufficient to induce the siSKP2-triggered senescence, but TP53 might contribute to this phenotype.

6.5 Role of *SKP2* and *CDKN1B* in siSRF797-triggered senescence

It has been recently shown that besides the well-known *TP53*-*CDKN1A*-axis another axis plays a role in senescence, the *SKP2*-*CDKN1B*-axis. CDKN1B is a CDK inhibitor like CDKN1A. It inhibits CDK2, thereby blocking G_1/S-transition (Knudsen et al., 1997). *CDKN1B* can be downregulated by different pathways. SCF^{SKP2} complex ubiquitinates CDKN1B leading to its proteasomal degradation (Pagano et al., 1995), but CDKN1B can also be ubiquitinated by KPC (KIP1 ubiquitination-promoting complex) (Kamura et al., 2004).

Downregulation of *SRF* led to decreased levels of SKP2 protein and increased levels of CDKN1B protein, which points to the establishment of senescence via the *SKP2*-*CDKN1B*-axis. *SKP2* mRNA was not affected upon siSRF797-transfection, whereas the protein was significantly downregulated. This fits to previous papers that demonstrate the posttranslational regulation of SKP2 (Wirbelauer et al., 2000; Bashir et al., 2004; Wei et al., 2004). Shin et al. showed in 2008 that a downregulation of *SKP2* by siRNAs led to a G_1 arrest in SK-OV-3 cells and Fujita et al could also show in 2008 that siSKP2-transfection slowed down the cell cycle in tumor cells. To analyze the role of *SKP2* in siSRF797-triggered senescence, siSKP2 was transfected into human SMCs. Downregulation of *SKP2* led also to an induction of senescence in human SMCs. This finding is in line with the publication of Shin et al. (2008). *CDKN1B* levels did not show any change upon siSKP2-transfection in human SMCs. Nakayama et al. showed in 2000 that Cdkn1b protein is upregulated in *Skp2* murine knockout cells and thereby induces senescence, but Shin et al. did not check in their experimental setup, if CDKN1B is upregulated upon downregulation of *SKP2.* Therefore, it is likely, that there is another mechanism, which contributes to the senescent phenotype after downregulation of *SKP2*, which is also activated in our experimental setup.

Several papers show that an upregulation of *CDKN1B* drives cells into senescence (Tamir et al., 2000; Alexander et al., 2001; Martinez et al., 2004). Downregulation of *SRF* led to a slight increase of *CDKN1B* mRNA, but a strong upregulation on protein level. To investigate, if the increased CDKN1B protein levels are important for

siSRF797-triggered senescence, we cotransfected siCDKN1B and siSRF797. The cotransfection showed no increase of senescence when compared to control siGL2-transfected cells. The amount of siRNAs was halved for cotransfection, so that the lower siRNA concentration might be reason for the basal level of senescence. But since the reduced amount led to a similar reduction of *SRF* and *CDKN1B* mRNA level when compared to single transfected using the double amount of siRNAs, this is not very likely. The rescue of the senescent phenotype upon cotransfection points to a key role for *CDKN1B* in siSRF797-triggered senescence.

6.6 Conclusions and Outlook

This thesis demonstrates that porcine and humans *SRF* have a high homology and that therefore *Sus scrofa* is suitable for a cardiologic model using siSRF797 to maybe overcome the hyperproliferative vascular pathologies after bypass surgeries.

The cellular mechanisms, which induce the senescent phenotype after downregulation of *SRF*, could be not completely clarified, but it is obvious that *SRF* plays a key role in the inhibition of senescence in human and porcine SMCs.

Supplemental experiments using siSKP2 led to the conclusion that *SKP2* downregulation upon SRF-depletion is probably not the only player responsible for the strong upregulation of *CDKN1B*. *CDKN1B* transcription might be transactivated by BRCA1, but since the mRNA level was not very strong upregulated, it is more likely that the downregulation of CDKN1B by KPC is disturbed.

The cotransfection of siSRF797+siCDKN1B points to *CDKN1B* as main inducer for siSRF797-triggered senescence, since the senescent phenotype was rescued and also *TP53* and *SKP2* did not show a change in expression upon cotransfection of siSRF797+siCDKN1B.

Several papers point to a cytoskeletal-related mechanism, how *SRF* affects *SKP2* and consequently *CDKN1B*. *SRF* is a well-known regulator of actin dynamics. Schratt et al. showed 2002 that Ptk2 is mislocalized in *Srf*-/- ES cells. Total Ptk2 protein was not changed, but its activity was reduced to about 50% in *Srf* knockout cells. Angstenberger et al. used primary colon SMCs and demonstrated reduced F-actin levels and a degenerated stress fiber network in *Srf*-/- SMCs (2007).

A link between cytoskeleton and SKP2 was published by Mammoto et al. 2004 and Bond et al., 2004 and 2008. Bond et al. showed in 2004 that Skp2 expression is dependent on Ptk2 in rat SMC. RhoA activity is also required for SKP2 expression in human endothelial cells (Mammoto et al. 2004). Bond et al. showed in 2008 using rat SMCs that Rac_1-dependent actin polymerization controls Skp2 levels.

These reports suggest a scenario, where SRF stabilizes PTK2, which in turn leads to actin polymerization. High F-actin increases SKP2 protein by reducing proteolysis of SKP2. Elevated SKP2 protein then leads to an increased degradation of CDKN1B and thereby to SMC proliferation.

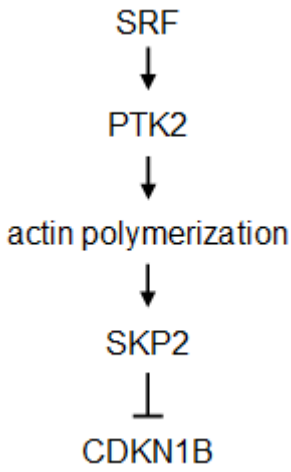

Figure 44 – hypothesis about how SRF controls smooth muscle cell proliferation

Primary vascular human and porcine smooth muscle cells have been used to study the role of *SRF* in these cells in more detail, since not much is known about the role of *SRF* in primary vascular SMCs.

The approach using siRNAs is a fast and efficient way to downregulate a specific protein and it has probably less influence on other cellular processes as other methods like shRNA-expressing plasmids.

The block of proliferation by usage of siSRF797 or siSKP2 might be a useful approach to handle hyperproliferative vascular pathologies like restenosis after bypass surgeries.

7 Summary

This PhD thesis deals with the role of the transcription factor *SRF* (*serum response factor*) in smooth muscle cell proliferation and cellular senescence. An siRNA approach was used to reduce *SRF* in human and porcine primary smooth muscle cells. These cells are much closer to the real *in vivo* situation than immortalized cell lines.

siRNA-transfection did not lead to an interferon response. siSRF797 showed a highly specific downregulation in human as well as in porcine SMCs. Sequencing of *Sus scrofa SRF* showed a very high evolutionary conservation when compared to *Homo sapiens*. Therefore, the siRNA can be tested in the porcine animal model and later in clinical trials.

Downregulation of *SRF* caused a block in G_1/S transition. *TP53* upregulation and SKP2 protein downregulation led to an increase in CDKN1B protein, which was responsible for the senescence induction. siSKP2-transfection showed a similar increase in senescent cells, but only a slight increase of *CDKN1B* could be determined. Therefore, the downregulation of *SKP2* is not the only reason for the strong increase of *CDKN1B* after siSRF797-transfection. A cotransfection of siCDKN1B+siSRF797 could rescue the senescent phenotype. So in conclusion, the *CDKN1B* upregulation is the main inducer of senescence after downregulation of *SRF*.

The data lead to the conclusion that *SRF* plays a key role in the inhibition of cellular senescence in human and porcine smooth muscle cells.

8 Zusammenfassung

Diese Dissertation untersucht die Rolle des Transkriptionsfaktors *SRF* (*Serum response factor*) in der Zellproliferation und zellulären Seneszenz von Glattmuskelzellen. Die siRNA-Technik wurde verwendet, um *SRF* in primären Glattmuskelzellen von Mensch und Schwein zu reduzieren. Diese Zellen kommen der in vivo Situation viel näher als immortalisierte Zelllinien.

Die Transfektion der siRNAs zeigte keine Induktion einer Interferon-Antwort. siSRF797 zeigte eine starke und spezifische Reduktion in Glattmuskelzellen von Mensch als auch von Schwein. Sequenzanalysen von *SRF* in *Sus scrofa* zeigten eine hohe Konservierung, so dass diese siRNA sowohl im Tiermodell Schwein als auch später in klinischen Studien verwendet werden kann.

Eine Reduktion von *SRF* führte zu einem Block im G_1/S-Übergang. Eine Hochregulierung von *TP53* und eine Runterregulierung des SKP2-Proteins hatten eine erhöhte Expression von *CDKN1B* zur Folge, die für die Induktion der Seneszenz verantwortlich ist. Eine siSKP2-Transfektion zeigte einen ähnlich hohen Anstieg der seneszenten Zellen, aber führte nur zu einer geringen Erhöhung von *CDKN1B*. Daher ist die Erniedrigung des SKP2-Proteins nicht der einzige Grund für den starken Anstieg von *CDKN1B* nach siSRF797-Transfektion. Eine Kotransfektion von siCDKN1B+siSRF797 konnte die Seneszenz verhindern. Zusammenfassend ist also die Hochregulierung von *CDKN1B* für die Induktion der Seneszenz nach Runterregulierung von *SRF* verantwortlich.

Diese Daten führen zu der Folgerung, dass *SRF* eine Schlüsselrolle in der Inhibition der zellulären Seneszenz in Glattmuskelzellen von Mensch und Schwein innehat.

9 Abbreviations

°C	°Celsius
µg	microgram
µl	microliters
µM	micromole
A	adenine
aa	amino acids
as	antisense strand
alpha	antibodies against
APC	Anaphase promoting complex
APS	Ammonium peroxodisulfate
ATP	Adenosine-tri-phosphate
β-ME	β-mercaptoethanole
b	bases
bp	base pairs
C	cytosine
CDK	Cyclin-dependent kinase
cDNA	complementary DNA
cm	centimeter
DAPI	4',6-diamidino-2-phenylindole
DBD	DNA binding domain
DMF	N,N-Dimethylformamide
DMSO	dimethylsulfoxide
DNA	desoxyribonucleic acid
dNTP	deoxy nucleotide-triphosphate
DTT	Dithiothreitol
dsRNA	double-stranded RNA
ECM	extracellular matrix
EDTA	ethylenediaminetetraacetic acid
ES	Embryonic stem cells
FBS	fetal bovine serum
G	guanine
GAPDH	Glycerinaldehyde 3-phosphate dehydrogenase
g	gram
hs	Homo sapiens
kDa	kilo Dalton

l	liter
M	Mol
mA	milliampere
MADS	MCM1, Agamous, Deficiens and SRF
min	minutes
ml	milliliter
mM	millimol
MPF	Mitosis or maturation promoting factor
mRNA	messenger RNA
NLS	nuclear localisation sequenz
PAA	Poly-acrylamide (Acrylamide-Solution)
PBS	phosphate-buffered saline
PCR	polymerase chain reaction
pH	potential of hydrogen
rel	relative
RISC	RNA-induced silencing complex
RNA	ribonucleic acid
RNAi	RNA interference
rpm	rounds per minute
RT-PCR	reverse-transcripase polymerase chain reaction
s	sense strand
SDS	sodium-dodecyl-sulfate
siRNA	small interfering RNA
SMC	smooth muscle cell
SRF	Serum Response Factor
ss	Sus scrofa
T	thymine
TAD	transactivation domain
TCF	Ternary complex factors
TEMED	Tetramethylethylenediamine
Tris	Trizma base
U	uracil
V	Volt

10 Table of figures

		Page
Figure 1	The *SRF* gene	9
Figure 2	SRF-dimer binding to DNA	10
Figure 3	Sequence logos of known and novel SRF-binding sequences	11
Figure 4	Schematic overview of two principal pathways that regulate SRF activity	12
Figure 5	Schema of SRF and its cofactors	13
Figure 6	Formation of a ternary complex	13
Figure 7	Model of mutually exculsive binding of MAL and TCFs to SRF	14
Figure 8	Schematic drawing of cell cycle	18
Figure 9	G_1/S transition-pathway	22
Figure 10	Comparison of artery and vein	28
Figure 11	Cross-bridge-cycling	29
Figure 12	Schematic model of phenotypic modulation	30
Figure 13	Mechanisms that contribute to SMC proliferation after bypass surgery	32
Figure 14	Basic steps of RNAi	35
Figure 15	Agarose gel with PCR products	62
Figure 16	Segment of raw data after sequencing of porcine SRF	63
Figure 17	Porcine SRF cDNA, siRNA target site is marked	64
Figure 18	Alignment of human and porcine cDNA. MADS box and siSRF797 recognition site are marked	65/66
Figure 19	Porcine SRF protein with MADS-box highlighted	67
Figure 20	Alignment of human and porcine SRF protein	68
Figure 21	relative mRNA levels of *SRF* in human SMCs	69
Figure 22	Relative mRNA levels of markers for interferon response	70
Figure 23	mRNA and protein levels of SRF in human SMCs	71
Figure 24	mRNA and protein levels of *SRF* in porcine SMCs	72
Figure 25	Downregulation of SRF target genes in human and porcine SMCs after depletion of SRF	73
Figure 26	Senescence staining and quantification of human SMCs after siSRF797-transfection	74
Figure 27	Senescence staining and quantification of porcine SMCs after *SRF* downregulation	75
Figure 28	Data for CDKN1B mRNA and protein levels in human SMCs after transfection	76

Figure 29	Summary of all results obtained for *SKP2* in transfected human SMCs	77
Figure 30	*TP53* levels in human SMCs after downregulation of *SRF*	78
Figure 31	Data for CDKN1A mRNA and protein levels in human SMCs after transfection	79
Figure 32	siSKP2-transfection leads to a decrease of SKP2 mRNA and protein	80
Figure 33	Senescence staining and quantification of human SMCs after *SKP2* downregulation	81
Figure 34	Analysis of *SRF* and *TAGLN* levels after transfection of siSKP2	82
Figure 35	Analysis of *CDKN1B* levels after transfection of siSKP2	83
Figure 36	Analysis of *TP53* levels after transfection of siSKP2	84
Figure 37	relative mRNA and protein levels of *CDKN1B*	85
Figure 38	relative mRNA and protein levels of *SRF*	86
Figure 39	relative mRNA of *TAGLN*	87
Figure 40	Senescence staining of human SMCs after transfection with different siRNAs	88
Figure 41	Quantification of senescence stainings of human SMCs	89
Figure 42	relative mRNA and protein levels of SKP2	90
Figure 43	relative mRNA and protein levels of TP53	91
Figure 44	Hypothesis about how SRF controls SMC proliferation	99

11 References

Abraham PA, Smith DW, Carnes BH (1974). Synthesis of soluble elastin by aortic medial cells in culture. *Biochem Biophys Res Comm 58*, 597-604

Agrawal S and Kandimalla ER (2004). Role of Toll-like receptors in antisense and siRNA. *Nat biotechnol 22*, 1533-1537

Alexander K, Hinds PW (2001). Requirement for p27(KIP1) in retinoblastoma protein-mediated senescence. *Mol Cell Biol 21*, 3616-3631

Amati B, Vlach J (1999). Kip1 meets SKP2: new links in cell-cycle control. *Nat Cell Biol 1*, 91-93

AmericanHA = American Heart Association (2004). http://www.americanheart.org

Angstenberger M, Wegener JW, Pichler BJ, Judenhofer MS, Feil S, Alberti S, Feil R, Nordheim A (2007). Severe intestinal obstruction on induced smooth muscle-specific ablation of the transcription factor SRF in adult mice. *Gastroenterology 133*, 1948-1959

Anitchkov N and Chalatow S (1913). Über experimentelle Cholesterinsteatose und ihre Bedeutung für die Entstehung einiger pathologischer Prozesse. *Zentrbl Allg Pathol Pathol Anat 24,* 1-9

Aravind L, Koonin EV (2000). SAP – a putative DNA-binding motif involved in chromosomal organization. *Trends Biochem Sci 25*, 112-114

Arsenain S, Weinhold B, Oelschlager M, Ruthner U, Nordheim A (1998). Serum response factor is essential for mesoderm formation during mouse embryogenesis. *Embo J 17*, 6289-6299

Aylon Y, Oren M (2007). Living with p53, Dying of p53. *Cell 130*, 597-600

Baserga R (1985). The Biology of Cell Reproduction. MA: *Harvard University Press*

Bashir T, Dorrello NV, Amador V, Guardavaccaro D, Pagano M (2004). Control of the SCF(Skp2-Cks1) ubiquitin ligase by the APC/C(Cdh1) ubiquitin ligase. *Nature 428*, 190-193

Belaguli NS, Zhou W, Trinh TH, Majesky MW, Schwartz RJ (1999). Dominant negative murine serum response factor: alternative splicing within the activation domain inhibits transactivation of serum response factor binding targets. *Mol Cell Biol 19*, 4582-4591

Benimetskaya L, Loike JD, Khaled Z, Loike G, Silverstein SC, Cao L, el Khoury J, Cai TQ, Stein CA (1997). Mac-1 (CD11b/CD18) is an oligodeoxynucleoride-binding protein. *Nat Med 3*, 414-420

Bertolotto C, Ricci JE, Luciano F, Mari B, Chambard JC, Auberger P (2000). Cleavage of the serum response factor during death receptor-induced apoptosis results in an inhibition of the c-FOS promoter transcriptional activita. *J Biol Chem 275*, 12941-12947

Blagosklonny MV (2006). Cell senescence: hypertrophic arrest beyond the restriction point. *J Cell Physiol 209*, 592-597

Bodnar AG, Ouellette M, Frolkis M, Holt SE, Chiu CP, Morin GB, Harley CB, Shay JW (1998). Extension of life-span by introduction of telomerase into normal human cells. *Science 279*, 349-352

Bond M, Sala-Newby GB, Newby AC (2004). Focal adhesion kinase (FAK)-dependent regulation of S-phase kinase associated protein-2 (Skp-2) stability. A novel mechanism regulating smooth muscle cell proliferation. *J Biol Chem 279*, 37304-37310

Bond M, Wu YJ, Sala-Newby GB, Newby AC (2008). Rho GTPase, Rac1, regulates Skp2 levels, vascular smooth muscle cell proliferation, and intima formation in vitro and in vivo. *Cardiovasc Res 80*, 290-298

Buchwalter G, Gross C, Wasylyk B (2004). Ets ternary complex transcription factors. *Gene 324*, 1-14

Campisi J, d'Adda di Fagagna F (2007). Cellular senescence: when bad things happen to good cells. *Nat Rev Mol Cell Biol 9*, 729-740

Carmichael GG (2003). Antisense starts making more sense. *Nat biotechnol 21*, 371-372

Carnac G, Primig M, Kitzmann M, Chafey P, Tuil C, Lamb N, Fernandez A (1998). RhoA GTPase and serum response factor control selectively the expression of MyoD without affecting Myf5 in mouse myoblasts. *Mol Biol Cell 9*, 1891-1902

Casscells W, Engler D, Willerson JT (1994). Mechanisms of restenosis. *Tex Heart Inst J 21*, 68-77

Chai J, Jones MK, Tarnawski AS (2004). Serum response factor is a critical requirement for VEGF signalling in endothelial cells and VEGF-induced angiogenesis. FASEB J 18, 1264-1266

Chamley-Campbell JH, Campbell GR, Ross R (1982). Phenotype-dependent response of cultured aortic smooth muscle to serum mitogens. *J Cell Biol. 89*, 379-383

Chen QM, Tu VC, Liu J (2000). Measurements of hydrogen peroxide induced premature senescence: senescence-associated beta-galactosidase and DNA synthesis index in human diploid fibroblasts with down-regulated p53 or Rb. *Biogerontology 1*, 335-339

Claassen GF, Hann SR (2000). A role for transcriptional repression of p21CIP1 by c-Myc in overcoming transforming growth factor beta-induced cell-cycle arrest. *Proc Natl Acad Sci USA 97*, 9498-9503

Cohen-Fix O, Peters JM, Kirschner MW, Koshland D (1996). Anaphase initiation in Saccaromyces cerevisiae is controlled by the APC-dependent degradation of the anaphase inhibitor Pds1p. *Genes Dev 10*, 3081-3093

Collado M, Blasco MA, Serrano M (2007). Cellular senescence in cancer and aging. *Cell 130*, 223-233

Couderc B, Penary M, Tohfe M, Pradines A, Casteignau A, Berg D, Favre G (2006). Reversible inactivation of the transcriptional function of P53 protein by farnesylation. *BMC Biotechnol 6:26*

Cristofalo VJ (2005). SA beta Gal staining: biomarker or delusion. *Exp Gerontol 40*, 836-838

Davis FJ, Gupta M, Pogwizd SM, Bacha E, Jeevanandam V, Gupta MP (2002). Increased expression of alternatively spliced dominant-negative isoform of SRF in human failing hearts. *Am J Physiol Heart Circ Physiol 282*, 1521-1533

Dettman RW, Denetclaw W Jr, Ordahl CP, Bristow J (1998). Common epicaridal origin of coronary vascular smooth muscle, perivascular fibroblasts, and intermyocardial fibroblasts in the avian heart. *Dev Biol 193*, 169-181

DeRuiter MC, Poelmann RE, VanMunsteren JC, Mironov V, Markwald RR, Gittenberger-de Groot AC (1997). Embryonic endothelial cells transdifferentiate into mesenchymal cells expressing smooth muscle actins in vivo and in vitro. *Circ Res 80*, 444-451

Díaz-Hernandez M, Torres-Peraza J, Salcatori-Abarca A, Morán MA, Gómez-Ramos P, Alberch J, Lucas JJ (2005). Full motor recovery despite striatal neuron loss and formation of irreversible amyloid-like inclusions in a conditional mouse model of Huntington's disease. *J Neurosci 25*, 9773-9781

Dimri GP, Lee X, Basile G, Acosta M, Scott G, Roskelley C, Medrano EE, Linskens M, Rubelj I, Pereira-Smith O, Peacocke M, Campisi J (1995). A biomarker that identifies senescent human cells in culture and in aging skin in vivo. *Proc Natl Acad Sci USA 92*, 9363-9367

Ding W, Gao S, Scott RE (2001). Senescence represses the nuclear localization of the serum response factor and differentiation regulates its nuclear localization with lineage specificity. *J Cell Sci 114*, 1011-1018

Dulic V, Stein GH, Far DF; Reed SI (1998). Nuclear accumulation of p21Cip1 at the onset of mitosis: a role at the G2/M-phase transition. *Mol Cell Biol 18*, 546-557

Dunphy WG (1994). The decision to enter mitosis. *Trends Cell Biol 4*, 202-207

El-Deiry WS, Tokino T, Velculescu VE, Levy DB, Parsons R, Trent JM, Lin D, Mercer WE, Kinzler KW, Vogelstein B (1993). WAF1, a potential mediator of p53 tumor suppression. *Cell 75*, 817-825

El-Deiry WS, Harper JW, O'Connor PM, Velculesco VE, Canman CE, Jackman J, Pietenpol JA, Burrell M, Hill DE, Wang Y, et al. (1994). WAF1/CIP1 is induced in p53-mediated G1 arrest and apoptosis. *Cancer Res 54*, 1169-1174

Elbashir SM, Lendeckel W, Tuschl T (2001). RNA interference is mediated by 21- and 22-nucleotide RNAs. *Genes Dev 15*, 188-200

Farhood H, Serbina N, Huang L (1995). The role of dioleoyl phophatidylethanolamine in cationic liposome mediated gene transfer. *Biochim Biophys Acta 1235*, 289-295

Fatigati V, Murphy RA (1984). Actin and tropomyosin variants in smooth muscles. Dependence on tissue type. *J Biol Chem 259*, 14383-14388

Felgner JH, Kumar R, Sridhar CN, Wheeler CJ, Tsai YJ, Border R, Ramsey P, Martin M, Felgner PL (1994). Enhanced gene delivery and mechnism studies with a novel series of cationic lipid formulations. *J Biol Chem 269*, 2550-2561

Fire A, Xu S, Montgomery MK, Kostas SA, Driver SE, Mello CC (1998). Potent and specific genetic interference by double-stranded RNA in Caenorhabditis elegans. *Nature 391*, 806-811

Flores-Rozas H, Kelman T, Dean FB, Pan ZQ, Harper JW, Elledge SJ, O'Donnell M, Hurwitz J (1994). Cdk-interacting protein 1 directly binds with proliferating cell nuclear antigen and inhibits DNA replication catalyzed by the DNA polymerase delta holoenzyme. *Proc Natl Acad Sci USA 91*, 8655-8659

Fox SI (1993). Human Physiology - 4th edition. *W.C. Brown Publishers*

Fu D, Richardson DR (2007). Iron chelation and regulation of the cell cycle: 2 mechanisms of posttranscriptional regulation of the universal cyclin-dependent kinase inhibitor p21CIP1/WAF1 by iron depletion. *Blood 110*, 752-761

Fujii M, Tsuchiya H, Chuhjo T, Minamino T, Miyamoto K, Seiki M (1994). Serum response factor has functional roles both in indirect binding to the CArG box and in the transcriptional activation function of human T-cell leukaemia virus type I Tax. *J Virol 68*, 7275-7283

Fujita T, Liu W, Doihara H, Date H, Wan Y (2008). Dissection of the APCCdh1-Skp2 cascade in breast cancer. *Clin Cancer Res 14*, 1966-1975

Gao X, Huang L (1995). Cationic liposome-mediated gene transfer. *Gene Ther 2*, 710-722

Gauthier-Rouviere C, Cavadore JC, Blanchard JM, Lamb N, Fernandez A (1991). p67SRF is constitutive nuclear protein implicated in the modulation of genes required throughout the G1 period. *Cell Regul 2*, 575–588

Geley S, Kramer E, Gieffers C, Gannon J, Peters JM, Hunt T (2001). Anaphase-promoting complex/cyclosome-dependent proteolysis of human cyclin A starts at the beginning of mitosis and is not subject to the spindle assembly checkpoint. *J Cell Biol 153*, 137-148

Giaccia AJ, Kastan MB (1998). The complexity of p53 modulation: emerging patterns from divergent signals. *Genes Dev 12*, 2973-83

Gil J, Peters G (2006). Regulation of the INK4b-ARF-INK4a tumour suppressor locus: all for one or one for all. *Nat Rev Mol Cell Biol 9*, 667-677

Gilman MZ, Wilson RN, Weinberg RA (1986). Multiple protein-binding sites in the 5'-flanking region regulate c-fos expression. *Mol Cell Biol 6*, 4305-4316

Gimona M, Herzog M, Vandekerckhove J, Small JV (1990). Smooth muscle specific expression of calponin. *FEBS Lett 274*, 159-162

Gineitis D, Treisman R (2001). Differential usage of signal transduction pathways defines two types of serum response factor target gene. *J Biol Chem 276*, 24531-24539

Gittenberger-de Groot AC, DeRuiter MC, Bergwerff M, Poelmann RE (1999). Smooth muscle cell origin and its relation to heterogeneity in development and disease. *Arterioscler Throm Vasc Biol 19*, 1589-1594

Glukhova MA, Frid MG, Koteliansky VE (1990). Developmental changes in expression of contractile and cytoskeletal proteins in human aortic smooth muscle. *J Biol Chem 562*, 13042-13046

Han YL, Yu HB, Yan CH, Kang J, Meng ZM; Zhang XL, Li SH, Wang SW (2006). Rac1 accelerates endothelial cell senescence induced by hypoxia in vitro. *Sheng Li Xue Bao 58*, 207-216

Harper JW, Elledge SJ, Keyomarsi K, Dynlacht B, Tsai LH, Zhang P, Dobrowolski S, Bai C, Connell-Crowley L, Swindell E, Pat Fox M, Wei N (1995). Inhibition of cycle-dependent kinases by p21. *Mol Biol Cell 6*, 387-400.

Harris SL, Levine AJ (2005). The p53 pathway: positive and negative feedback loops. *Oncogene 24*, 2899-2908

Hautmann MB, Madsen CS, Mack CP, Owens GK (1998). Substitution of the degenrate smooth muscle (SM) alpha-actin CC(A/Trich)6GG elements with c-fos serum response elements results in increased basal expression but relaxed SM cell specificity and reduced angiotensin II inducibility. *J Biol Chem 14*, 8398-8406

Hayflick L, Moorhead PS (1961). The serial cultivation of human diploid cell strains. *Exp Cell Res 25*, 585-621

Heidel JD, Hu S, Liu XF, Triche TJ, Davis ME (2004). Lack of interferon response in animals to naked siRNAs. *Nat biotechnol 22*, 1579-1582

Heidenreich O, Neininger A, Schratt G, Zinck R, Cahill MA, Engel K, Kotlyarov A, Kraft R, Kosta S, Gaestel M, Nordheim A (1999). MAPKAP kinase 2 phosphorylates serum response factor in vitro and in vivo. *J Biol Chem 274*, 14434-14443

Herzinger T, Funk JO, Hillmer K, Eick D, Wolf DA, Kind P (1995). Ultraviolet B irradiation-induced G2 cell cycle arrest in human keratinocytes by inhibitory phoshorylation of the cdc2 cell cycle kinase. *Oncogene 11*, 2151-2156

Hipskind RA, Rao VN, Mueller CG, Reddy ES, Nordheim A (1991). Ets-related protein Elk-1 is homologous to the c-fos regulatory factor p62TCF. *Nature 354*, 531-534

Hill CS, Wynne J, Treisman R (1994). Serum-regulated transcription by serum response factor (SRF): a novel role for the DNA binding domain. *EMBO J 13*, 5421-5432

Hill CS, Wynne J, Treisman R (1995). The Rho family GTPases RhoA, Rac1, and CDC42Hs regulate transcriptional activation by SRF. *Cell 81*, 1159-1170

Hornung V, Guenthner-Biller M, Bourquin C, Ablasser A, Schlee M, Uematsu S, Noronha A, Manoharan M, Akira S, de Fougerolles A, Endres S, Hartmann G (2005). Sequence-specific potent induction of IFN-α by short interfering RNA in plasmacytoid dendritic cells through TLR7. *Nat Med 11*, 263-270

Howard A, Pelc SR (1951). Synthesis of nucleoprotein in bean root cells. *Nature 167*, 599-600

Jacobs JJ, de Lange T (2005). p16INK4a as a second effector of the telomere damage pathway. *Cell Cycle 4*, 1364-1369

Johansen FE and Prywes R (1993). Identification of Transcriptional Activation and Inhibitory Domains in Serum Response Factor (SRF) by using GAL4-SRF constructs. *Mol Cell Biol 13*, 4640-4647

Kalmanson D, Veyrat C, Abitbol G, Bouchareine F, Cholot N (1977). Non-invasive exploration of valvular heart disease using Pulsed Doppler Flowmetry with echography. *Nouv Presse Med 6*, 2849-2853

Kamura T, Hara T, Matsumoto M, Ishida N, Okumura F, Hatakeyama S, Yoshida M, Nakayama K, Nakayama KI (2004). Cytoplasmic ubiquitin ligase KPC regulates proteolysis of p27 (Kip1) at G1 phase. *Nat Cell Biol 6*, 1229-1235

Kardinal C, Dangers M, Kardinal A, Koch A, Brandt DT, Tamura T, Welte K (2006). Tyrosine phosphorylation modulates binding preference to cyclin-dependent kinases and subcellular localization of p27Kip1 in the acute promyelocytic leukemia cell line NB4. *Blood 107*, 1133-1140

Kastan MB, Onyekere O, Sidransky D, Volgelstein B, Craig RW (1991). Participation of p53 protein in the cellular response to DNA damage. *Cancer Res 51*, 6304-6311

Kemp PR, Metcalfe JC (2000). Four isoforms of serum response factor that increase or inhibit smooth-muscle-specific promoter activity. *Biochem J 345*, 445-451

Khachigian LM, Collins T (1997). Inducible expression of Egr-1-dependent genes: a paradigm of transcriptional activation in vascular endothelium. *Circ Res 81*, 457–461

Khvorova A, Reynolds A, Javasena SD (2003). Functional siRNAs and miRNAs exhibit strand bias. *Cell 115*, 209-216

King RW, Deshaies RJ, Peters JM, Kirschner MW (1996). How proteolysis drives the cell cycle. *Science 274*, 1652-1659

King RW, Peters JM, Tugendreich S, Rolfe M, Hieter P, Kirschner MW (1995). A 20S complex containing CDC27 and CDC16 catalyzes the mitosis-specific conjugation of ubiquitin to cyclin B. *Cell 81*, 279-288

Knöll B, Kretz O, Fiedler C, Alberti S, Schütz G, Frotscher M, Nordheim A (2006). Serum response factor controls neuronal circuit assembly in the hippocampus. *Nat Neurosci 9*, 195-204

Knudsen ES and Wang JY (1997). Dual mechanisms for the inhibition of E2F binding to RB by cyclin-dependent kinase-mediated RB phosphorylation. *Mol Cell Biol 17*, 5771-5783

Krause K, Wasner M, Reinhard W, Haugwitz U, Dohna CL, Mössner J, Engeland K (2000). The tumour suppressor protein p53 can repress transcription of cyclin B. *Nucleic Acids Res 15*, 4410-4418

Krek W, Xu G, Livingston DM (1995). Cyclin A-kinase regulation of E2F-1 DNA binding function underlies suppression of an S phase checkpoint. *Cell 83*, 1149-1158

Kreutzer R, John M, Limmer S, Vornlocher HP (2004). siRNA – Entwicklung einer neuen Klasse von Therapeutika. *Laborwelt 5*, 21-25

Krishna DR, Sperker B, Fritz P, Klotz U (1999). Does pH 6 beta-galactosidase activity indicate cell senescence? *Mech Ageing Dev 109*, 113-123

Krishnamurthy J, Torrice C, Ramsey MR, Grigriy KI, Al-Regaiey K, Su L, Sharpless NE (2004). Ink4a/Arf expression is a biomarker of aging. *J Clin Invest 114*, 1299-1307

Kumar V, Fausto N, Abbas A, Robbins and Cotran – Pathologic Basis of Disease, 6th edition, *W.B. Saunders Publishing*

Kuo CH, Wells WW (1978). beta-Galactosidase from rat mammary gland. Its purification, properties and role in the biosynthesis of 6beta-O-D-galactopyranosyl myo-inositol. *J Biol Chem 253*, 3550-3556

Kurz DJ, Decary S, Hong Y, Erusalimsky JD (2000). Senescence-associated (beta)-galactosidase reflects an increase in lysosomal mass during replicative aging of human endothelial cells. *J Cell Sci 113*, 3612-3622

Labbe JC, Capony JP, Caput D, Cavadore JC, Derancourt J, Kaqhad M, Lelias JM, Picard A, Doree M (1989). MPF from starfish oocytes at first meiotic metaphase is a heterodimer containing one molecule of cdc2 and one molecule of cyclin B. *EMBO J 8*, 3053-3058

Landen CN Jr, Chavez-Reyes A, Bucana C, Schmandt R, Deavers MT, Lopez-Berestein G, Sood AK (2005). Therapeutic EphA2 gene targeting in vivo using neutral liposomal small interfering RNA delivery. *Cancer Res 65*, 6910-6918

Landerholm TE, Dong XR, Lu J, Belaguli NS, Schwartz RJ, Majesky MW (1999). A role for serum response factor in coronary smooth muscle differentiation from proepicardial cells. *Development 126*, 2053-2062

Laptenko O, Prives C (2006). Transcriptional regulation of p53: one protein, many possibilities. *Cell Death Differ 13*, 951-961

Le NT, Richardson DR (2003). Potent iron chelators increase the mRNA levels of the universal cyclin-dependent kinase inhibitor p21(CIP/WAF1), but paradoxically inhibit its translation: a potential mechanism of cell cycle dysregulation. *Carcinogenesis 24*, 1045-1058

Lee BY, Han JA, Im JS, Morrone A, Johung K, Goodwin EC, Kleijer WJ, DiMaio D, Hwang ES (2006). Senescence-associated beta-galactosidase is lysosomal beta-galactosidase. *Aging Cell 5*, 187-195

Lees-Miller JP, Heeley DH, Smillie LB, Kay CM (1987). Isolation and characterization of an abundant and novel 22-kDa protein (SM22) from chicken gizzard smooth muscle. *J Biol Chem 262*, 2988-2993

Leung S, Miyamoto NG (1989). Point mutational analysis of the human c-fos serum response factor binding site. *Nucleic Acids Res 17*, 1177-1195

Levedakou EN, Kaufmann WK, Alcorta DA, Galloway DA, Paules RS (1995). p21CIP1 is not required for the early G2 checkpoint response to ionizing radiation. *Caner Res 55*, 2500-2502

Li L, Miano JM, Mercer B, Olson EN (1996). Expression of the SM22alpha promoter in transgenic mice provides evidence for distinct transcriptional regulatory programs in vascualr and visceral smooth muscle cells. *J Cell Biol 132*, 849-859

Li L, Liu Z, Mercer B, Overbeek P, Olson EN (1997). Evidence for serum response factor-mediated regulatory networks geverning SM22alpha transcription in smooth, skeletal and cardiac muscle cells. *Dev Biol 187*, 311-321

Li S, Wang DZ, Wang Z, Richardson JA, Olson EN (2003). The serum response factor coactivator Myocardin is required for vascular smooth muscle development. *Proc Natl Acad Sci USA 100*, 9366-9370

Li S, Czubryt MP, McAnally J, Bassel-Duby R, Richardson JA, Wiebel FF, Nordheim A, Olson EN (2005). Requirement for serum response factor for skeletal muscle growth and maturation revealed by tissue-specific gene deletion in mice. *Proc Natl Acad Sci USA 102*, 1082-1087

Little JB (1968). Delayed initiation of DNA synthesis in irradiated human diploid cells. *Nature 218*, 1064-1065

Liu B, Itoh H, Louie O, Kubota K, Kent KC (2004). The role of phospholipase C and phosphatidylinositol 3-kinase in vascular smooth muscle cell migration and proliferation. *J Surg Res 120*, 256-265

Liu J, Carmell MA, Rivas FV, Marsden CG, Thomson JM, Song JJ, Hammond SM, Joshua-Tor L, Hannon GJ (2004). Argonaute2 is the catalytic engine of mammalian RNAi. *Science 305*, 1437-1441

Lwin T, Hazlehurst LA, Dessureault S, Lai R, Bai W, Sotomayor E, Moscinski LC, Dalton WS, Tao J (2007). Cell adhesion induces p27Kip1-associated cell-cycle arrest through down-regulation of the SCFSkp2 ubiquitin ligase pathway in mantle-cell and other non-Hodgkin B-cell lymphomas. *Blood 110*, 1631-1638

Mack CP, Owens GK (1999). Regulation of smooth muscle α-actin expression in vivo is dependent on CArG elements within the 5' and first intron promoter regions. *Circ Res 84*, 852-861

Mammoto A, Huang S, Moore K, Oh P, Ingber DE (2004). Role of RhoA, mDia, and ROCK in cell shape-dependent control of the Skp2-p27kip1 pathway and the G1/S transition. *J Biol Chem 279*, 26323-26330

Martinez N, Drescher B, Riehle H, Cullmann C, Vornlocher HP, Ganser A, Heil G, Nordheim A, Krauter J, Heidenreich O (2004). The oncogenic fusion protein RUNX1-CBFA2T1 supports proliferation and inhibits senescence in t(8;21)-positive leukaemic cells. *BMC Cancer 6*, 4:44

Masui Y, Markert CL (1971). Cytoplasmic control of nuclear behaviour during meiotic maturation of frog oocytes. *J Exp Zool 177*, 129-145

Matsushime H, Roussel MF, Sherr CJ (1991). Novel mammalian cyclins (CYL genes) expressed during G_1. *Cold Spring Harbor Symp Quant Biol 56*, 69-74

Matsuzaki K, Minami T, Tojo M, Honda Y, Uchimura Y, Saitoh H, Yasuda H, Nagahiro S, Saya H, Nakao M (2003). Serum response factor is modulated by the SUMO-1 conjugation system. *Biochem Biophys Res Commun 306*, 32-38

McDonald OG, Wamhoff BR, Hoofnagle MH, Owens GK (2006). Control of SRF binding to CArG box chromatin regulates smooth muscle gene expression in vivo. *J Clin Invest 116*, 36-48

Meyyappan M, Wheaton K, Riabowol KT (1999). Decreased expression and activity of the immediate-early growth response (Egr-1) gene product during cellular senescence. *J Cell Physiol 179*, 29-39

Miano JM, Carlson MJ, Spencer JA, Misra RP (2000). Serum response factor-dependent regulation of the smooth muscle calponin gene. *J Biol Chem 275*, 9814-9822

Miano JM (2003). Serum response factor: toggling between disparate programs of gene expression. *J Mol Cell Cardiol 35*, 577-593

Miano JM, Ramanan N, Georger MA, de Mesy Bentley KL, Emerson RL, Balza RO Jr, Xiao Q, Weiler H, Ginty DD, Misry RP (2004). Restricted inactivation of serum response factor to the cardiovascular system. *Proc Natl Acad Sci USA 101*, 17132–17137.

Miano JM, Long X, Fujiwara K (2006). Serum response factor: master regulator of the actin cytoskeleton and contractile apparatus. *Am J Physiol Cell Physiol 292*, 70-81.

Michieli P, Chedid M, Lin D, Pierce JH, Mercer WE, Givol D (1994). Induction of WAF1/CIP1 by a p53-independent pathway. *Cancer Res 54*, 3391-3395

Minshull J, Golsteyn R, Hill CS, Hunt T (1990). The A- and B-type cyclin associated cdc2 kinases in Xenopus turn on and off at different times in the cell cycle. *EMBO J 9*, 2865-2875

Minty A, Kedes L (1986). Upstream regions of the human cardiac actin gene that modulate its transcription in muscle cells: presence of an evolutionarily conserved repeated motif. *Mol Cell Biol 6*, 2125-2136

Misra RP, Rivera VM, Wang JM, Fan DP, Greenberg ME (1991). The serum response factor is extensively modified by phosphorylation following its synthesis in serum-stimulated fibroblasts. *Mol Cell Biol 11*, 4545-4554

Moiseeva EP (2001). Adhesion receptors of vascular smooth muscle cells and their functions. *Cardiovasc Res 52*, 372-386

Momand J, Zambretti GP, Olson DC, George D, Levine AJ (1992). The mdm-2 oncogene product forms a complex with the p53 protein and inhibits p53-mediated transactivation. *Cell 69*, 1237-1245

Momand J, Wu HH, Dasgupta G (2000). MDM2—master regulator of the p53 tumor suppressor protein. *Gene 242*, 15-29

Monica BP, Lesnik EA, Gonzalez C, Lima WF, McGee D, Guinosso CJ, Kawasaki AM, Cook PD, Freier SM (1993). Evaluation of 2'-modified oligonucleotides containing 2'-deoxy gaps as antisense inhibitors of gene expression. *J Biol Chem 5*, 14514-14522

Montagnoli A, Fiore F, Eytan E, Carrano AC, Draetta GF, Hershko A, Pagano M (1999). Ubiquitination of p27 is regulated by Cdk-dependent phosphorylation and trimeric complex formation. *Genes Dev 13*, 1181-1189

Morgan DO (1995). Principles of CDK regulation. *Nature 374*, 131-134

Motwani JG and Topol EJ (1998). Aortocoronary saphenous vein graft disease: pathogenesis, predisposition, and prevention. *Circulation 97*, 916–931

Mullany CJ (2003). Coronary Artery Bypass Surgery. *Circulation 107*, 21-22

Nakayama K, Nagahama H, Minamishima YA, Matsumoto M, Nakamichi I, Kitagawa K, Shirane M, Tsunematsu R, Tsukiyama T, Ishisa N, Kitagawa M, Nakayama K, Hatakeyama S (2000). Targeted disruption of Skp2 results in accumulation of cyclin E and p27(Kip1), polyploidy and cotrosome overduplication. *EMBO J 19*, 2069-2081

Nellen W, Sczakiel G (1996). In vitro and in vivo action of antisense RNA. *Mol Biotechnol 6*, 7-15

Nigg EA (1995). Cyclin-dependent protein kinases: key regulators of the eukaryotic cell cycle. *Bioessays 17*, 471-480

Nigg EA (2001). Mitotic kinases as regulators of cell cycle divisions and its checkpoints. Nat *Rev Mol Cell Biol 2*, 21-32

Niu Z, Yu W, Zhang SX, Barron M, Belaguli NS, Schneider MD, Parmacek M, Nordheim A, Schwartz RJ (2005). Conditional mutagenesis of the murine serum response factor gene blocks cardiogenesis and the transcription of downstream gene targets. *J Biol Chem 280*, 32531-32538

Noda A, Ning Y, Venable SF, Pereira-Smith OM, Smith JR (1994). Cloning of senescent cell-derived inhibitors of DNA synthesis using an expression screen. *Exp Cell Res 21*, 90-98

Norman C, Runswick M, Pollock R, Treisman R (1988). Isolation and properties of cDNA clones encoding SRF, a transcription factor that binds to the c-fos serum response element. *Cell 55*, 989-1003

Nykänen A, Haley B, Zamore PD (2001). ATP requirements and small interfering RNA structure in the RNA interference pathway. *Cell 107*, 309-321

Owens CD (1996). Atherosclerosis and Coronary Artery Disease. *Chap 3*, p 401 ff

Owens GK, Kumar MS, Wamhoff BR (2004). Molecular regulation of vascular smooth muscle cell differentiation in development and disease. *Physiol Rev 84*, 767-801

Pagano M, Pepperkok R, Verde F, Ansorge W, Draetta G (1992). Cyclin A is required at two points in the human cell cycle. *EMBO J 11*, 961-971

Pagano M, Tam SW, Theodoras AM, Beer-Romero P, Del Sal G, Chau V, Yew PR, Draetta GF, Rolfe M (1995). Role of the ubiquitin-proteasome pathway in regulating abundance of the cyclin-dependent kinase inhibitor p27. *Science 269*, 682-685

Pardee AB, Dubrow R, Hamlin JL, Kletzien RF (1978). Animal cell cycle. *Annu Rev Biochem 47*, 715-750

Pellegrini L, Tan S, Richmond TJ (1995). Structure of serum response factor core bound to DNA. *Nature 376*, 490-498

Phan-Dinh-Tuy F, Tuil D, Schweighoffer F, Pinset C, Kahn A, Minty A (1988). The 'CC.Ar.GG' box. A protein-binding site common to transcription-regulatory regions of the cardiac actin, c-fos and interleukin-2 receptor genes. *Eur J Biochem 173*, 507-515

Polyak K, Kato JY, Solomon MJ, Sherr CJ, Massague J, Roberts JM, Koff A (1994). p27Kip1, a cyclin-Cdk inhibitor, links transforming growth factor-beta and contact inhibition to cell cycle arrest. *Genes Dev 8*, 9-22

Poser S, Impey S, Trinh K, Xia Z, Storm DR (2000). SRF-dependent gene expression is required for PI3-kinase-regulated cell proliferation. *EMBO J 19*, 4955-4966

Posern G, Treisman R (2006). Actin' together: serum response factor, its cofactors and the link to signal transduction. *Trends Cell Biol 11*, 588-596

Prywes R, Roeder RG (1987). Purification of the c-fos enhancer-binding protein. *Mol Cell Biol 7*, 3482-3489

Reason AJ, Morris HR, Panico M, Marais R, Treisman RH, Haltiwanger RS, Hart GW, Kelly WG, Dell A (1992). Localization of O-GlcNAc modification on the serum response transcription factor. *J Biol Chem 267*, 16911-16921

Rensen SSM, Doevendans PAFM, van Eys GJJM (2007). Regulation and characteristics of vascular smooth muscle cell phenotypic diversity. *Neth Heart J 15*, 100-108

Reynolds A, Leake D, Boese Q, Scaringe S, Marshall SW, Khvorova A (2004). Rational siRNA design for RNA interference. *Nat biotechnol 22*, 326-330

Rieder CL, Schultz A, Cole R, Sluder G (1994). Anaphase onset in vertebrate somatic cells is controlled by a checkpoint that monitors sister kinetochore attachment to the spindle. *J Cell Biol 127*, 1301-1310

Rosenquist TH, Beall AC (1990). Elastogenic cells in the developing cardiovascular system. Smooth muscle, nonmuscle, and cardiac neural crest. *Ann N Y Acad Sci 588*, 106-119

Ross R (1993). The pathogenesis of atherosclerosis: a perspective for the 1990s. *Nature 362*, 801-809

Rossi JJ (2004). Medicine: A cholesterol connection in RNAi. *Nature 432*, 155-156

Rudner AD, Murray AW (1996). The spindle assembly checkpoint. *Curr Opin Cell Biol 8*, 773-780

Saga H, Kimura K, Hayashi K, Gotow T, Uchiyama Y, Momiyama T, Tadokoro S, Kawashima N, Jimbou A, Sobue K (1999). Phenotype-dependent expression of α-smooth muscle actin in visceral smooth muscle cells. *Exp Cell Res 247*, 279-292

Samuel CE (2001). Antiviral actions of interferons. *Clin Microbiol Rev 4*, 778-809

Sanger F, Nicklen S, Coulson AR (1977). DNA sequencing with chain-terminating inhibitors. *Proc Natl Acad Sci USA 74*, 5463-5467

Samuel CE (2003). Knockdown by RNAi – proceed with caution. *Nat biotechnol 22*, 280-282

Schratt G, Weinhold B, Lundberg AS, Schuck S, Berger J, Schwarz J, Weinberg RA Ruther U, Nordheim A (2001). Serum response factor is required for immediate-early gene activation yet is dispensable for proliferation of embryonic stem cells. *Mol Cell Biol 21*, 2933-2943

Schratt G, Philippar U, Berger J, Schwarz H, Heidenreich O, Nordheim A (2002). Serum response factor is crucial for actin cytoskeletal organization and focal adhesion assembly in embryonic stem cells. *J Cell Biol 156*, 737-750

Schratt G, Philippar U, Hockemeyer D, Schwarz H, Alberti S, Nordheim A (2004). SRF regulates Bcl-2 expression and promotes cell survival during murine embryonic development. *EMBO J 23*, 1834-1844

Schröter H, Mueller CG, Meese K, Nordheim A (1990). Synergism in ternary complex formation between the dimeric glycoprotein p67SRF, polypeptide p62TCF and the c-fos serum response element. *EMBO J 4*, 1123-1130

Schwartz RS, Holmes DR Jr, Topol EJ (1992). The restenosis paradigm revisited: an alternative proposal for cellular mechanisms. *J Am Coll Cardiol 20*, 1284-1293

Schwartz RS, Edelman ER, Carter A, Chronos NA, Rogers C, Robinson KA, Waksman R, Machan L, Weinberger J, Wilensky RL, Goode JL, Hottenstein OD, Zuckerman BD, Virmani R (2004). Preclinical evaluation of drug-eluting stents for peripheral applications: recommendations from an expert consensus group. *Circulation 110*, 2498-2505

Schwartz SM, Campbell GR, Campbell JH (1986). Replication of smooth muscle cells in vascular disease. *Circ Res 58*, 427-444

Schwarz-Sommer Z, Huijser P, Nacken W, Saedler H & Sommer H (1990). Genetic control of flower development by homeotic genes in *Antirrhinum majus*. *Science 250*, 931 -936.

Semizarov D, Frost L, Sarthy A, Kroeger P, Halbert DN, Fesik SW (2003). Specificity of short interfering RNA determined through gene expression signatures. *Proc Natl Acad Sci USA 100*, 6347-6352.

Shaw PE, Schroter H, Nordheim A (1989). The ability of a ternary complex to form over the serum response element correlates with serum inducibility of the human c-fos promoter. *Cell 56*, 563-572

Sheaff RJ, Singer JD, Swanger J, Smitherman M, Roberts JM, Clurman BE (2000). Proteasomal turnover of p21Cip1 does not require p21Cip1 ubiquitination. *Mol Cell 5*, 403-410

Sheng M, Dougan ST, McFadden G, Greenberg ME (1988). Calcium and growth factor pathways of c-fos transcriptional activation require distinct upstream regulatory sequences. *Mol Cell Biol 8*, 2787-2796

Shimizu RT, Blank RS, Jervis R, Lawrenz-Smith SC, Owens GK (1995). The smooth muscle α-actin gene promoter is differentially regulated in smooth muscle versus non-smooth

Shin JS, Hong SW, Lee SL, Kim TH, Park IC, An SK, Lee WK, Lim JS, Kim KI, Yang Y, Lee SS, Jin H, Lee MS (2008). Serum starvation induces G1 arrest through suppression of SKP2-CDK2 and CDK2 in SK-OV-3 cells. *Int J Oncol 32*, 435-439

Sinanan AC, Buxton PG, Lewis MP (2006). Muscling in on stem cells. *Biol Cell 98*, 203-214

Sledz CA, Holko M, de Veer MJ, Silverman RH, Williams BR (2003). Activation of the interferon system by short-interfering RNAs. *Nat Cell Biol 5*, 834-839

Small JV, Gimona M (1998). The cytoskeleton of the vertebrate smooth muscle cell. *Acta Physiol Scand 164*, 341-348

Sobue K, Hayashi K, Nishida W (1999). Expessional regulation of smooth muscle cell-specific genes in association with phenotypic modulation. *Mol Cell Biochem 190*, 105-118

Solway J, Seltzer J, Samaha FF, Kim S, Alger LE, Niu Q, Morrisey EE, Ip HS, Parmacek MS (1995). Structure and expression of a smooth muscle cell-specific gene, SM22 alpha. *J Biol Chem 270*, 13460-13469

Song E, Lee SK, Wang J, Ince N, Ouyang N, Min J, Chen J, Shankar P, Lieberman J (2003). RNA interference targeting Fas protects mice from fulminant hepatitis. Nat Med 9, 347-351

Soulez M, Gauthier-Rouviere C, Chafey P, Hentzen D, Vandromme M, Lautredou N, Lamb N, Kahn A, Tuil D (1996). Growth and differentiation of C2 myogenic cells are dependent on serum response factor. *Mol Cell Biol 16*, 6065–6074

Soulez M, Tuil D, Kahn A, Gilgenkrantz H (1996). The serum response factor (SRF) is needed for muscle-specific activation of CArG boxes. *Biochem Biophys Res Commun 219*, 418-422

Stein CA (1995). Does antisense exist? *Nat Med 1*, 1119-1121

Stix G (2004). Hitting the genetic off switch. *Sci Am 291*, 98-101

Sudakin V, Ganoth D, Dahan A, Heller H, Hershko J, Luca FC, Ruderman JV, Hershko A (1995). The cyclosome, a large complex containing cyclin-selective ubiquitin ligase activity, targets cyclins for destruction at the end of mitosis. *Mol Biol Cell 6*, 185-197

Sun Q, Chen G, Streb JW, Long X, Yang Y, Stoeckert CJ Jr, Miano JM (2006). Defining the mammalian CArGome. *Genome Res 16*, 197-207

Szak ST, Mays D, Pietenpol JA (2001). Kinetics of p53 binding to promoter sites in vivo. *Mol Cell Biol 21*, 3375-3386

Takahashi K, Abe M, Hiwada K, Kokubu T (1988). A novel troponin T-like protein (calponin) in vascular smooth muscle: interaction with tropomyosin paracrystals. *J Hypertens Suppl 6*, 40-43

Takai H, Smogorzewska A, de Lange T (2003). DNA damage foci at dysfunctional telomeres. Curr Biol 13, 1549-1556

Tamir A, Petrocelli T, Stetler K, Chu W, Howard J, Croix BS, Slingerland J, Ben-David Y (2000). Stem cell factor inhibits erythroid differentiation by modulating the activity of G1-cyclin-dependent kinase complexes: a role for p27 in erythroid differentitation coupled G1 arrest. *Cell Growth Differ 11*, 269-277

Tang G, Galili G (2004). Using RNAi to improve plant nutritional value: from mechanism to application. *Trends Biotechnol 22*, 463-469

Taylor WR, Schonthal AH, Galante J, Stark GR (2001). p130/E2F4 binds to and represses the cdc2 promoter in response to p53. *J Biol Chem 276*, 1998-2006

Thomas M, Gessner A, Vornlocher HP, Hadwiger P, Greil J, Heidenreich O (2005). Targeting MLL-AF4 with short interfering RNAs inhibits clonogenicity and engraftment of t(4;11)-positive human leukemic cells. *Blood 106*, 3559-3566

Thyberg J, Blomgren K, Roy J, Tran PK, Hedin U (1997). Phenotypic modulation of smooth muscle cells after arterial injury is associated with changes in the distribution of laminin and fibronectin. *J Histocheim Cytochem 45*, 837-846

Ting LH (2005). Short double-stranded RNA induces transcriptional gene silencing in human cancer cells in the absence of DNA methylation. *Nat genet 37*, 906-910

Toledo F, Wahln GM (2006). Regulating the p53 pathway: in vitry hypotheses, in vivo veritas. *Nat Rev Cancer 6*, 909-923

Tolentino MJ, Bruckner AJ, Fosnot J, Ying GS, Wu IH, Malik G, Wan S, Reich SJ (2004). Intravitreal injection of vascular endothelial growth factor small interfering RNA inhibits growth and leakage in a nonhuman primate, laser-induced model of choroidal neovascularization. *Retina 24*, 660-661

Toyoshima H, Hunter T (1994). p27, a novel inhibitor of G_1 cyclin-Cdk protein kinase activity, is related to p21. *Cell 78*, 67-74

Treisman R (1986). Identification of a protein-binding site that mediates transcriptional response of the c-fos gene to serum factors. *Cell 46*, 567-574

Treisman R (1987). Identification and purification of a polypeptide that binds to the c-fos serum response element. *EMBO J 6*, 2711-2717

Vandekerckhove J, Weber K (1987). At least six different actins are expressed in a higher mammal: an analysis based on the amino acid sequence of the amino-terminal tryptic peptide. *J Mol Biol 126*, 783-802

Vousden KH, Lu X (2002). Live or let die: the cell's response to p53. *Nat Rev Cancer 2*, 594-604

Wagner AJ, Kokontis JM, Hay N (1994). Myc-mediated apoptosis requires wild-type p53 in a manner independent of cell cycle arrest and the ability of p53 to induce p21Waf1/Cip1. *Genes Dev 8*, 2817–2830

Wagner S and Selzer A (1982). Patterns of progression of aortic stenosis: a longitudinal hemodynamic study. *Circulation 65*, 709-712

Walker T, Wendel HP, Raabe C, Wyechnik P, Spranger L, Heidenreich O, Scheule AM, Nordheim A, Ziemer G (2009). Graft protection in bypass surgery: siRNA-mediated silencing of adhesion molecules. *Oligonucleotides 2009*

Wang D, Chang PS, Wang Z, Sutherland L, Richardson JA, Small E, Krieg PA, Olson EA (2001). Activation of cardiac gene expression by myocardin, a transcriptional cofactor of serum response factor. *Cell 105*, 851-862

Wang DZ, Li S, Hockemeyer D, Sutherland L, Wang Z, Schratt G, Richardson JA, Nordheim A, Olson EN (2002). Potentiation of serum response factor activity by a family of myocardin-related transcription factors. *Proc Natl Acad Sci USA 99*, 14855-14860

Wang Z, Wang DZ, Hockemeyer D, McAnally J, Nordheim A, Olson EN (2004). Myocardin and ternary complex factors compete for SRF to control smooth muscle gene expression. *Nature 428*, 185-189

Wei W, Ayad NG, Wan Y, Zhang GJ, Kirschner MW, Kaelin WG Jr (2004). Degradation of the SCF component Skp2 in cell-cycle phase G1 by the anaphase-promoting complex. *Nature 428*, 194-198

Wirbelauer C, Sutterlüty H, Blondel M, Gstaiger M, Peter M, Reymond F, Krek W (2000). The F-box protein Skp2 is a ubiquitylation target of a Cul1-based core ubiquitin ligase complex: evidence for a role of Cul1 in the suppression of Skp2 expression in quiescent fibroblasts. *EMBO J 19*, 5362-5375

Yang NC, Hu ML (2005). The limitations and validities of senescence associated-beta-galactosidase activity as an aging marker for human foreskin fibroblast Hs68 cells. *Exp Gerontol 40*, 813-819

Zhang H, Somasundaram K, Peng Y, Tian H, Zhang H, Bi D, Weber BL, El-Deiry WS (1998). BRCA1 physically associates with p53 and stimulates its transcriptional activity. *Oncogene 16*, 1713-1721

Zhang X, Azhar G, Chai J, Sheridan P, Nagano K, Brown T, Yang J, Khrapko K, Borras AM, Lawitts J, Misra RP, Wei JY (2001). Cardiomyopathy in transgenic mice with cardiac-specific overexpression of serum response factor. *Am J Physiol Heart Circ Physiol 280*, 1782-1792

Zhang X, Chai J, Azhar G, Sheridan P, Borras AM, Furr MC, Khrapko K, Lawitts J, Misra RP, Wei JY (2001). Early postnatal cardiac changes and premature death in transgenis mice overexpressing a mutant form of serum response factor. *J Biol Chem 276*, 40033-40040

12 Acknowledgement

I would like to thank Prof. Dr. Nordheim and Dr. Heidenreich for giving me the opportunity to do this research and for supervising me. Thanks for letting me work on this interesting topic.

Thanks to Dr. Wendel in Tuebingen and Dr. Grassi in Trieste for the great collaboration.

Special thanks to Heidemie and David for their help and always having answers for every conceivable question. Sunny thanks to Natalia for always showing us the bright side of life. Thanks to Christine for her help and funny trips to Kopenhavn or Rust. Thanks to Jenny for always having an ear for me and the great cocktails on her balcony. Not to forget Stefan for keeping the safety up in the lab and bringing music to the lab, thank you.

The whole “mouse lab” a big thank you for your support, help and discussions: Siggi, Seba, Katja, Anke, Bilge and Meike, it was a great time!

Dr. Bernd Knöll: Thank you for great discussion in the research reports. Special thanks to Daniela for her great social engagemant, Kai for interesting discussions about sports or movies, Tine and her husband for always having a space for me in their wonderful home and Sina for spreading good mood and movie trips!

I am very grateful to Heide for always supporting me in every conceivable situation, especially when it came to burocracy!

My thanks are also expressed to all the colleagues in this department.

My special thanks go to my parents for their support and encouragement in whatever I am doing, my grandma for all the Sunday-phone calls and my whole family. Of course, thanks to all other friends all over the world, who make my life my life.